Cell Matrix Adhesions and Collective Cell Migration:

The Role of X-chef-1

Melissa Turan

A thesis submitted in partial fulfilment for the degree
of Doctor of Philosophy

University College London

February 2021

I declare that the work presented in this thesis is my own, unless otherwise stated

Melissa Turan

Abstract

Collective cell migration is involved in a plethora of developmental and physiological processes. One well-studied example is the collective migration of the cephalic neural crest (NC); an embryonic stem cell population that gives rise to a diverse cell lineage in vertebrate embryos. NC migration requires the formation of integrin-based cell matrix adhesions. However, the exact molecular composition of these adhesions and how they regulate cell polarity during NC migration remains unclear. Furthermore, it was recently demonstrated that stiffening of the migratory substrate is required to trigger the onset of NC migration. This finding raises the question of how the neural crest transduces mechanical cues from its substrate to trigger migration. Whilst integrin-based adhesions serve as the mechanosensory unit of adherent cells, their functional relevance in mechanotransduction during NC migration remains unknown.

Here, we investigate the role of Crk Associated Substrate (CAS) protein, X-chef-1, within the cephalic neural crest in *Xenopus laevis*. This scaffolding protein within the integrin signaling pathway is expressed in the neural crest prior to the onset of migration, however its function is unknown. Through loss of function experiments, we investigated the requirement of X-chef-1 during NC migration. Knock down of X-chef-1 inhibited migration *in vivo* and cell dispersion and motility *in vitro.* Through the targeted expression of X-chef-1 dominant negative constructs, we observed that the migratory deficit was primarily attributed to the loss of tyrosine phosphorylation of the X-chef-1 substrate domain. Taken together, we propose that tyrosine phosphorylation of the X-chef-1 substrate domain promotes migration through activating the cell polarity effector Rac-1 at the leading edge of the neural crest. Furthermore, preliminary experiments suggested that constitutive phosphorylation of the X-chef-1 substrate domain may rescue NC migration on mechanically non-permissive substrates *in vivo*. Hence, our results set up

the framework for further investigation into the role of X-chef-1 in the response to mechanical cues during NC migration.

Impact Statement

The work presented in this study aims to elucidate mechanisms of the cephalic neural crest migration. The cephalic neural crest migrates in a directional manner during migration to give rise to a diverse cell lineage including the cartilage, bone, cranial neurons, glia, and connective tissues of the face. Perturbing migration of the cephalic neural crest can manifest in severe craniofacial defects during development. For example, deficits in the formation and migration of the neural crest can result in the reduced translocation of cells to their required destinations. This can lead to the development of Treacher Collins syndrome, characterized by birth defects including small noses, jaws, and ears as well as cleft palate. For this reason, elucidating mechanisms of neural crest migration is critical to advance current knowledge of the etiology and pathology of inherited craniofacial malformation disorders. Furthermore, it can also provide the foundation for developing future therapeutics to prevent and treat craniofacial abnormalities.

The neural crest is also a suitable model to investigate cancer metastasis. Neural crest migration possesses many commonalities with tumour cell invasion. Like many tumour cells the neural crest undergo an epithelial to mesenchymal manner and migrate as a collective cell population. Furthermore, many of the genes expressed in the migratory neural crest are also expressed in cancer cells. In this thesis, we examine the role of cell-matrix adhesion component Cass4, in the migration of the neural crest. While Cass4 is expressed in the cephalic neural crest of *Xenopus laevis,* Cass4 is also upregulated in lung adenocarcinoma and lung squamous carcinoma tissues and associated with poor prognosis. Hence, clarifying the role of CAS proteins in neural crest migration can have important implications for cancer metastasis.

Acknowledgements

First of all, I would like to thank my supervisor Professor Roberto Mayor for his continued support and guidance throughout my PhD. I would like to thank my thesis committee, composed of David Wilkinson and Buzz Baum for their useful inputs into my project and the Wellcome Trust for the funding of my project.

Special thanks go to members of the Mayor lab over the course of my PhD. I would like to thank Dr. Elias Barriga for providing experimental assistance when needed and for always motivating to me to keep going, even when I ran into technical difficulties. I would like to thank Soraya Villaseca for the sharing PAK-GBD-GFP construct with me (and sometimes her lunch). I would like to thank Louise Van Bergen and Sven Hey for always managing to put a smile on my face, during their time in the lab. Finally I would like to thank Zahra and Marta for giving me the opportunity to teach them during their Undergraduate and Master's project.

Outside of the lab, I would like to thank Virginia, Vicki and Ivana for always making time for weekend brunches. I would like to thank Marc for standing by me in the highs and lows of the final year of my PhD (and in ensuring that I was always properly fed). Finally, I would like to thank my parents for their unconditional support and motivation over the years.

Table of Contents

Abstract **3**

Impact Statement **5**

Acknowledgements **6**

List of Figures and Tables **11**

List of Supplementary Movies **14**

List of Abbreviations **15**

1.Introduction **17**

1.1 Principles of Cell Migration **18**

1.1.1 Introduction to Cell Migration **18**

1.1.2 Single cell migration **19**

1.1.3 Cell Polarity during single cell migration **19**

1.1.4 Collective Cell Migration **21**

1.1.5 Cell Polarity during Collective cell migration **21**

1.1.6 Molecular structures that govern cell motility **22**

1.2 Cell Matrix Adhesions **26**

1.2.1 Introduction to cell matrix adhesions **26**

1.2.2 Cell matrix Adhesion Assembly, Maturation and Disassembly **27**

1.2.3 Cell matrix adhesions as mechanosensors **31**

1.3 The Crk Associated Substrate (CAS) proteins **37**

1.3.1 Discovery of CAS family proteins **37**

1.3.2 CAS protein Domain structure **38**

1.3.3 CAS protein expression in *Xenopus laevis* 39
1.3.4 CAS proteins as docking proteins 40
1.3.5 Functional roles behind CAS protein signaling 44

1.4 The neural crest 50
1.4.1 Introduction to the neural crest 50
1.4.2 Neural crest induction 51
1.4.3 Delamination 52
1.4.4 EMT 53
1.4.5 Neural Crest Migration 55

1.5 Hypothesis 63
1.5.1 Hypothesis Background 63
1.5.2 Hypothesis 64

2.Experimental Procedures 65
2.1 Solutions 66

2.2 Embryological Procedures 69
2.2.1 *Xenopus Laevis* Oocyte collection and Fertilization 69
2.2.2 Microinjection 69
2.2.3 Neural crest dissection and culture 72

2.3 Molecular Biology 73
2.3.1 Amplification of DNA clones 73
2.3.2 Molecular cloning 73
2.3.3 *In vitro* transcription 75
2.3.4 *In situ* hybridisation 76
2.3.5 Immunofluorescence 77
2.3.6 Morpholinos (MO) 79
2.3.7 Inhibitors 79
2.3.8 Polyacrylamide gels 80

2.4 Analysis 82

2.4.1 *In vivo* migration 82

2.4.2 Single Cell Motility 82

2.4.3 Dispersion 83

2.4.4 Phosphopaxilin analysis 83

2.4.5 FAK-GFP analysis 84

2.4.6 Protrusion analysis 84

2.4.7 Rac-GTP analysis 84

2.4.8Pak-gdb analysis 85

2.4.9 Statistical analysis 85

3. Results 86

3.1 Investigating the functional role of X-chef-1 in NC migration 87

3.1.1 X-chef-1 localises to cell matrix adhesions 87

3.1.2 X-chef-1 is required for neural crest migration *in vivo* 88

3.1.3 X-chef-1 is required for cell dispersion and motility *in vitro* 89

3.1.4 Discussion 90

3.2. Elucidating the molecular mechanism of X-chef-1 dependent migration 97

3.2.1 Loss of the SH3 and C terminus domains of X-chef-1 mildly impairs migration *in vivo* and cell motility *in vitro* 97

3.2.2 Loss of tyrosine phosphorylation of the Xchef-1 substrate domain strongly impairs migration *in vivo* and dispersion and cell motility *in vitro* 99

3.2.3 Discussion 100

3.3 Identifying downstream targets of X-chef-1 that promote NC migration 111

3.3.1 Loss of X-chef-1 tyrosine phosphorylation reduces size and number of cell matrix adhesions 112

3.3.2 Loss of X-chef-1 SD tyrosine phosphorylation impairs cell matrix adhesion and lamellipodial dynamics 112

3.3.3 Loss of X-chef-1 SD phosphorylation inhibits Rac-1 activation at leading edge ... 113

3.3.4 Constitutive activation of X-chef-1 SD tyrosine phosphorylation increases cell matrix adhesion number, protrusion size and promotes Rac-1 activation 115

3.3.5 Discussion 116

3.4 Investigating the role of X-chef-1 in the response to substrate stiffness during NC migration 132

3.4.1 Expression of phosphomimetic construct leads to expansion of neural crest territory at pre migratory stages 132

3.4.2 Expression of phosphomimetic construct does not improve cell spreading/polarity on soft substrates *in vitro* 133

3.4.3 Expression of phosphomimetic construct rescues migration of neural crest on softened mesoderm *in vivo* 134

3.4.4 Discussion 135

4.Discussion 141

4.1 Summary of Results and Working Model 142

4.2 The role of X-chef-1 in neural crest migration 143

4.3 The role of X-chef-1 in Rac-1 activation 144

4.4 The role of X-chef-1 in EMT 147

4.5 The role of X-chef-1 in the response to mechanical cues 148

4.6 The role of X-chef-1 in the response to chemical cues 151

4.7 Concluding remarks 154

5.References 156

List of Figures and Tables

Figure 1.1 Mechanisms of adhesion dependent single and collective cell migration **25**

Figure 1.2 Cell Matrix Adhesion lifecycle **35**

Figure 1.3 Mechanisms of integrin activation **36**

Figure 1.4 Diagram of Cas family member domain structures **47**

Figure 1.5 The CAS/FAK/SRC signaling complex **48**

Figure 1.6 CAS proteins in mechanotransduction **49**

Figure 1.7 The migration of the neural crest **62**

Table 1 A list of injected constructs **72**

Table 2 A list of cloning strategies and primers **75**

Table 3 Primary and Secondary Antibodies **78**

Figure 3.1 Subcellular localisation of X-chef-1 in the neural crest **92**

Figure 3.2 X-chef-1 is required for neural crest migration *in vivo* **93**

Figure 3.3 X-chef-1 full length mRNA rescues migration deficit resulting from morpholino **94**

Figure 3.4 X-chef-1 is required for cell dispersion *in vitro* **95**

Figure 3.5 X-chef is required for cell motility *in vitro* **96**

Figure 3.6 Design and subcellular localization of truncated X-chef-1 constructs **103**

Figure 3.7 Loss of SH3 and C terminus domains mildly impairs neural crest migration *in vivo* **105**

Figure 3.8 Loss of SH3 and C terminus domains impairs cell motility but not dispersion **107**

Figure 3.9 Design and subcellular localisation X-chef-1 Fxxp constuct **108**

Figure 3.10 Loss of tyrosine phosphorylation of the X-chef-1 substrate domain impairs migration *in vivo* **109**

Figure 3.11 Loss of tyrosine phosphorylation of the Xchef-1 substrate domain impairs dispersion and cell motility *in vitro* **110**

Figure 3.12 Loss of X-chef-1 SD tyrosine phosphorylation reduces size and number of cell matrix adhesions **120**

Figure 3.13 Loss of X-chef SD tyrosine phosphorylation reduces cell matrix adhesion size and stability **122**

Figure 3.14 Loss of X-chef SD tyrosine phosphorylation impairs formation and stability of protrusions *vivo* **124**

Figure 3.15 Validating the specificity of the Rac-GTP antibody **125**

Figure 3.16 Loss of X-chef-1 SD phosphorylation reduces Rac-1 activation at leading edge (1) **126**

Figure 3.17 Loss of X-chef-1 SD phosphorylation reduces Rac-1 activation at leading edge (2) **127**

Figure 3.18 Design and localization of X-chef-1 phosphomimetic substrate domain construct **128**

Figure 3.19 Constitutive activation of X-chef SD tyrosine phosphorylation results in an increased number of cell matrix adhesions at the leading edge **129**

Figure 3.20 Constitutive activation of X-chef SD tyrosine phosphorylation results in an increase in the size of protrusions at the leading edge **130**

Figure 3.21 Constitutive activation of X-chef SD tyrosine phosphorylation promotes Rac-1 activation at the leading edge **131**

Figure 3.22 Expression of phosphomimetic construct leads to expansion of neural crest territory at pre migratory stages **138**

Figure 3.23 Expression of phosphomimic construct does not improve cell spreading/polarity on soft substrates *in vitro* **139**

Figure 3.24 Expression of phosphomimetic construct rescues migration of neural crest on softened mesoderm *in vivo* **140**

Figure 4.1 Working Model **155**

List of Supplementary movies

1. Dispersion Assay (Wildtype vs. X-chef-1 MO)

X-chef-1 MO show a lower degree of dispersion in comparison with wildtype explants. Scale bar 100µm. Frame rate 5 mins per frame.

2. Dispersion Assay (Wildtype vs. ΔSH3 and ΔCT)

No significant difference is observed with regards to the degree of dispersion in ΔSH3 and ΔCT expressing explants, with respect to the control. Scale bar 100µm. Frame rate 5 mins per frame.

3. Dispersion Assay (Wildtype vs. X-chef-1-Fxxp)

Fxxp explants show a lower degree of dispersion in comparison with wildtype explants. Scale bar 100µm. Frame rate 5 mins per frame.

4. Cell Matrix adhesion dynamics (Wildtype vs. X-chef-1 MO and Fxxp)

Wildtype, X-chef-1 MO and Fxxp explants expressing FAK-GFP to label cell matrix adhesions at the leading edge were also imaged with the brightfield. Cell matrix adhesions at the leading edge of X-chef-1 MO and Fxxp explants are smaller and more unstable with respect to wildtype. Scale bar 10 µm. Frame rate 6 secs per frame.

5. Membrane protrusion dynamics (Wildtype vs. X-chef-1 MO and Fxxp)

Wildtype, X-chef-1 MO and Fxxp explants are imaged with the brightfield. Membrane protrusions are defined as the region devoid of yolk platelets. Membrane protrusions at the leading edge of X-chef-1 MO and Fxxp explants are smaller and shorter lived in duration with respect to wildtype. Scale bar 10 µm. Frame rate 6 secs per frame.

List of Abbreviations

ADAM	A disintegrin and metalloprotease
AFM	Atomic Force Microscopy
ANOVA	Analysis of variance
AP	Alkaline Phosphatase
ARP2/3	Actin related protein 2/3
BCAR1	Breast cancer anti-estrogen resistance 1
BCIP	5-bromo-4-chloro-3-indoyl-phosphate
BMBR	Boehringer Mannheim Blocking Reagent
BMP	Bone morphogenic protein
BSA	Bovine serum albumin
C3a	Complement component 3a
C3aR	Complement component 3a receptor
CAS	Crk associated substrate
CCH	Cas-family C terminal homology
CCM	Collective cell migration
CIL	Contact inhibition of locomotion
Crk	Crk proto-oncogene, adaptor protein
Cxcr4	C-X-C motif ligand receptor 4
DFA	Danilchick's Medium for Amy
ECM	Extracellular matrix
EMT	Epithelial-to-mesenchymal transition
ERK	Extracellular signal-regulated kinase
FA	Focal adhesion
FAB	Antigen binding fragment
F-actin	Filamentous actin

FAK	Focal adhesion kinase
FGF	Fibroblast Growth Factor
FRET	Fluorescence/Förster resonance energy transfer
GAP	GTPase-activating protein
GEF	Guanine-nucleotide exchange factor
GFP	Green fluorescent protein
HEF-1	Human enhancer of filamentation 1
MAB	Maleic acid buffer
MEMFA	Minimum essential medium with formaldehyde
MET	Mesenchymal-to-epithelial transition
MLCK	Myosin light chain kinase
MO	Morpholino
NAM	Normal amphibian medium
NBT	4-nitro blue-tetrazolium-chloride
NC	Neural crest
Nedd9	Neural precursor cell expressed developmentally down-regulated 9
NIK	Nck interacting kinase
NSP	Novel SH2-containing proteins
P130cas	p130 Crk-associated substrate
PDGF	Platelet-derived growth factor
PDGFRα	Platelet-derived growth factor receptor
ROCK	Rho-associated kinase
SDF-1	Stromal cell-derived factor
SEM	Semaphorin
SH3	Src homology 3
SHIP-2	Src-homology 2 containing inositol phosphatase-2
VEGF	Vascular endothelial growth factor
X-chef-1	Xenopus C*as/*HEF-*Like*-1 protein

1.Introduction

1.1 Principles of cell migration

1.1.1Introduction to cell migration

Cell migration is an essential biological process, required for a vast range of physiological events during embryogenesis, tissue and organ formation, wound healing, and immunological surveillance (Horwitz and Webb, 2003, Lauffenburger and Horwitz, 1996, Ridley et al., 2003). Furthermore, cell migration is involved in several pathophysiological processes and can lead to a range of disease states including mental retardation, osteoporosis, atherosclerosis, chronic inflammation, and cancer (Horwitz and Webb, 2003, Lauffenburger and Horwitz, 1996, Ridley et al., 2003, Hall, 2009). Fundamentally, the movement of cells is a highly complex and intricate process and relies on the integration and coordination of numerous signaling pathways. Cells can utilize different migratory strategies depending on the environmental context. For example, depending on the degree of cellular contractility and substrate adhesion, cells can assume different modes of migration (Friedl and Wolf.,2010). Cells can migrate in adhesion independent manner by amoeboid migration; a rapid cell movement associated with highly contractile cells, which generate weak traction force (Lämmermann and Sixt,2009). In contrast, mesenchymal cell migration, the primary focus of this thesis, involves the strong adherence of cells to the extracellular matrix (ECM), which allows them to generate the traction required for forward movement (Friedl et Wolf.,2010). In a further layer of complexity, cells which undergo adhesion dependent migration can migrate individually or collectively. Whilst much of our understanding of mesenchymal migration comes from studies in single cells, many of the fundamental principles also translate to collective cell migration. In the following section, we will outline general aspects of adhesion dependent motility, drawing parallels between single cells and collectives. We will

discuss mechanisms of collective migration in greater detail, within the context of the neural crest in section 1.4.

1.1.2 Single cell migration

Cell migration is an intricate multi-phase process, involving the integration of several complex regulatory pathways (Ridley et al., 2003). Broadly speaking, cell migration proceeds through a cyclical mechanism (figure1.1a) (Lauffenburger and Horwitz, 1996). Cells first acquire a front to rear polarity. Through actin polymerization at the leading edge, cells generate membrane protrusions, such as lamellipodia and filopodia, oriented in the direction of motion (Ananthakrishnan and Ehrlicher, 2007). Protrusions are stabilised via adherence to the ECM through cell substrate adhesions, which also facilitates the generation of traction forces (Geiger et al.,2001). Cell-substrate adhesions begin as small punctate adhesions known as focal complexes. Subsequently, they can grow to form focal adhesions (FA's) which associate with stress fibres and further mature. As focal adhesions reach the back of cells, where actomyosin contractility is predominant, focal adhesions disassemble and the cell retracts. Thus, in this way, repeated assembly and disassembly of adhesions and protrusions facilitates the progression of cell migration.

1.1.3 Cell Polarity during single cell migration

The cytoskeletal rearrangements which facilitate cell migration are governed by the activity of the small Rho GTPase family, including Rac-1, RhoA and Cdc42 (Ridley et al.,2001). Small Rho GTPases act as molecular switches, transferring from an inactive to an active state, through the exchange of the GDP molecule for a GTP molecule respectively and vice versa. The activation and

inactivation of Rho GTPases is facilitated by guanosine exchange factors (GEFs) and GTPase activating proteins (GAP's) respectively. Importantly, the activity of small Rho-GTPases is required to be carefully regulated to coordinate actin and microtubule assembly, needed for efficient migration.

During cell migration, Cdc42 and Rac-1 are generally active at the leading edge, whilst RhoA is primarily active at the cell rear. Cdc42 drives actin polymerization within filopodia at the leading edge (Itoh et al., 2002). Rac-1 activity, on the other hand, facilitates the formation of lamellipodia through promoting actin polymerization (Ridley et al.,1992).Rac1 is also required for the formation of early substrate adhesion sites, known as focal complexes (Nobes and Hall, 1995; Rottner et al., 1999). Active RhoA leads to the formation of stress fibers (Wheeler and Ridley,2004) and the maturation of focal adhesions (Rottner et al.,1999). Furthermore, RhoA can promote cell body retraction at the final stages of the cell migration cycle, through promoting activation of Rho-kinases or Rho-associated protein kinase (ROCK) (Kaibuchi et al.,1999).

In general, a mutual antagonism between Rac-1 and RhoA further promotes the acquisition of a front to rear polarity (Rottner et al.,1999). There are however certain contexts, where Rho-RAC mutual antagonism is not applicable. For example, in migrating neutrophils, Rac-1 activity was required for the detachment of focal adhesions and retraction of the cell body at the trailing edge of the cell (Gardiner et al.,2002). RhoA has also been shown to be involved in early protrusion formation (Pertz et al., 2006; MacHacek et al., 2009). Furthermore, during fibroblast migration, RhoA has been shown, in fact, to activate Rac-1 (Tsuji et al., 2002). Taken together, these findings highlight the complexity of cell polarization during migration.

1.1.4 Collective Cell Migration

Collective cell migration (CCM) describes the coordinated and cooperative movement of cell groups (Friedl and Gilmour.,2009, Rørth 2009). This term encompasses vastly differing modes of multicellular migration. Cells can migrate collectively as tightly coupled epithelial sheets, as observed during the migration of carcinoma cells (Nabeshima et al.,1999) and the migration of the Xenopus mesoderm (Winklbauer et al.,1992). Closely associated clusters can also migrate collectively, such as in the case of the zebra fish line primordium (Haas and Gilmour.,2006). On the other end of the spectrum, cells can migrate as loosely associated streams, communicating with one another through chemical signals, such as during the collective migration of the neural crest (Theveneau & Mayor,2012).

1.1.5 Cell Polarity during Collective cell migration

During collective migration, cells utilize the same principles underlying single cell migration but regulate them on a supracellular scale, to synchronize cell behavior within the cohort (Etienne-Manneville, 2014; Montell et al., 2012). Collectively migrating cell populations are composed of leader cells, located at the front of the group, which dictate the direction of migration and follower cells, which trail behind the leaders (figure 1.1B) (Mayor and Etienne-Manneville.,2016). Similarly, to single cell migration, migration at the multicellular level is usually driven by lamellipodia and filopodia at the front of leader cells, through the activation of Rac-1 and Cdc42. The main modification during collective cell migration, however, is that the cells remain coupled to one another (Friedl at el., 2004; Lecaudey and Gilmour, 2006; Rørth, 2007). As a result, cells can influence the behavior of one another and thereby modulate and refine the collective cell polarity, resulting in the more efficient mode of migration compared to that of single cells.

Different collective cell populations utilize vastly different strategies to obtain a supracellular polarity to drive collective cell migration. The mechanisms which facilitate the establishment of collective cell polarity during neural crest migration will be discussed in later sections.

1.1.6 Molecular structures that govern cell motility

Fundamental to individual and collective cell migration alike, cells utilize a range of actin rich structures to drive locomotion. In the following section, we will describe the assembly and regulation of cytoskeletal structures, which facilitate the acquisition of cell polarity and migration. The dynamic nature of cell substrate adhesions, which couple to cytoskeletal elements to drive migration, will be discussed in section 1.2.

Cell crawling during mesenchymal migration is governed by the assembly and the disassembly of filamentous actin (F-actin). F-actin is a filamentous structure of polymers which assembles from the addition of actin monomers (globular actin; G-actin). The sequential addition of G-actin monomers leads to the formation of double-helix microfilaments that span 7 nm in diameter, with the helix reiterating at 37 nm intervals (Gittes et al.,1993). Actin filaments grow from the preferential assembly of actin monomers at its barbed end and disassemble through the loss of actin monomers from its pointed end.

The organized assembly of actin filaments drives the extension of sheet-like protrusions known as lamellipodia. The assembly of lamellipodial protrusions requires the activation and recruitment of the SCAR/WAVE complex to the plasma membrane (Miki et al.,1998). Recruitment of the SCAR/WAVE complex promotes the activation of actin nucleators, such as the actin-related protein 2/3 (ARP2/3) complex, which facilitate branching of new actin filaments from existing ones. Subsequently, elongators such as formins and ENA/VASP protein promote the extension of

the barbed end of actin filaments (Romero et al.,2004, Bear et al.,2002.). Thus, sustained actin polymerization acts to push the membrane forward. Opposing this, resistance from the membrane, along with myosin contractility furthermore acts to pull the network back, creating a retrograde flow of actin. The retrograde flow of actin (Lai et al., 2008, Wang, 1985) in combination with the coupling of actin filaments to focal adhesions, allows for the extension of the leading edge in order to propel cells forward (Wehrle-Haller and Imhof, 2003, Alexandrova et al., 2008).

Aside from lamellipodia, assembly of filamentous actin gives rise to finer, finger-like structures known as filopodia. Filopodia are arranged into crosslinked parallel bundles by actin binding proteins such as fascin (Welch and Mullins, 2002). Unlike lamellipodia, which primarily form via Arp2/3 mediated branching nucleation, filopodia are postulated to form either from the convergence and bundling of preexisting branched filaments, in a mechanism known as convergent elongation (Svitkina et al.,2003) or from nucleation mediated by formins (tip nucleation) (Faix et al.,2009). Moreover, filopodia and lamellipodia are thought to serve different purposes. Filopodia act as sensors of the extracellular environment, whereas the fan shaped structure of lamellipodia allows them to occupy a large surface during migration. Despite their functional differences however, filopodia, similarly to lamellipodia, undergo actin polymerization at their barbed end, and thereby promote membrane protrusion and retrograde flow (Mellor, 2010, Faix et al., 2009).

In addition to facilitating the formation of lamellipodia and filopodia, actin polymerization leads to the formation of stress fibres. Three types of stress fibres can form in mammalian cells; ventral stress fibres which attach to focal adhesions at both ends, dorsal stress fibres that anchor to a focal adhesion on one end dorsally into a loose actin network, and transverse arcs (form at the base of the lamella, not connected to FAs at either end) (Small et al., 1998). Stress fibres can develop from nascent actin assembly at focal adhesions or by end-to-end linkage of short actin

and myosin bundles to form ventral stress fibres (Hotulainen and Lappalainen., 2006). Crucially, the presence of myosin permits stress fibres to function as contractile structures within the cell which is required for cell motility. Stress fibres also act as a template to facilitate focal adhesion growth and maturation (Choi et al.,2008).

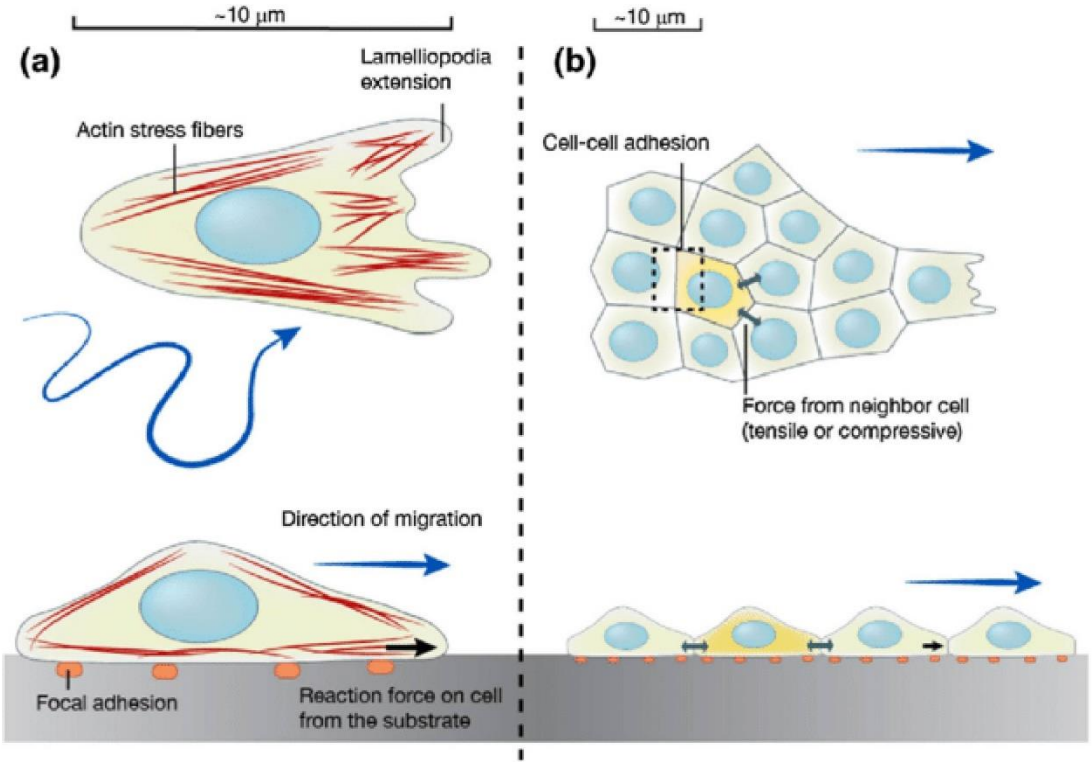

Figure 1.1 Mechanisms of adhesion dependent single and collective cell migration: (A)Single cell migration involves the formation and extension of protrusive structures, such as lamellipodia, at the leading edge, adhesion to the substrate, and rear cell contractility. (B) Similarly to single cell migration, collective cell migration involves polarization of the leader cells. However, cells remain coupled with one another e.g. through cell-cell adhesions, which refine collective cell polarity to facilitate more efficient migration. Reprinted by permission from Springer Nature: Springer Nature, Cellular and Molecular Bioengineering, Mechanobiology of Collective Cell Migration, Saw, T. B., Jain, S., Ladoux, B., & Lim, C. T., Copyright (2015).

1.2 Cell Matrix Adhesions

1.2.1 Introduction to cell matrix adhesions

During mesenchymal migration, cells adhere to the extracellular matrix through integrin-based cell substrate adhesions. Integrin based adhesions are macromolecular complexes composed of a large assembly of signaling molecules, scaffolding and adaptor proteins. Indeed, a study investigating the molecular composition of cell matrix adhesions identified over 150 proteins in the "integrin adhesome", including both integral adhesion components and transiently interacting proteins (Zaidel-Bar et al., 2007a). These cell matrix adhesions serve as a link between the actin cytoskeleton and the ECM and allow forces to be bidirectionally propagated between the cell and the ECM (Choquet et al., 1997, Wang et al.,1993) to elicit a range of cellular responses in addition to cell migration, including changes in gene expression, cell proliferation and survival (Wolfenson et al., 2013). Integrin based cell matrix adhesions are dynamic structures that begin as small punctate structures, known as focal complexes(figure1.2). Subsequently, cell matrix adhesions can grow to form focal adhesions which associate with stress fibres and further mature to fibrillar adhesions that align with ECM fibers before disassembly (Dubash et al., 2009). In this section, we will discuss the dynamic nature of the integrin-based adhesion, describing the sequential assembly and turnover of cell matrix adhesions and outlining their functional roles within the cell.

1.2.2 Cell Matrix Adhesion Assembly, Maturation and Disassembly

Integrin activation

The first step of cell matrix adhesion formation involves the activation of integrins, the primary matrix binding receptor. Integrins are heterodimeric transmembrane proteins, with large multidomain extracellular subunits and small cytoplasmic tails. In their inactive state, they assume a bent conformation, with no connection to the ECM or the actin cytoskeleton. During the process of activation, integrins passage from a bent low ligand affinity state into an extended open conformation with high ligand affinity, by sequentially transitioning through a series of intermediate affinity states. One way in which this can take place is through the binding of integrin receptors to the ECM, in a mechanism known as inside out signaling (figure 1.3). Intercellular signaling from other receptors can activate talin or kindlin and facilitates their binding to the cytoplasmic domain of β integrin subunit at sites of actin polymerization (Watanabe et al., 2008). The engagement of talin and integrin results in the perturbation of a salt bridge between the integrin α and β subunits. This, in turn, triggers a conformational extension of integrin and reveals a higher affinity binding site within the extracellular subunits of integrin for ligands within the ECM (Anthis et al.,2009). Alternatively, integrins can be activated via a mechanism known as "outside in signaling" (figure 1.3). Using a Förster resonance energy transfer (FRET) based technique, it was shown that upon binding to the extracellular matrix, integrin alpha and beta subunits undergo conformational changes, leading to the extension of the cytoplasmic tail of integrins (Kim et al.,2003). The unraveling of the cytoplasmic domain leads to the binding of adapter proteins talin and kindlin (Calderwood et al.,2002, Margadant et al.,2013), which in turn triggers the crosslinking of integrin to the actin cytoskeleton.

Integrin coupling to cytoskeleton and clustering

Upon ligand binding, integrins become preferentially coupled to the actin cytoskeleton and begin to cluster. The binding of adaptor proteins such as talin and kindlin facilitates linkage to the actin cytoskeleton and integrin clustering. Cytoskeletal linkage is further reinforced by the talin mediated recruitment of other adaptor proteins such as vinculin (Burridge and Mangeat, 1984; Johnson and Craig, 1995) alpha actinin(Otey et al.,1990) and paxillin (Liu et al., 1999)

Assembly of focal complexes

Integrin clusters constitute the earliest detectable adhesive structures. Such adhesions have been detected as spots, approximately 100nm in diameter (Geiger et al.,2009), and have been described to withstand forces no greater than 2pN (Jiang et al.,2003). Whilst earliest detectable structures have been proposed to consist of two α/β integrins linked to a talin dimer(Jiang et al.,2003), vinculin, p130cas, paxillin and low levels of Focal Adhesion Kinase (FAK) have also been found within focal complexes (Zaidel-bar et al .,2003, Donato et al.,2010). Focal complexes are found at the tip of the lamellipodial protrusions and their assembly is reliant on the fast actin retrograde flow within the lamellipodium. Hence, formation of such adhesion sites is dependent on Rac-1 activity (Nobes et Hall,1995). It is important to note that focal complexes are transient structures which either undergo rapid turnover or mature into focal adhesions (Zaidel-Bar et al., 2003).

Maturation of focal adhesions

The maturation of focal adhesions is dependent on their assembly and association to actomyosin stress fibres, mediated by mdia1 (Riveline et al.2001), alpha-actinin and myosin II (Choi et al.,2008). During maturation, adhesions elongate centripetally along the stress fibres, generated within the llamelipodium-llamela axis, forming structures of approximately 1 µm in width and 3-5µms in length (Zaidel-Bar et al.,2007b). The evolution of focal complexes into focal adhesions is

also accompanied by changes in the molecular composition of the adhesion proteins. Maturing focal adhesions have increased levels of paxillin, vinculin and FAK, with respect to focal complexes (Zaidel-bar et al.,2003). Additionally, they begin to express zyxin, which is not observed in focal complexes. Furthermore, maturation of focal adhesions is accompanied by conformational changes in many constituent proteins such as p130cas (Sawada et al.,2006) and vinculin (Grashoff et al.,2010) which unveil to expose further binding sites for adaptor proteins and increased levels of tyrosine phosphorylation.

Fibrillar adhesions

Focal adhesions can further mature into fibrillar adhesions in a manner dependent on Rho-GTPases. Fibrillar adhesions appear as long streaks or an array of dots which bind to fibronectin via integrin $\alpha 5_{\beta}1$ (Pankov et al.,2000). Rather than connecting to stress fibres, they are associated with thin actin cables which are linked by the protein tensin (Zamir et al.,2000). Notably, fibrillar adhesions have lower levels of tyrosine phosphorylation than focal adhesions. Fibrillar adhesions are required for fibronectin matrix assembly.

Disassembly

Cell substrate adhesions are dynamic structures which undergo turnover over time. Focal complexes can undergo disassembly, at the leading edge of the cell, during a transient turnover phase. Alternatively, mature adhesions within the retracting tail can disassemble by a phenomenon called focal adhesion sliding, during which adhesive components move inwards towards the centre of the cell via a Rho/myosin dependent mechanism (Ballestrem et al.,2001). At the molecular level, many signaling pathways have been described to promote focal adhesion disassembly. Below, we outline a few of the main mechanisms leading to adhesion disassembly. Microtubules can be targeted to early focal complexes at the cell front and trailing focal adhesions at the back of the cell, to promote adhesion disassembly (Kaverina et al.,1999). Indeed, it has been

shown that the induction of microtubule depolymerization through nocodazole results in an inhibition of adhesion disassembly (Ezratty et al.,2005). Microtubules can trigger cell matrix adhesion disassembly through negative regulation of actomyosin contractility, by localizing to focal adhesions and promoting the relaxation of actin bundles (Kaverina et al.,1999). Alternatively, they can facilitate disassembly through the modulation of Rho GTPase signaling pathways (Rooney et al.,2010). For example, microtubule mediated disassembly of adhesions was found to be dependent on the Rac GEF Tiam (Rooney et al,2010). Another potential way in which microtubules could affect adhesion disassembly is through their role in cargo transport from the cell matrix adhesions. For example, microtubules could promote disassembly through clathrin mediated endocytosis of integrin (Ezratty et al.,2009). As well as transporting cargo away from cell matrix adhesions, microtubules can trigger disassembly by transporting cargo to adhesive sites. In line with this, the microtubule motor protein kinesin-1 has been implicated in the regulation of microtubule mediated cell matrix adhesion disassembly (Krylyshkina et al., 2002). It is thought that kinesin-1 may enable the delivery of disassembly factors to adhesion sites along microtubules.

Fak-Src signaling is another mechanism by which focal adhesion disassembly is mediated. Indeed, the loss of function of either Fak or Src resulted in perturbed focal adhesion disassembly and a reduction in cell motility (Webb et al., 2004). Fak-Src signaling is believed to promote focal adhesion disassembly through localized inhibition of RhoA (Ren et al.,2000) which stabilizes focal adhesions. Fak-Src signaling at cell matrix adhesions can modulate the activity of extracellular signal regulated kinase (ERK) which subsequently phosphorylates myosin light chain kinase to trigger actomyosin contractility (Webb et al.,2004). Furthermore, Fak-Src signaling has been suggested to be required for microtubule mediated cell matrix adhesion disassembly (Ezratty et

al.,2005). The GTPase dynamin is thought to be targeted to cell matrix adhesions through an interaction with FAK

1.2.3 Cell Matrix adhesions as mechanosensors

Integrin based adhesions serve as a link between the extracellular matrix and the actin cytoskeleton, allowing forces to be propagated bidirectionally. Moreover, cell matrix adhesions themselves have been demonstrated to act as mechanosensitive structures. The application of mechanical stimuli to immature, punctate adhesions at the leading edge using a micropipette promoted the formation of mature focal adhesions (Riveline et al., 2001). Aside from intact cells, exerting force on Triton treated cytoskeletons resulted in recruitment of new adhesion molecules (Sawada and Sheetz, 2002), highlighting the role of focal adhesions in mechanosensation. In fact, several components of cell matrix adhesions themselves have been shown to act as mechanoresponsive elements.

Integrins play an essential role in mechanosensing at adhesion sites. Integrins can serve as primary force transducers or can act indirectly to transduce force to other mechanosensitive elements. One way by which integrins respond to the application to force is through altering their aggregation state. Indeed, the aggregation and inward movement of integrin clusters is dependent on actomyosin contractility (Yu et al.,2011). Additionally, simulations have indicated that mechanical force may promote the conversion of β-integrin from an inactive to an active conformational state (Puklin-Faucher et al., 2006). This was further supported by studies in NIH3T3 cells which assessed levels of the high affinity active conformation of integrin $\alpha_v\beta_3$ heterodimer upon cell stretching, using an engineered antigen binding fragment (FAB) that recognizes active integrin $\alpha_v\beta_3$ (Katsumi et al.,2005). The results indicated a conformational

transition from a low affinity integrin $\alpha_v\beta_3$ state to high affinity state resulting in the enhanced binding of the integrins to the extracellular matrix as described above. Furthermore, through experiments performed on cells adhering to optically trapped fibronectin beads to which a restraining force was applied, it was found that increasing the force exerted on the cells strengthened the integrin cytoskeleton linkage (Choquet el al.,1997). This reinforcement of the integrin actin cytoskeleton linkage is mediated by force dependent conformational changes, undertaken by molecular components downstream of integrins.

Integrins make a direct linkage with the actin cytoskeleton via talin. Upon the exertion of mechanical stimuli on individual talin molecules *in vitro* (del Rio et al., 2009), the protein was observed to unfold. Notably, the application of force resulted in the unveiling of cryptic binding sites for the actin-binding protein vinculin. Taken together, this implied that mechanotransduction at cell substrate adhesion takes places through exposing cryptic vinculin binding sites in the talin upon the exertion of mechanical stimuli (del Rio et al., 2009). Moreover, the targeting of vinculin to cell matrix adhesions is dependent on force (Galbraith et al., 2002; Grashoff et al., 2010). Indeed, recruitment of vinculin to cell matrix adhesions increased when increasing magnitudes of force were applied to cells adhering to optically trapped fibronectin coated beads (Galbraith et al., 2002)

A number of other adaptor proteins have been shown to act as mechanoresponsive elements at cell matrix adhesions. One such protein found in cell matrix adhesions is filamin A. Filamin A binds to the cytoplasmic tail of integrin. Upon the exertion of mechanical force, filamin A increasingly binds to the beta subunit of integrin (Ehrlicher et al.,2011). Furthermore, a subset of adaptor proteins provides a scaffold for phosphorylation events upon mechanical stretching. Stretching of p130cas increases its susceptibility to Src phosphorylation (Sawada et al., 2006), likely by revealing

cryptic tyrosine phosphorylation sites. As the focus of this thesis is on CAS proteins, this will be discussed in greater depth in section 1.3.

Mechanotransduction via cell matrix adhesions can be explained via the molecular clutch model (Chan et Odde, 2008). The molecular clutch model postulates that integrin-based adhesions are coupled to the actin cytoskeleton and the myosin driven actin retrograde flow. This clutch facilitates the growth of lamellipodial protrusions and enables contractile forces to be transmitted from the cytoskeleton to the cell substrate. Molecular clutch dynamics differ on substrates of different stiffnesses and this is thought to dictate the cell's ability to sense and respond to substrate stiffness. On stiff substrates, cells constantly exhibit frictional slippage during which actin filaments slide relative to the substrate. This is believed to manifest in higher rates of actin retrograde flow and lower traction forces. By contrast, cells adhering to softer substrates display load-and-fail dynamics, during which F-actin moves concomitantly with the compliant substrate until coupling failure. This is predicted to result in slower F actin retrograde movement and higher traction forces.

Alternative models of mechanotransduction, such as the active gel theory, allude to a more global mechanism of mechanosensing, rather than local rigidity sensing mechanisms postulated by the molecular clutch model. In a model by Trichet et al, actin stress fibres were proposed to act as a global tension sensor (Trichet et al.,2012). Actin cytoskeleton shifts from an isotropic phase on soft substrates to a nematic phase on stiff substrates. In this model, the actin cytoskeleton behaves as a fluid-like material on compliant substrates and as a solid-like material on stiffer ones. The solid-like behaviour observed on stiffer substrates is accompanied by a transition to a large-scale order of actin filament alignment and higher cytoskeletal tension.

In summary, transduction of mechanical stimuli into biochemical signals involves the various mechanosensitive components that act at various length-scales and timescales. Additional work must be done to further consolidate the described models of mechanotransduction and in understanding the interplay between different mechanosensitive units.

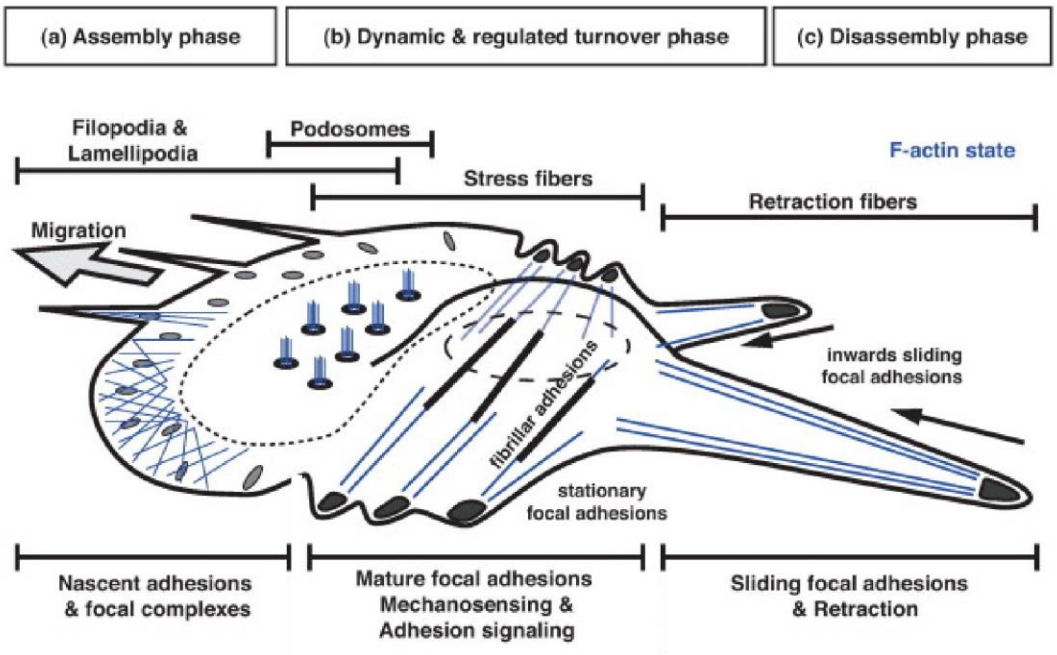

Figure 1.2 Cell Matrix adhesion lifecycle: A schematic to show the assembly of focal complexes, and maturation and diassembly of focal adhesions. Reprinted from Current Opinion in Cell Biology, 24(5), Wehrle-Haller, B , Assembly and disassembly of cell matrix adhesions, pp.569-581, Copyright (2012), with permission from Elsevier.

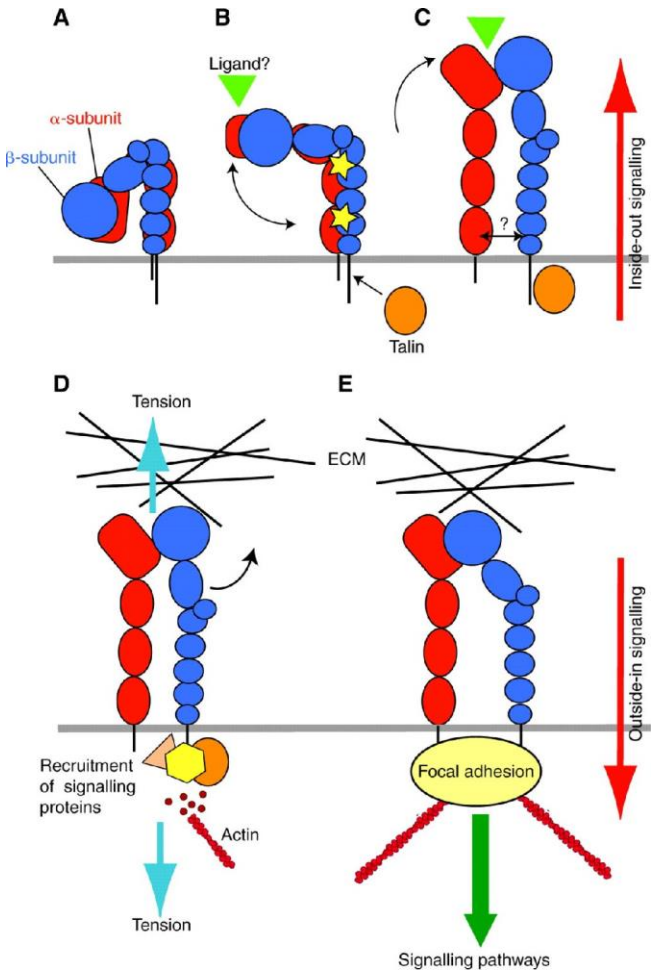

Figure 1.3 Mechanisms of integrin activation: (A-C) Inside out signalling: Adaptor proteins such as talin can bind to the cytoplasmic domain of β integrin subunit at sites of actin polymerization. The binding of talin to integrin perturbs a salt bridge between the integrin α and β subunits. exposes a higher affinity binding site within extracellular subunits of integrins for ligands within the ECM. **(D-E)** Outside in signaling**:** Binding to the extracellular matrix enables integrin alpha and beta subunits to undergo conformational changes, leading to the extension of the cytoplasmic tail of integrins, the recruitment of signaling proteins, the subsequent linkage to the actin cytoskeleton. Reproduced from Askari et al., 2009, Journal of Cell Science with permission from COMPANY OF BIOLOGISTS LTD.

1.3 The Crk Associated Substrate (CAS) proteins

1.3.1 Discovery of CAS family proteins

A crucial component of the integrin signaling pathway is the Crk Associated substrate (CAS) family of adaptor proteins (Tikhmyanova et al.,2010) Whilst they possess no enzymatic activity, this protein family functions as scaffolding proteins within cell-substrate adhesions. CAS proteins are major substrates for Src tyrosine kinases and have been shown to regulate a number of cellular responses including cell migration, proliferation and cell transformation (Tikhmyanova et al.,2010). Whilst only one Cas family member is present in lower vertebrates, chordates, and insects, corresponding to p130cas (Singh et al., 2008), four CAS family members proteins were identified in higher vertebrates, including *Xenopus laevis.* The CAS family is comprised of p130 Crk-associated substrate, also known as Breast cancer anti-estrogen resistance 1 **(p130cas/BCAR1)** (Sakai et al.,1994), Neural precursor cell expressed developmentally down-regulated 9; also called Human enhancer of filamentation 1 or Cas-L **(Nedd9/HEF-1/Cas-L)** (Law et al.,1996 Minegishi et ak.,1996), Embryonal Fyn Substrate or Src interacting protein **(Efs/Sin**) (Ishino et al.,1995. Alexandropoulos and Balitmore., 1996), and the fourth member, known as HEF1-Efs-p130CAS-like protein or Cas scaffolding protein family member 4 **(HEPL/Cass4)** (Singh et al.,2008).

P130cas was the first member of the CAS family to be discovered as a hyper-tyrosine-phosphorylated protein in v-src and v-crk transformed cells (Sakai et al.,1994). Subsequently, Nedd9/HEF-1/Cas-L was identified by two independent studies. HEF-1 was identified in a screen for human proteins involved in the regulation of cell polarity and in the induction of filamentous

budding phenotype *in S.cerevisae (*Law et al.,1996). Independently in lymphocytes, the cDNA of a highly tyrosine phosphorylated protein upon integrin ligation was cloned and identified as Cas-L (Minegishi et al.,1996). The third member of the CAS family, Efs/Sin, was also detected and characterized from two separate cDNA screens in mouse embryonal libraries; one searching for proteins possessing an SH3-interacting domain (Ishino et al.,1995) and the other identifying proteins which interact with the Src SH3 domain (Alexandropoulos and Balitmore., 1996). The fourth and final member, HEPL or Cass4, was most recently identified following an *in silico* screening for CAS related sequences from an evolutionarily diverse group of organisms(Singh et al.,2008). The gene of the novel CAS family member was subsequently cloned and its function in cell spreading and migration was characterized. However, since the seminal discovery of Cass4 by Singh et al., very few follow up studies have attempted to elucidate its functional role. Hence, whilst Cass4 is the focus of this thesis, in this section we will provide a more general discussion on the structure of CAS proteins and their functions in signal transduction.

1.3.2 CAS protein domain structure

CAS proteins contain several protein interaction domains which are highly conserved. All members of the CAS family possess a highly conserved N terminal Src homology 3 (SH3) domain which facilitates interactions with proline rich motif containing proteins, a central substrate domain containing multiple YxxP tyrosine motifs that are phosphorylated by Src and Src related kinases , a serine rich region, and a C terminal region containing a conserved “Cas-family C terminal homology” (CCH) domain. Furthermore, all CAS protein family members, apart from Cass4, possess a Src binding domain containing proline rich and/or YDYVHL motifs which bind the

SH3 and SH2 domains of Src respectively. The function of each domain will be discussed in more depth in this chapter.

Homologous CAS proteins found in *Xenopus Laevis* have retained all of the functional domains and binding motifs of mammalian CAS proteins. The secondary structure of the CAS homologues in *Xenopus Laevis* is detailed in the figure 1.4.

1.3.3 CAS protein expression in *Xenopus laevis*

Homologous proteins for all four CAS family genes have been detected in *Xenopus laevis.* However, limited data regarding the expression patterns is currently available. No information is available with regards to the expression patterns of EFS. Expression of p130cas has been detected as early as blastula stages, within the animal hemisphere (Green et al.,2016). An *in-situ* hybridization, against p130cas at neurula stages indicated that p130cas is expressed in the epidermis and anterior neural plate. At later tailbud stages expression is restricted to the brain, eye branchial arches and propnephros. *In situ* hybridizations of Nedd9 reveal that the mRNA is expressed in the presomatic mesoderm at neurula stages (Pollet et al.,2005). At later tailbud stages, expression is observed within the trigeminal ganglion and the heart. Expression of Cass4, also known as Xenopus C*as/*HEF-*Like*-1 protein (X-chef-1), is observed in the dorsal lip at gastrula stages (Meek et al.,2004). At neurula stages, Cass4/X-chef-1 is expressed specifically within the neural crest.

1.3.4 CAS proteins as docking proteins

The ability of CAS family proteins to function as signal transducers relies on its correct localization and activation. The N terminal SH3 and CCH domain function predominantly to target CAS proteins to cell matrix adhesions (Donato et al.,2010). Subsequent to adhesion targeting, CAS proteins become activated by tyrosine phosphorylation of the substrate domain via Src and Src related kinases. This creates docking sites for effector proteins which trigger the activation of downstream signaling cascades. In this section, we will discuss further the mechanisms of CAS targeting to adhesion site and CAS signaling.

Cas targeting

In non-adherent cells, CAS proteins localise to the cytoplasm. Upon integrin engagement, CAS proteins re-localize to cell matrix adhesions (Donato et al.,2010, Law et al.,1996). Whilst the dynamics of cell matrix adhesion targeting have not been very well described, in the case of p130cas, it is observed to localize to early focal complexes at the leading edge of cells, reach peak levels in mature focal adhesions and dissociate from focal adhesions in the later stages of their disassembly (Donato et al.2010). Furthermore, through FRAP experiments, it was observed that p130cas makes transient contacts with its binding partners and exists in a highly mobile fraction of focal adhesions relative to the adhesion marker paxillin.

Targeting of CAS proteins to integrin-based adhesions is achieved via the SH3 and C-terminal domain. Notably deletion of either SH3 or C terminal domains resulted in a decrease in localization to paxillin positive cell matrix adhesions, with a deletion of both domains resulting in a complete exclusion of CAS from cell matrix adhesions (Donato et al.,2010). The dual targeting mechanism

of CAS proteins plays a crucial role in signal transduction and mechanotransduction, allowing for the mechanical extension of the substrate domain and the exposure of cryptic tyrosine residues, which become phosphorylated. In the following section, the known interactions of the cell matrix adhesion anchoring domains are detailed.

SH3 domain

All members of the CAS family possess a highly conserved N terminal SH3 domain which facilitates interactions with proline rich motif containing proteins. One of the most crucial protein-protein interactions facilitated by the SH3 domain is with protein tyrosine kinase FAK (Minegishi et al.,1996, Singh et al.,2008), which plays a critical role in CAS mediated signal transduction. In non-adherent cells FAK assumes an autoinhibited conformation. Integrin activation and clustering leads to a release of the autoinhibitory interactions of FAK, possibly through the interaction of the FAK FERM domain with the β cytoplasmic tail of integrin (Cooper et al.,2003). This results in FAK autophosphorylation at residue Y397 which facilitates the recruitment of Src kinase (Ruest et al.,2001). Src kinase, in turn phosphorylates the substrate domain of the CAS proteins that are bound to FAK.

Additionally, CAS proteins interact with other tyrosine kinases such as PTK2B (Astier et al.,1997), as well as phosphatases such as PTP-PPEST (Garton et al., 1997), responsible for the dephosphorylation of CAS proteins. The SH3 domain of p130cas has also been reported to bind guanosine exchange factor C3G (Kirsch et al.,1999).

CCH domain

The C terminal homology domain, which contains a helix-loop-helix motif, is the second highest conserved domain within CAS proteins. This domain is required for cell matrix adhesion targeting and anchoring, although it still remains unclear as to what interactions facilitate this. It has been suggested that p130cas and Nedd9 can form homodimers using the CCH domain (Braniš et al 2017, Law et al.,1999). P130cas and Nedd9 have also been shown to interact with other signaling molecules such as novel SH2-containing proteins (NSP) which facilitate connections to receptor tyrosine kinase signaling. Little however is known with regards to the interactions of Efs and Cass4 in this region.

Cas signaling

Src binding domain

All CAS protein family members, apart from Cass4, possess a Src binding domain, containing proline rich and/or a YDYVHL motif. Phosphorylation of the YDYVHL motif results in the formation of a binding site for the SH2 domain of Src kinase (Tachibana et al.,1997), which in turn phosphorylates the substrate domain. Furthermore, proline-rich motifs found in p130cas and Efs (Alexandropoulos and Baltimore, 1996), similarly promote the binding and phosphorylation by Src family kinases, via interactions with the SH3 domain of Src kinase (Pellicena and Miller, 2001). Whilst Cass4 is the only family member lacking both Src kinase binding motifs, it has still been shown to undergo phosphorylation by Src kinase, implying that compensatory interactions between Cass4, FAK, and Src are sufficient to facilitate this process (Singh et al.,2008).

The substrate domain

On the carboxy terminal of the SH3 domain, CAS proteins contain a substrate domain which contains a series of tyrosine motif sequence, which can be phosphorylated by Src or Src related kinases. Tyrosine phosphorylation of such YxxP motifs has been largely validated using mass spectrometry phosphoproteomic approaches (Rush et al.,2005). Phosphorylated tyrosine motifs form binding sites for SH2 domain containing proteins. For example, Crk and Nck adaptor proteins have been identified as direct CAS binding partners that interact with SD phosphotyrosine motifs via their SH2 domains (Sakai et al., 1994, Schlaepfer et al., 1997). These proteins regulate the activity of downstream signaling associated with cell motility and invasion. The SH2 domain of Src-homology 2 containing inositol phosphatase-2 (SHIP-2) and growth factor receptor bound 2 (Grb2) have also been shown to bind to phosphorylated tyrosine motifs within the substrate domain of p130Cas (Wang et al., 2000).

The serine rich domain

In addition to tyrosine phosphorylation, CAS proteins can be serine phosphorylated (Schlaepfer et al., 1997), but significantly less is known about the function of the serine rich domain. Serine phosphorylation has been reported to facilitate an interaction of p130cas with 14-3-3 (Garcia-guzman et al.,1999), however, direct interacting proteins have not been identified for the serine rich domain of other CAS proteins.

1.3.5 Functional roles behind CAS protein signaling

Cell migration

CAS family proteins have been described as important regulators of cell migration in diverse contexts ranging from cancer to development. Overexpression of the p130cas is sufficient to activate downstream signaling pathways, associated with cell motility, to thereby promote migration (Klemke et al.,1998). Overexpression of Nedd9, in some contexts, has been described to serve a pro-migratory function (Natarajan et al.,2006, Fashena et al.,2002) and an anti-migratory function in others (Simpson et al.,2008), which may suggest that its functional role is tissue specific. Although less well characterized, one study has suggested that Cass4 plays a role in cell migration (Singh et al.,2008). Notably, loss of Cass4 induced a bimodal effect on cell motility, resulting in a subset of cells exhibiting a lower velocity and a subset of cells exhibiting a higher velocity than control cells.

Regulation of cell migration by CAS proteins is primarily initiated when CAS proteins localise to cell matrix adhesions and become phosphorylated at specific tyrosine motifs within the substrate domain. Tyrosine phosphorylation leads to the activation of signaling cascades to promote migration, through mediating effects on cytoskeletal rearrangements, membrane protrusion formation and cell matrix adhesion dynamics. In line with this, a number of promigratory signaling cascades have been so far identified downstream of CAS proteins p130cas and Nedd9. As described above, phosphorylated tyrosine motifs can form binding sites for CRK adaptor proteins (Klemke et al.,1998.) These adaptor proteins can subsequently form a complex with GDP-exchange factors such as C3G (Ohashi et al.,1998), DOC3 (Sanz-Moreno et al.,2008) and DOCK180

(Kiyokawa et al.,1998), to in turn activate Rac-1. Activated RAC induces actin polymerization at the leading edge of cells as previously described (Ridley et al.,1992). A Crk- C3G complex can lead to the activation of small GTPase, RAP1 (Sawada et al.,2006), thereby activating an additional promigratory pathway. Rap-1 can promote migration through promoting integrin activation and signaling and through regulation of cytoskeletal arrangements.

Aside from the CAS-CRK-C3G/DOCK pathway, additional CAS-dependent promigratory signaling pathways have also been identified. In addition to facilitating interactions with GDP exchange factors such as C3G and DOCK, CAS proteins also interact with GTPase activating proteins. For example, Nedd9 promoted the migration of trunk neural crest through its association with Rho Gap DLC1, resulting in the asymmetric distribution of RhoA and the acquisition of a front to rear polarity (Liu et al.,2017). CAS proteins can also regulate migration through interactions with other cell matrix adhesion proteins. For example, both P130cas and NEDD9 can associate with Zyxin family proteins, including zyxin, Ajuba, and TRIP6 to promote cell motility (Pratt et al.,2005, Yi et al.,2002). Zyxin family member Ajuba has been shown to bind to p130cas and activate Rac-1(Pratt et al.,2005). As well as regulating signaling cascades which influence cell motility on a shorter time scale, a zyxin CAS interaction can facilitate longer term gene expression changes. Notably, Zyxin has been shown to form a complex with p130cas and nucleocytoplasmic transcription factor, CIZ/NMP4/ZNF384 (Janssen et al.,2006). Given that this transcription factor regulates the expression of matrix metalloproteinases (Nakamoto et al.2000), such an interaction is likely to promote cell migration. In a similar fashion, induced overexpression of Nedd9 resulted in an upregulation of genes associated with promotion of cell motility, including myosin light chain kinase (MLCK), Nck interacting kinase (NIK), ROCK and matrix metalloproteases (Fashena et al.2002). Taken together, CAS proteins can promote migration through the regulation of a multitude of signaling pathways.

Mechanotransduction

As cell matrix adhesions serve as a mechanosensitive hub of the cell and as CAS proteins are important components in focal adhesion signaling, it is likely that CAS proteins have a role in the transduction of mechanical cues into biochemical signals. In the case of p130cas, the substrate domain has been described to be an intrinsically disordered domain. The substrate domain of p130cas has been shown to unfold and become increasingly phosphorylated in response to external mechanical cues such as the application of stretch (intact cells and purified proteins), leading to the recruitment of a Crk-C3G complex and the subsequent activation of RAP-1, demonstrating its potential to act as mechanosensor/transducers (Sawada et al., 2006). P130cas has further been implicated to have a role in rigidity sensing (Kostic and Sheetz.,2006). P130Cas is localises to the leading edge of cells and becomes increasingly phosphorylated in the substrate domain with increasing substrate stiffness. More recently, the requirement of p130cas for stretch-induced reorientation of cells was demonstrated in a manner dependent on the phosphorylation of tyrosine residues present in the substrate domain (Niediek et al., 2012).

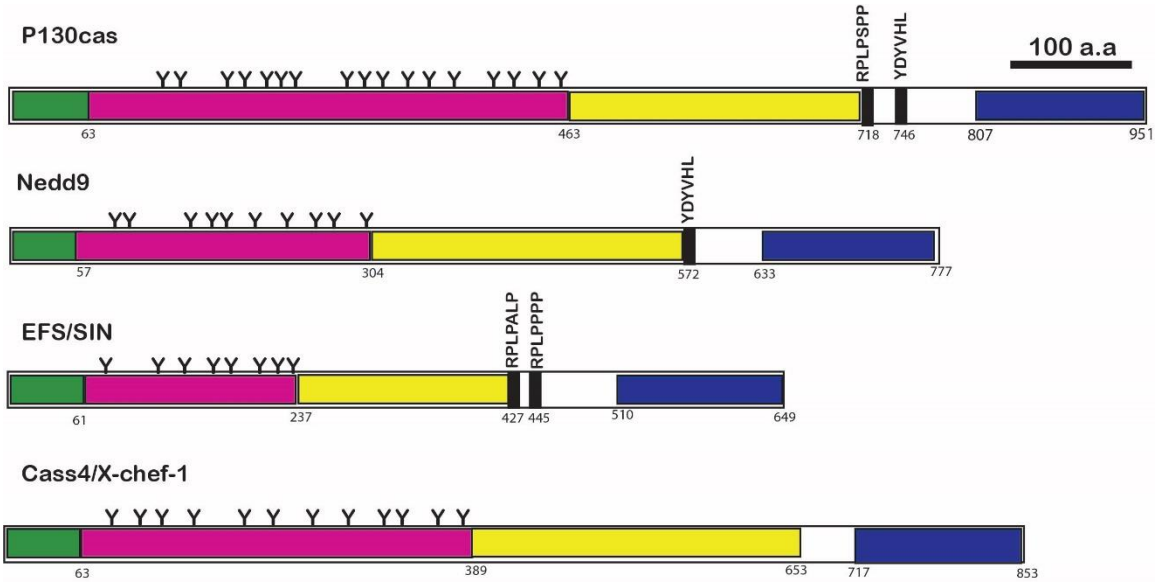

Figure 1.4 Diagram of Cas family member domain structures: The key interaction domains of the four Cas family members in *Xenopus laevis* have been depicted to scale. P130cas (Uniprot ID: Q6PAF8) is 951 amino acids long and possesses an N-terminal SH3 domain (GREEN) aa 7-63; a substrate domain (PINK) aa 63-463 with 18 YxxP motifs ; a serine rich region (YELLOW) aa 463-718; a bipartite Src-binding domain (BLACK) with a proline-rich motif RPLPSPP beginning at aa718, and a YDYVHL beginning at aa 746; and a Cas-family C-terminal homology (CCH) domain (BLUE) aa 807-951.Nedd9 (Uniprot ID: A0A1L8FXZ9) is 777 amino acids and possesses an SH3 domain aa 7-57; an SD aa 57-304 with 10 YxxP motifs; a serine rich region aa304-572; a SBD domain containing YDYVHL SH2 binding motif beginning at aa572; and a CCH domain aa 633-777. Efs/Sin (Uniprot ID: A0A1L8HPK8) is 649 amino acids and contains an SH3 domain aa 9-61; an SD aa 61-237 with 8 YxxP tyrosine motifs; a serine rich region aa237-427; a SBD with two proline-rich motifs RPLPALP beginning at aa427 and RPLPPPP beginning at aa 445,and a CCH domain aa 510-69. Cass4/ X-chef-1 (Uniprot ID: Q6RCJ1) is 853 amino acids and contains an SH3 domain aa 15-63; an SD aa 63-289 12 YxxP motifs, a serine rich region aa.389-447 and a CCH domain aa 719-853.

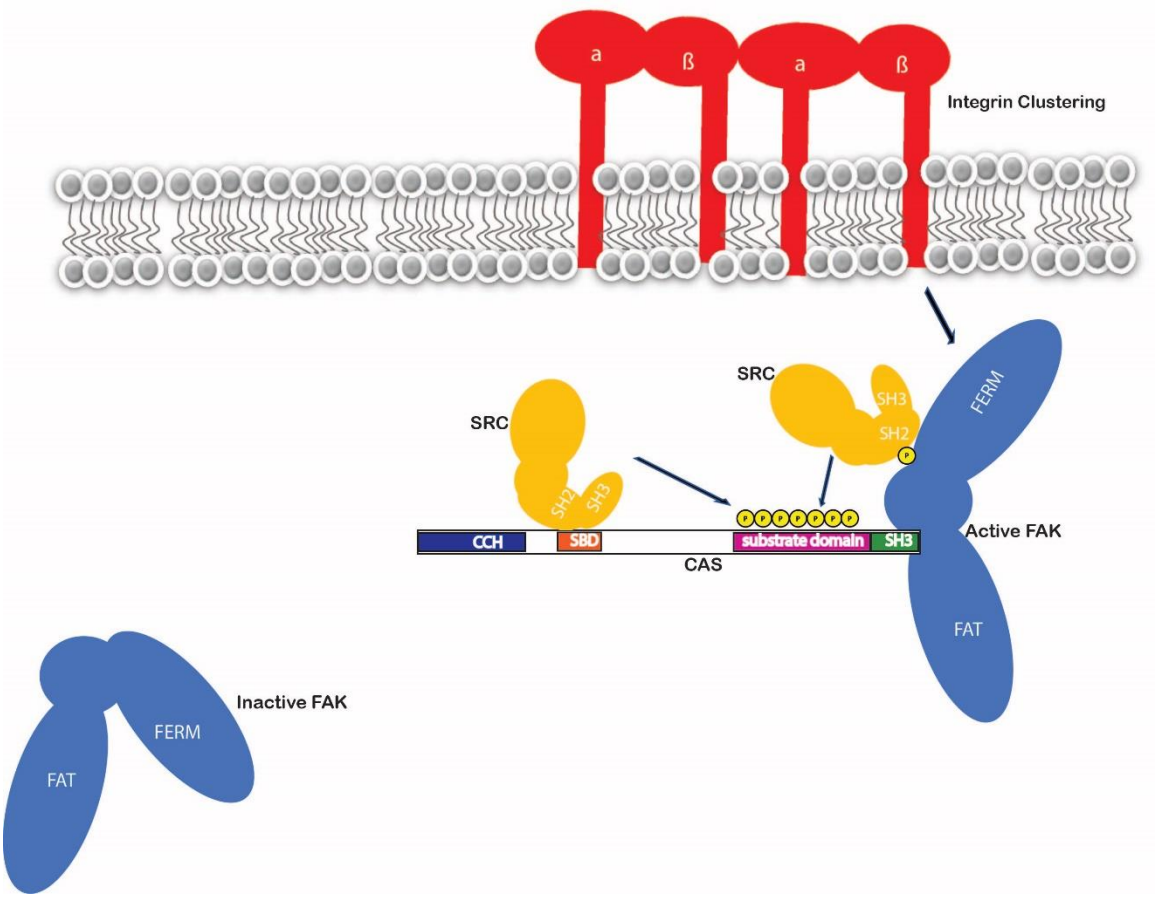

Figure 1.5 The CAS/FAK/SRC signaling complex: In non-adherent cells FAK assumes an autoinhibited conformation. Integrin activation and clustering leads to a release of autoinhibitory interactions, possibly through the interaction of the FAK FERM domain with the β cytoplasmic tail of integrin. This results in FAK autophosphorylation at residue Y397 which facilitates the recruitment of Src kinase (Ruest et al.,2001). Src kinase, in turn phosphorylates the substrate domain of the CAS protein that are bound to FAK. Src can also be activated through binding to the SBD, in all CAS family proteins, apart from Cass4.

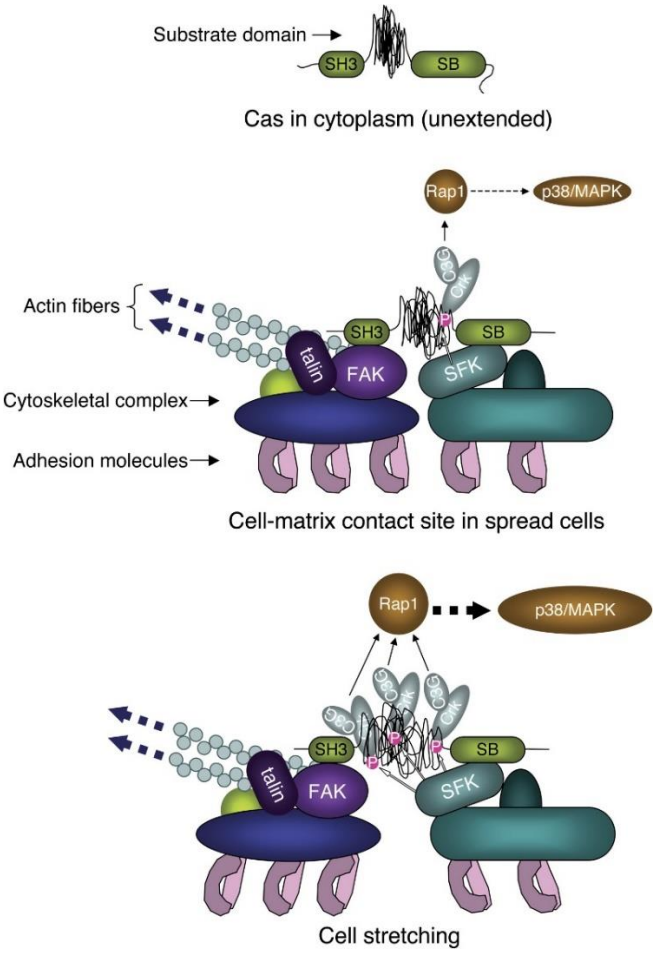

Figure 1.6 CAS proteins in mechanotransduction: The substrate domain of p130cas assumes a folded conformation in the cytoplasm. Once p130cas localizes and anchors to cell matrix adhesions, it becomes partially unfolded and weakly phosphorylated. Upon the application of mechanical stimuli, the substrate domain unfolds to a larger extent and is increasingly phosphorylated, resulting in the recruitment of adaptor proteins and the activation of downstream signaling cascades. Reprinted from Cell, 127(5), Sawada, Y., Tamada, M., Dubin-Thaler, B. J., Cherniavskaya, O., Sakai, R., Tanaka, S., & Sheetz, M, Force Sensing by Mechanical Extension of the Src Family Kinase Substrate p130Cas. 1015–26., Copyright (2006), with permission from Elsevier.

1.4 The neural crest

1.4.1 Introduction

The neural crest is a transient, highly motile cell population, specific to vertebrate embryos. Commonly described as the fourth germ layer (Gans and Northcutt,1983), the evolution of this stem cell population is considered to be a crucial event in distinguishing vertebrates from other metazoans. The neural crest was first discovered by WIlheim His, who referred to the cell population as "Zwischenstrang" or intermediate chord in his treatise on the topic written in 1868. Since its initial discovery in the 19th century, great advances have been made in elucidating the role of this stem cell population during development.

The neural crest cell population is induced during gastrulation and resides between the epidermis and the mesoderm. Subsequent to induction, the neural crest dissociates from the neural tube in a process known as delamination and undergoes an epithelial to mesenchymal transition (EMT), before migrating in a directed fashion in collective streams. After migration, the neural crest differentiates to establish a diverse cell lineage (reviewed in Theveneau and Mayor,2012). It is important to note that the neural crest is a heterogeneous stem cell population, composed of cranial or cephalic neural crest (NC), truncal, vagal and sacral NC and cardiac subpopulations (Le Dourain and Kalcheim.,1999). As such, the fate of the progenitor cells is dependent on the subpopulation to which they belong to. The cephalic neural crest, the primary focus of this thesis, migrates in a dorsoventral direction into the pharyngeal arches, differentiating to generate a number of craniofacial features including cartilage, bone, cranial neurons, glia and connective

tissue (Le Dourain and Kalcheim.,1999). The truncal neural crest either move in a dorsolateral direction over the ectoderm, giving rise to the melanocytes or in a ventrolateral direction, to differentiate to the dorsal root ganglion neurons or the cells of the adrenal medulla (Le Dourain and Kalcheim.,1999). The vagal and sacral neural crest differentiate to form the enteric ganglia of the gut.

1.4.2 Neural crest induction

The neural crest is induced at the border of the neural plate, through the interaction of neural ectoderm and non-neural ectoderm at blastula stages (Selleck and BronnerFraser.,1995, Mancilla and Mayor., 1996, Sauka-Spengler and Bronner-Fraser., 2008). The induction of the neural crest is a two-phase process, reliant on extracellular molecules which are produced by the epidermis, neuroepithelium and underlying mesodermal tissue. Briefly, in *Xenopus*, the initial induction phase, involves the establishment of a bone morphogenic protein (BMP) signaling gradient along the dorso-ventral axis of the embryo. An intermediate level of BMP signaling is required for induction of the neural crest itself (Marchant et al., 1998, Nguyen et al., 1998). In combination with the activity of other signaling molecules, including Wnt, fibroblast growth factor (FGF), Retinoic Acid and Notch, a genetic cascade is triggered which is required for the initial specification of the neural crest. A network comprising of genes including *Msx*, *Dlx*, *Ap2*, *Pax3*, *Zic* and *cMyc* is activated, which functions to define the neural plate territory (Tribulo et al., 2003, Woda et al., 2003, Luo et al., 2002). In the second phase, subsequent to neural crest specification, genes involved in cell maintenance begin to be expressed in the presumptive territory of the neural crest. This includes transcriptions factors of the *Snail* family (Mayor et al.,2000, LaBonne and Bronner-Fraser, 2000, del Barrio and Nieto, 2002, Shi et al., 2011). Expression of Snail

transcription factors leads to further activation of genes, including *FoxD3*, *Id3* and *Twist,* which serve to maintain the cell population through inhibition of proliferation and apoptosis (Aybar et al.,2003). Thus, in this way, the combined expression of cell specification and cell survival genes in the neural crest paves the way for their subsequent delamination, migration and differentiation.

1.4.3 Delamination

After induction and specification, the neural crest undergo an epithelial to mesenchymal transition and depart from their original niche, through delamination from the neural tube. It should be noted that these processes are distinct from one another. Delamination, in this instance, refers to the process by which the neural crest dissociates from the neural tube and surrounding tissue. In contrast, EMT is a highly coordinated sequence of molecular events, which facilitates a transformation from an epithelial to a mesenchymal phenotype (Yang et al., 2020, Thiery et al., 2009) and involves the loss of apico-basal polarity and the acquisition of a front-rear polarity and a mesenchymal migratory phenotype. Whilst delamination and EMT are distinct processes, they are, however, dependent on one another. In order for delamination to take place, the neural crest must undergo either complete or partial EMT, depending on the species in question (Duband, 2006). The timing and dynamics of delamination have also been observed to vary depending on species as well as the subpopulation of neural crest. For example, whilst the cephalic neural crest in *Xenopus laevis* and *Mus musculus* delaminates all at once, prior to neural tube closure (Sadaghiani and Thiébaud, 1987,Nichols,1981,Nichols,1987), across all species the trunk neural crest has been observed to delaminate one by one, after the closure of the neural tube (Clay and Halloran, 2010, Duband, 2010).

The genetic programme which facilitates neural crest delamination involves a number of molecular players, which form part of the gene regulatory network coordinating neural crest induction. Delamination is triggered by BMP/WNT signaling, which activates a set of transcription factors including Snail2, Foxd3, Sox9 and Sox10 (Cheung et al.,2005, Sauka-Spengler andBronner-Fraser,2008). Transient inhibition of WNT signaling is also required for the delamination of the neural crest from the neural tube (Rabadan et al.,2016, Hutchins et al.,2018).

1.4.4 EMT

Before delaminating from the neural tube, the neural crest behaves as an epithelial cell population. Epithelial cells maintain an apico-basal polarity and strong cell-cell adhesions. They are arranged into sheets, supported by a basement membrane (Nieto et al.,2016). In order to begin collective migration, the neural crest must transition from a steady epithelial cell population to a highly migratory mesenchymal population, in a process known as EMT. EMT is critical to several other developmental processes including gastrulation, heart morphogenesis and the development of the sclerotome (Larue and Bellacosa, 2005). As well as its roles during development, EMT is central to many pathophysiological processes such as cancer cell invasion (Nieto et al, 2016; Thiery and Morgan, 2004). Notably, EMT is a reversible event and cells are able to transition back to an epithelial state (MET) (Chaffer et al., 2007).

The downregulation of epithelial cell- cell adhesion molecules in apical, tight and gap junctions is a hallmark of EMT (Vandewalle et al., 2005, Kirby and Hutson, 2010). Crucially, the neural crest undergoes an E-to-N cadherin switch during EMT (Scarpa et al.,2015, Dady et al.,2012). The pre-migratory neural crest express type I E-cadherin. Prior to migration, E-cadherin is repressed with a concomitant upregulation of weaker adhesion type N-cadherin (Rogers et al., 2013, Scarpa et

al., 2015,). The E-to-N cadherin switch in the neural crest is facilitated by the activation of transcription factors, including Twist, Snail/slug and SIP1 (Carl et al.,1999,Kang and Massagué, 2004,Nieto et al.1994, Rogers et al.,2013).

The activity of internal transcription factors is necessary for the neural crest to undergo EMT, as described above. However external environmental cues are also required to facilitate the transition. Through the use of atomic force microscopy (AFM), it has been shown that the mesoderm, the migratory substrate of the neural crest, increases in stiffness prior to neural crest migration (Barriga et al.,2018). Barriga et al, demonstrated that the stiffening of the substrate of the neural crest was required to trigger the EMT programme. Importantly, culturing neural crest cells on soft compliant polyacrylamide gels, resulted in increased levels of E-cadherin. Furthermore, the increase of mesodermal stiffness was also required to trigger the onset of NC migration. In line with this, when mesodermal stiffness was reduced, through introducing physical ablations of surrounding tissue or through targeted injection of myosin inhibitors (myosin light chain 9 morpholino), severe migratory deficits were observed *in vivo*. On the contrary, when mesodermal stiffness was increased, through the application of a sustained compressive force or through expression of a constitutively active myosin light chain construct, this was sufficient to trigger the premature migration of the neural crest. When the authors investigated the mechanism by which mesodermal tissue stiffens during development, they observed that it was a consequence of the increase in mesodermal cell density, leading to a thickening of the tissue. In agreement with this idea, the aforementioned mechanical and molecular manipulations which functioned to decrease tissue stiffness also resulted in a reduction in mesodermal cell density, whilst perturbations leading to increases in tissue stiffness correspondingly increased mesodermal cell accumulation. The increase in cell accumulation was found to result from the convergent extension of the mesoderm, mediated by the planar cell polarity (PCP) pathway.

Notably, targeted injections of PCP dominant negative constructs resulted in a reduction in substrate stiffness, mesodermal cell accumulation and an inhibition of neural crest migration. Taken together, these results indicate that the onset of EMT and migration of the cephalic neural crest are controlled by environmental mechanics (Barriga et al.,2018).In addition to changes in cell- cell adhesion molecules during EMT, the neural crest undergoes a number of molecular and morphological changes, linked to the acquisition of a migratory phenotype. For example, the neural crest begins to express a number of intermediate filament proteins, adopt a flattened morphology and form stable lamellipodial and filapodial protrusions (Berndt et al.,2008). Furthermore, the neural crest also start to express a disintegrin and metalloproteinase 10 and 13 (ADAM10 and ADAM13) which degrade cadherins at cell-cell contacts as well components of the extra cellular matrix (Alfandari et al.,2001) giving rise to a more invasive migratory cell population.

Taken together, EMT is a multifaceted event, which gives rise to alterations in cellular morphology and polarity, cell-cell adhesion and gene expression within the neural crest, in preparation for migration. As EMT is also considered to be a hallmark of cancer, the neural crest is a commonly used model system to investigate the molecular mechanisms behind metastasis.

1.4.5 Neural Crest Migration

Subsequent to delamination and EMT, the neural crest begin to migrate in collective streams along the dorso-ventral axis. Neural crest migration relies on the polarized formation of lamellipodia in leader cells (Matthews et al.2008), which couple to the ECM, via cell matrix adhesions(as described in section 1.1) In the case of the cephalic neural crest in *Xenopus laevis*, cells require ECM component fibronectin for migration(Alfandari et al.,2003). Migration on fibronectin is permitted through expression of α5β1 integrin (Alfandari et al., 2003.) as well as

downstream components of the integrin signaling pathway including FAK (Roycroft et al.,2018), vinculin and talin (Barriga et al.,2018). Additionally, the cephalic neural crest also expresses adhesion molecule syndecan-4, which binds to fibronectin and promotes the formation of cell matrix adhesions (Matthews et al.,2008).

Whilst cell-substrate interactions are required for the adhesion dependent migration of the neural crest, directional migration is driven through mechanisms of physical and chemical confinement. Furthermore, the neural crest employs a number of mechanisms which confer them with a collective cell polarity, to facilitate coordinated and directional migration. These aspects of neural crest migration will be discussed further below.

Physical and Chemical confinement

During migration, the neural crest subjected to both physical and chemical confinement by surrounding tissue, which helps them to achieve directed locomotion. When NC cells initiate migration along the fibronectin network, they are physically confined by a number of neighbouring epithelial tissues , including the neural tube, the eye, the epidermis, and the cranial placodes. The cranial placodes are progressively displaced by NC cells during the onset of migration. Such emergent interactions between the neural crest and placodal cell population leads to the formation of dorsoventral corridors of migration ,which are lined by placodes (Szabo et al.,2019).The neural crest subsequently migrate into these corridors as three well defined streams, termed as the mandibular, hyoid and branchial streams (Sadaghiani and Thibaud, 1987). The stream which the neural crest are restricted into ultimately dictates their imminent cell fate, once migration is complete.

Whilst the neural crest are restrained to their respective streams by the physical confinement of the placodes and surrounding tissue, they are also subjected to a further layer of chemical confinement which arises from repulsive cues secreted from neighbouring tissue. The neural crest express receptors that bind to and interact with repulsive ligands, which are expressed by cells and tissues in adjacent territory. Thus, through a mechanism of lateral inhibition, the neural crest are maintained in funneled streams and prevented from invading surrounding territory. Three types of receptor/ligand families are thought to be responsible for this; the Eph receptors and Ephrin ligands, Neuropilin receptors and Semaphorin ligands and Robo receptors and Slit ligands.

Ephs are tyrosine kinases, which upon interaction with their ligand, known as ephrins, facilitate bidirectional signaling. Notably, disrupting the activity of Ephs and Ephrins resulted in aberrant migration of the neural crest into non permissive territory (Smith et al.,1997), highlighting their role as confinement signals. Whilst the subtype of Ephs and Ephrins expressed in the neural crest and surrounding tissue respectively is species dependent, the role of eph-ephrin signaling in maintaining migratory streams of the neural crest appears to be conserved across species (Davy and Soriano, 2007, Mellott and Burke, 2008, Smith et al., 1997, Wang and Anderson, 1997).

In a similar manner, Neuropilin receptors 1 and 2 as well their coreceptor plexinA1 are expressed by the neural crest, whilst Class 3 semaphorins (sem3A 3F 3G) are expressed in the neighbouring tissues (Koestner et al., 2008). Indeed, perturbing the function of Neuropilin 2 or Sem3F resulted in ectopic migration of the mouse cephalic NC (Gammill et al.,2007). More recently, a study was performed to elucidate the mechanism by which Sem3A promotes directional neural crest migration within constrained streams (Bajanca et al.,2019). The study postulated that Sem3A, which is highly expressed in the dorsal medial regions of the embryo, inhibits Rac-1 activation and cell matrix adhesion formation in follower cells. In parallel, the attractive signal SDF-1 (discussed later) is expressed in ventral -lateral regions and antagonizes SEM3A mediated inhibition of Rac-

1 and focal adhesion formation, to promote polarization in leader cells and the directional migration of the neural crest.

Finally, the Slit/Robo receptor ligand family plays an important role in constraining the trunk neural crest in defined streams. The trunk neural crest presents Robo1 and Robo2 receptors which interact with Slit2, which is expressed by adjacent tissue (Jia et al., 2005, Giovannone et al., 2012). This interaction restricts migration of the trunk neural crest to a ventral-medial pathway.

Chemotaxis and Co-attraction

The directional migration of the neural crest is also dependent on a number of positive chemical guidance cues. The neural crest is known to respond to attractive chemical cues, including Stromal cell-derived factor (SDF-1), Platelet-derived growth factor (PDGF), Vascular endothelial growth factor (VEGF) over long ranges. In the chick NC, VEGF was found to be expressed in the neuroectoderm and required to direct the migration from rhombomere 4 into the second branchial arch (McLennan and Kulesa, 2007, McLennan and Kulesa, 2010, McLennan et al.,2010.) Notably, introduction of VEGF immersed beads or VEGF expressing cells by rhombomere 4 resulted in aberrant migration away from the second branchial arch (McLennan et al.,2010). Furthermore, VEGF was suggested to establish the identity of the leader cells within the collectively migrating neural crest, as exposure to VEGF altered the gene expression pattern and behavior of cells at the leading edge (McLennan et al., 2015).

The PDGF receptor (PDGFRα) is expressed in the migratory NC (Bahm et al.,2017, Eberhart et al.,2008 Ho et al., 1999,) and ligands PDGF-A and PDGF-C in neighbouring territory including the optic stalk, nasal cavity and branchial arches. When the *Xenopus* migratory cephalic neural crest were exposed to an exogenous source of PDGF-A *in vitro,* they demonstrated the ability to

undergo efficient chemotaxis (Bahm et al.,2017) and introduction of an exogenous source similarly biased the migration of mouse NC *in vivo.* Additionally, PDGF signaling was shown to be required to direct trunk neural crest cells to the dorsal aorta, prior to initiation of haemopoietic stem cell specification (Damm et al.,2017).

Another chemical cue, which promotes neural crest migration, is SDF1. SDF-1 has been found to be expressed in the pharyngeal arches and in the ectoderm, where it functions as a long range chemoattractant for the migration of the neural crest (Olesnicky Killian et al., 2009., Theveneau et al.,2010). However, SDF-1 can also act as a short-range chemoattractant. In addition to the pharyngeal arches, the epibranchial placodes which directly surround the neural crest also express SDF-1 at pre-migratory developmental stages (Theveneau et al.,2013). *In vitro* neural crest explants are observed to migrate directionally towards placodal explants. Hence, in this way, SDF-1 can also act as a short-range attractive cue to initiate directional migration *in vivo*. This 'chase and run' mechanism will be discussed further later.

Mechanistically, SDF-1 binds to the G-protein coupled receptor Cxcr4, expressed in the cephalic neural crest. Indeed, SDF-1/ Cxcr4 signaling was shown to be required for migration of the neural crest around the eye and into the pharyngeal arches (Olesnicky Killian et al., 2009, Theveneau et al.,2010).Downstream of Cxcr4, SDF-1 promotes Rac-1 activity at the leading edge of the neural crest, thereby stabilizing lamellipodia in the direction the chemoattractant (Theveneau et al.,2010). Furthermore, SDF-1 promotes the acquisition of a supracellular polarity, by inhibiting the contractility of a tensile actomyosin cable in leader cells (Shellard et al.,2018). The polarised contractility of the actomyosin cable at the rear of the collective has been shown to promote the directional migration of the cephalic neural crest.

In addition to long range attractive cues, the neural crest also exhibits a short-range mutual attraction known as co-attraction (Carmona-Fontaine et al., 2011). Co-attraction is required to maintain the integrity of the collective, by keeping cells in proximity of one another. Importantly, perturbing co-attraction results in the dispersion of the neural crest and the loss of directional migration towards a chemoattractant (Carmona-Fontaine et al., 2011; Woods et al., 2014).The process of co-attraction is mediated by components of the complement pathway, which play an important role in the immune response. Crucial mediators of co-attraction include the complement factor C3a and the receptor C3aR, which are both expressed by the neural crest.

Contact Inhibition of Locomotion

As well as co-attraction, the neural crest also undergoes contact inhibition of locomotion to facilitate efficient directional migration. Contact inhibition of locomotion (CIL) is the process during which two cells, which come into contact, collapse their protrusions, repolarize and migrate in opposing directions (Roycroft and Mayor, 2015). In the context of the collective migration of the neural crest, contact inhibition of locomotion ensures efficient directional migration, by polarizing the leader cells away from the cell-cell contact and by inhibiting protrusion formation in follower cells (Carmona-Fontaine et al., 2008; Theveneau et al., 2010). At the molecular level, CIL requires WNT signaling which activates RhoA at the cell-cell contact (Carmona-Fontaine et al., 2008). Activation of RhoA polarizes Rac-1 away from intercellular contacts and towards the leading edge. In addition to WNT signaling, a number of molecular players function in CIL. Syndecan-4, for example, works in concert with the non-canonical Wnt signaling pathway to promote CIL by inhibiting Rac-1 at the cell-cell contact (Matthews et al.,2008). Cell- cell adhesion molecules also play an important role in CIL. N cadherin, for example,

acts to inhibit Rac-1 activity at cell contacts (Theveneau et al.,2010). In contrast, E-cadherin has the opposite effect on Rac-1 activity. In fact, the E to N cadherin switch during EMT is required for the acquisition of CIL behavior in the neural crest (Scarpa et al.,2015). Additionally, Par3, a component of the tight junctions, has also been shown to mediate CIL, through inhibition of Rac-1 and through promoting microtubule catastrophe, which acts to polarize cells in the opposite direction (Moore et al.,2013).

Directional migration of the neural crest is not only driven by homotypic CIL but also by heterotypic CIL between the neural crest and the placodes (Theveneau et al.,2013). As discussed above, the neural crest migrate directionally towards the placodes, which express SDF-1. When the neural crest come into contact with the placodes, both cell population collapse their protrusions. The placodal cell population then repolarizes and migrates away from the neural crest. As such, directional migration is accomplished through a chase and run mechanism, during which the neural crest pursue the placodes that “run” away upon interaction with the neural crest. Taken together, the neural crest requires a fine balance between the attractive forces, mediated by co-attraction, and cell -cell repulsion, which manifests as a consequence of contact inhibition of locomotion, to facilitate coordinated directed migration.

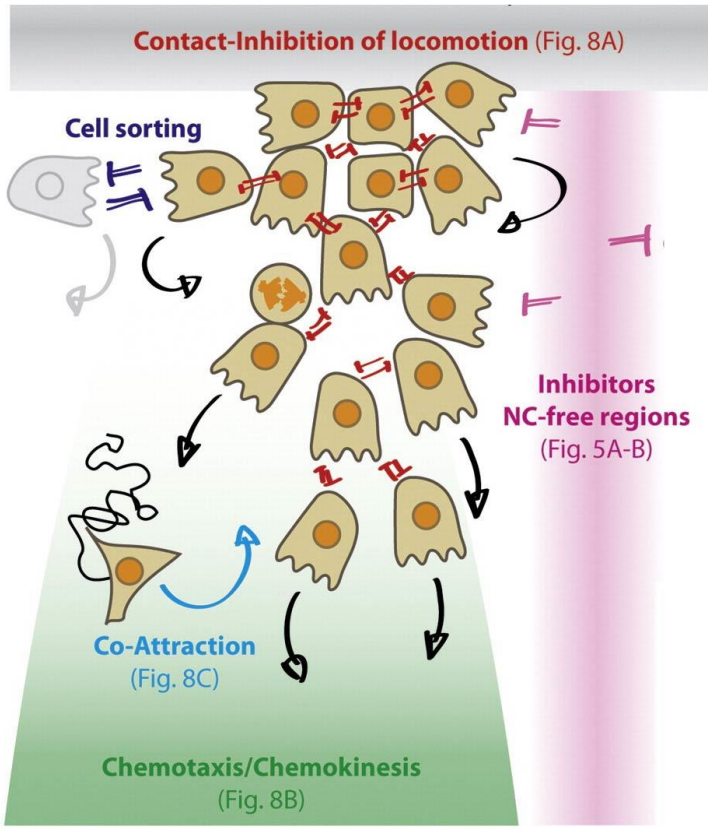

Figure 1.7 The migration of the neural crest: The migration of the cephalic neural crest is facilitated by intercellular interactions and inhibitory and attractive cues signals. Coordination between the opposing mechanisms of contact inhibition of locomotion (red) and co-attraction (blue) directs the collective polarity while maintaining the integrity of cohort. Contact inhibition of locomotion results in the collapse of protrusions at the cell-cell interface, and a reorientation of protrusions into free space. On the other hand, co-attraction, mediated by C3 signaling, enables cells to maintain close proximity with one another. The neural crest undergo chemotaxis in response to a number of chemoattractant in sdf-1 PDGF and VEGF. The neural crest are restrained in migratory streams by inhibitory cues in the surrounding territory (pink), such as semaphorins and ephrins. *Adapted from Theveneau and Mayor.,2012*

1.5 Hypothesis

1.5.1 Hypothesis Background

The body of work presented in this thesis focuses on the collective migration of the *Xenopus laevis* cephalic neural crest. While detaching from the dorsal neural tube, neural crest cells adopt a mesenchymal morphology which allows them to invade their surrounding territory (Duband et al.,2013). Indeed, conversion of NC cells from a non-motile into a motile state involves interactions with various extracellular matrix components via cell matrix adhesions (Alfandari et al., 2003,Roycroft et al.,2018). However, how components of cell matrix adhesions function to regulate cell attachment and polarity during the onset of NC migration remains unclear. Furthermore, it was recently demonstrated that stiffening of the substrate is required to trigger an epithelial to mesenchymal transition, and the subsequent onset of migration (Barriga et al.2018). One question which arises from this is how the neural crest transduces mechanical cues from its substrate to trigger migration. Focal adhesions have been described as the mechanosensory unit of adherent cells. However, the functional relevance of constituent cell matrix adhesion proteins in mechanotransduction during neural crest migration remains unknown.

Here, we investigate the role of CAS protein, X-chef-1 during neural crest migration. The CAS family of proteins are scaffolding proteins within the integrin signaling pathway, which have established roles in the regulation of cell migration and rigidity sensing (Honda et al., 1999, Sawada et al.2006). The Cass4 homologue X-chef-1 was shown to be specifically expressed in the neural crest prior to the onset of migration (Meek et al.2004).

1.5.2 Hypothesis

Hence, given this information, the thesis proposes to address the following hypothesis:

X-chef-1 participates in neural crest migration as part of the machinery required to respond to changes in substrate stiffness.

To address this hypothesis, this thesis addresses the following questions:

Questions

1. Is X-chef-1 required for neural crest migration *in vivo*?
2. What is the molecular mechanism by which X-chef-1 promotes migration?
3. What are the downstream targets of X-chef-1 that affect neural crest migration?
4. Can X-chef-1 promote cell spreading and migration in a substrate stiffness dependent manner?

2. Experimental procedures

2.1 Solutions

Solutions for embryological procedures

Cysteine solution

2% L-cysteine in H_2O with 50 mM NaOH.

Danilchick's medium for Amy (DFA)

53 mM NaCl, 5 mM Na2CO3, 4.5 mM K-Gluconate, 32 mM Na-Gluconate, 1 mM $MgSO_4$, 1 mM $CaCl_2$, 0.1% bovine calf serum albumin, pH 8.3

adjusted with bicine.

Ficoll solution

3% polysucrose in NAM 3/8.

Marc's modified ringer's (MMR)

100 mM NaCl, 2 mM KCl, 1 mM $MgSO_4$, 2 mM $CaCl_2$, 5 mM HEPES, 0.1 mM EDTA, pH 7.6.

Normal amphibian medium (NAM 1/10)

11 mM NaCl, 0.2 mM KCl, 0.1 mM $Ca(NO_3)_2$,, 0.1 mM MgSO4, 10 mM EDTA, 0.2 mM NaH_2PO_4, 0.1 mM $NaHCO_3$, pH 7.5, 50 µm/mL streptomycin.

NAM 3/8

40.7 mM NaCl , 0.74 KCl, 0.37 mM $Ca(NO_3)_2$, 0.37 mM $MgSO_4$, 37 M EDTA, 0.37 mM NaH_2PO_4, 0.1 mM NaH_2PO_4, pH 7.5, 50 µm/mL streptomycin.

Solutions for molecular biology

Anti-digoxigenin-alkaline phosphatase (AP) buffer

100 mM NaCl, 50 mM $MgCl_2$, 100 mM Tris-HCl, pH 9.8, 0.1% Tween-20.

Bleaching buffer

20% H_2O_2, 2.5% 20X SSC, 5% formamide.

Diethylpyrocarbonate water (DEPC)

0.1% diethylpyrocarbonate.

Formamide/SSC post-hybridisation washing solutions 1-5

Solution 1

50% formamide, 10% 20X SSC, 0.1% Tween-20.

Solution 2

25% formamide, 10% 20X SSC, 0.1% Tween-20.

Solution 3

12.5% formamide, 10% 20X SSC, 0.1% Tween-20.

Solution 4

10% 20X SSC, 0.1% Tween-20.

Solution 5

1% 20X SSC, 0.1% Tween-20.

Hybridisation buffer

50% formamide, 5X SSC, 1X Denhardt's solution, 1 mg/mL ribonucleic acid, 100mg/mL heparin, 0.1%

CHAPS, 10 mM EDTA, 0.1% Tween-20, pH 5.5.

Maleic acid buffer (MAB)

100 mM maleic acid, 100 mM NaCl, 0.1% Tween-20, pH 7.6.

MEMFA

100 mM MOPS, 1 mM $MgSO_4$, 2 mM EGTA, 3.7% formaldehyde.

Phosphate buffer saline (PBS)

137 mM NaCl, 2.7 mM KCl, 4.3 mM NaH_2PO_4, 1.4 mM H_2PO_4, pH 7.3.

PBS with Tween (PBT)

1X PBS with 0.1% Tween-20.

20X saline-sodium citrate buffer (SSC)

3 M NaCl, 0.3 M tri-sodium citrate, pH 7.0.

2.1 Embryological Procedures

2.2.1 *Xenopus Laevis* Oocyte collection and Fertilization

Xenopus laevis were acquired from Portsmouth Animal Facility, UK and Nasco, USA. In order to induce superovulation, mature female frogs first underwent pre-priming 2-3 days prior to oocyte collection, via an injection of 100 units of gonadotropic hormone PMSG (Intervet). This was followed by a subcutaneous injection of 500 units of Human Chorionic Gonadotrophin (Intervet), on the day prior to experimentation. Injected frogs were kept overnight at 17°C in MMR solution. Testes were extracted from mature male frogs, which were culled by anaesthetisation in 0.5% Tricaine solution for at least 40 minutes and subsequent decapitation. Extracted testes were maintained in Leibovitz L-15 medium (Invitrogen) with streptomycin added at 5 $\mu g.ml^{-1}$ (Sigma) at 4°C. The oocytes were gathered into in a petri dish and fertilized using a small piece of testis, homogenized in MMR solution. Following 30 minutes of incubation, NAM 1/10 solution was added to the petri dish. Subsequent to the first embryonic cleavage, embryos were submerged in a 2% L-cysteine (Sigma) solution for 5 minutes, to dissociate the surrounding jelly. The embryos were maintained in NAM 1/10 at 14.5°C. The developmental stage of embryos was determined using the Nieuwkoop and Faber method, 1967.

2.2.2 Microinjection

Borosilicate glass capillaries (Harvard Apparatus) with a 0.58mm inner diameter were used to produce needles for microinjection. Needles were generated by pulling the capillaries on a Narishige PC-10, set to 2 step mode, with the initial step set to 88% capacity and the second step set to 99.4% capacity. Needles were then calibrated with an eye piece graticule, to inject a defined volume of 10nl. Prior to injection, the glass capillaries were loaded with suspensions of either

mRNA or antisense morpholinos. Injection of *Xenopus laevis* embryos was performed using a Narishige IM300 Microinjector. The embryos were maintained in Ficoll solution (Sigma) during injection, a highly branched hydrophilic polymer solution, used to preserve the integrity of the embryo. Embryos were injected at either 8, or 16 cell embryonic stage, depending on the cell population to be targeted. Injection to target the neural crest was performed at the 8-cell stage, into the dorsal animal blastomere and the ventral animal blastomere. For targeting of the mesoderm, two dorso-vegetal blastomeres were injected at the 16-cell stage. Embryos were maintained in Ficoll solution overnight in 14.5°C, following injection. Subsequently they were maintained to NAM 1/10. Embryos were primarily kept at 14.5°C, however temperature could be changed from 14°C - 18°C, in order to alter rates of development.

Construct	Type	Amount injected	Stage
Fak-GFP	mRNA	200pg per blastomere	8 cell stage
Nuclear-RFP	mRNA	150pg per blastomere	8 cell stage
Pak-gbd-GFP	mRNA	100pg per blastomere	8 cell stage
X-chef-1-GFP	mRNA	200-400 pg per blastomere	8 cell stage
X-chef-1- Δ-CT-GFP	mRNA	400 pg per blastomere	8 cell stage
X-chef-1- Δ-SH3-GFP	mRNA	400pg per blastomere	8-cell stage
X-chef-1- Δ/Δ-GFP	mRNA	400pg per blastomere	8-cell stage
X-chef-1-fxxp-GFP	mRNA	800pg per blastomere	8 cell stage
X-chef-1-fxxp	mRNA	800pg per blastomere	8 cell stage
X-chef-1-Exxp-GFP	mRNA	300pg per blastomere	8 cell stage
X-chef-1 MO(Sequence 5'5'GTTTGTAACCTTCATTTTCCTCAGC 3')	Morpholino oligomer	5ng per blastomere	8 cell stage

Myo19 MO (sequence 5' TGGCTTTTGTCTTCTTGCTGGACAT3')	Morpholino oligomer	5ng per blastomere	16 cell stage

Table 1: A list of injected constructs

2.2.3 Neural crest dissection and culture

Embryos were left to develop until stage 17. At this point, the cranial neural crest cells were extracted from the embryos. Neural crest dissection was performed at 18°C in normal amphibian medium 3/8 (NAM 3/8) to maintain the integrity of the embryo. Forceps were used to dissociate the vitelline membrane which encompasses the embryos. Embryos were subsequently allowed to recover for half an hour. Once embryos had healed, they were suspended in a plasticine dish and the superficial layer of the ectoderm was removed to expose the neural crest. The neural crest was dissected from the embryo, using a hair knife and transferred to a plastic or glass dish containing Danilchick's Medium for Amy (DFA), prior to further dissociation into smaller sized explants and plating on a fibronectin coated glass or plastic dish containing DFA. NC explants were left to attach and spread for a time frame of 30mins- 1hr before imaging.

Plastic dishes (Falcon 50 x 9 mm; used in *in vitro* dispersion assays) were coated with fibronectin (Sigma) at 10 $\mu g.ml^{-1}$ for 1 hour at 37°C. Glass bottomed dishes (FluoroDish 35 mm; used for immunohistochemistry and live imaging of cell matrix adhesions) were incubated with fibronectin (100 $\mu g.ml^{-1}$) for an hour at 37°C. Following fibronectin incubation, the dishes were subjected to 3 PBS washes and blocked with 0.1% bovine serum albumin (BSA) (Sigma) in PBS for 20 minutes at 37°C. Following blocking, dishes were washed a final time with PBS. Before usage, DFA medium was added to dishes.

2.3 Molecular Biology

2.3.1 Amplification of DNA clones

Plasmid DNA was transformed into DH5a competent cells in order amplify DNA clones. In brief, 1-2 microlitres of plasmid DNA was added to 50 microlitres of bacterial cells. Cells were incubated on ice for 30 minutes, before being subjected to a heat shock at 42 degrees for one minute. Cells were then incubated on ice once again for a further 5 minutes. 800 microlitres of LB broth was added to cells which were then incubated at 37 degrees for two hours. Cells were then plated to Ampicillin or Kanamycin resistant LB agar plates and incubated overnight at 37 degrees. Colonies were picked the following day and cultured in 20 microlitres of LB broth containing either Ampilcin or Kanomycin overnight at 37 degrees. Plasmid DNA purification was performed using a Plasmid Miniprep Kit (Qiagen). DNA concentration was determined using a Nanodrop Spectrophotometer-ND-2000.

2.3.2 Molecular Cloning

The cloning strategies and primers used to generate X-chef-1 constructs are described below in Table 2. X-chef-1-full length, X-chef-1-Fxxp and X-chef-1-Exxp cDNA fragments were synthesized by GeneArt Gene Synthesis (Invitrogen). Synthesized DNA fragments were amplified by PCR using a Go Taq DNA polymerase kit (Promega). Amplicons were purified using a PCR purification kit (Qiagen) and were digested using restriction enzymes (New England Biolabs) to be cloned into a PCS2+ or PCS2+-GFP vector. Digested fragments were confirmed to be of the correct size by gel electrophoresis and were once again purified using a PCR purification kit. DNA concentration was

quantified using a Nanodrop Spectrophotometer- ND-2000. A DNA ligation was then preformed using a Quick Ligation kit (New England Biolabs). Digested Amplicons were mixed with the digested PCS2+ vector at a ratio of 3:1. A T4 DNA ligase was then added to the mix and the ligation incubated at 16 degrees overnight. The following day the ligation mixture was transformed to Dh5a competent and plated onto Ampicillin resistant agar plates which were incubated at 37 degrees overnight. 10-15 colonies were isolated from the agar plates the following day. Colonies were cultured in LB broth containing ampicillin overnight at 37 degrees. Plasmid DNA was purified using a Plasmid mini kit (Qiagen). Plasmid DNA from the colonies was then digested with appropriate enzymes to identify positive clones. Identified positive clones were confirmed by sequencing at the Source Biosciences sequencing facilities. X-chef-1- Δ-CT-GFP ,X-chef-1- Δ-SH3-GFP and X-chef-1-Δ/ Δ-GFP constructs were cloned by Elias Barriga, using the cloning strategy primers documented in Table 2. Ligation and transformation steps were performed as described above.

Construct	Destination Plasmid	Forward Primer	Reverse Primer	Restriction Digest
X-chef-1-FL-GFP	PCS2+GFP	5'GCGCGCGGATCCATGAAGGTTACAAACATG-3	5'GCGCGCCTCGAGCATTGCCCTGAATATCTG-3'	XhoI and BamHI
X-chef-1-Fxxp-GFP	PCS2+GFP	5'GCGCGCGGATCCATGAAGGTTACAAACATG-3	5'GCGCGCCTCGAGCATTGCCCTGAATATCTG-3'	XhoI and BamHI
X-chef-1-Fxxp	PCS2+	5'GCGCGCGGATCCATGAAGGTTACAAACATG-3	5'GCGCGCCTCGAGCATTGCCCTGAATATCTG-3'	XhoI and BamHI

X-chef-1-Exxp-GFP	PCS2+GFP	5'GCGCGCGGATCCATGAAGGTTACAAACATG-3	5'GCGCGCCTCGAGCATTGCCCTGAATATCTG-3'	XhoI and BamHI
X-chef-1-ΔCT-GFP	PCS2+GFP	5'GCGCGCGGATCCATGAAGGTTACAAACATG-3	5'GCGCGCCTCGAGAGTTTTTTGCCTTGGGAG-3'	XhoI and BamHI
X-chef-1-ΔSH3-GFP	PCS2+GFP	5'-GCGCGC-GGATCC-ATG CTT TTT ACT ATT ACA AAG-3'	5'GCGCGCCTCGAGCATTGCCCTGAATATCTG-3'	XhoI and BamHI
X-chef-1-Δ/Δ -GFP	PCS2+GFP	5'-GCGCGC-GGATCC-ATG CTT TTT ACT ATT ACA AAG-3'	5'-GCGCGC-CTCGAG-AGT TTT TTG CCT TGG GAG-3'	XhoI and BamHI

Table 2: A list of Cloning Strategies and Primers

2.3.3 *In vitro* transcription

In order to synthesize sense mRNA for injection, plasmid DNA was first linearized by restriction digestion using a suitable restriction enzyme (Promega Restriction enzymes). The digestion was incubated at 37 degrees for 2 hours then subsequently purified using a PCR purification kit (Qiagen). The linearization of DNA was confirmed by preforming gel electrophoresis. The concentration of linearized DNA was determined using a Nanodrop Spectrophotometer- ND-2000. 1 microgram of purified linearized DNA was used for an i*n vitro* transcription reaction with the Sp6 or T7 Ambion mMessage Machine kit (Invitrogen). The reaction was incubated at 37 degrees for two hours. Subsequently, one microlitre of turbo DNAse was added to the mixture and the reaction was further incubated at 37 degrees for half an hour to degrade the remaining DNA template. The mRNA transcript was then purified using an RNeasy Mini Kit (Qiagen). RNA concentration was determined using a Nanodrop Spectrophotometer- ND-2000.

2.3.4 *In situ* hybridisation

Whole mount *in situ* hybridisation were performed as described previously (Harland, 1991). Embryos were fixed in MEMFA for 1 hour at room temperature and were subsequently dehydrated in 100% methanol for 30 minutes. Embryos were rehydrated by sequentially washing with 75%, 50% and 25% methanol in PBS, followed by PBS-tween. Using a bleaching solution containing hydrogen peroxide, embryos were bleached for 30 minutes and subsequently washed in PBS-tween. Embryos were then fixed once again in MEMFA for 20 minutes and washed with PBS-tween. This was followed by an incubation in hybridisation buffer, for 6 hours at 62°C. The hybridization buffer was then discarded, and embryos were incubated with a digoxigenin labelled *Twist* or *Slug* probe at a concentration of 1 µg.ml-1 at 62°C overnight. After removal of the digoxigenin labelled probe, embryos were washed sequentially with Formamide/SSC post hybridisation solutions 1-5 at 62°C. Embryos were washed with solutions 1-4 for 10 minutes each and solution 5 for half an hour. Subsequently, embryos were washed in PBS-tween for 5 minutes, followed by MAB at room temperature, for a further 5 minutes. Embryos were then subjected to blocking with 2% Boehringer Mannheim Blocking Reagent (BMBR) (Roche) dissolved in Maleic acid buffer (MAB) for 2 hours at room temperature. An anti— digoxigenin-alkaline phosphatase conjugated antibody (Roche) (dissolved in 2% BMBR in MAB at a dilution of 1/4000) was added to embryos which were incubated overnight at 4 degrees. The following day, embryos were subjected to 6 washes in MAB of 30 minutes at room temperature, to get rid of any residual antibody, prior to washing with AP buffer twice, for 5 minutes each. 4nitroblue tetrazolium chloride (NBT, Roche) & 5-bromo-4-chloro-3-indoylphosphate (BCIP, Roche) were added to Alkaline Phosphatase (AP) buffer to develop the AP colour reaction at 150 $\mu g.ml^{-1}$ and 75 $\mu g.ml^{-1}$

respectively. After the signal had fully developed, the reaction was inhibited by washing in PBS-tween before fixation in 4% formaldehyde.

2.3.5 Immunofluorescence

Cells were plated onto glass bottomed dishes and allowed to attach for one hour. For immunostainings against phosphopaxilin, explants were then fixed in 4% formaldehyde for 30 minutes at room temperature (RT) and washed with PBS 3 times for 5 minutes. Fixed explants were then subjected to permeabilization in PBS-triton X 100 for 5 minutes and blocking in 5% Normal Goat Serum (NGS) in PBS for two hours. For immunostainings against Rac-gtp, cells were fixed in 4% paraformaldehyde for one hour and washed several times in PBS. Cells were then permeabilized in 0.1 %PBS-triton X100 on ice for 10 minutes and blocked in 5% PBS-BSA for half an hour. Primary antibodies were diluted in 5% NGS-PBS for phosphopaxilin or 5% PBS-BSA for Rac-GTP . Incubation protocols with primary antibody are described below. Secondary antibodies were diluted in 5% PBS-NGS or 5% PBS-BSA for phosphopaxilin and Rac-gtp immunostainings respectively and added to cells for an incubation period of two hours. Cells were subsequently imaged with an Olympus Fluoview FV1000 confocal microscope and a 63x objective and 2x digital zoom.

Antibody	Type	Supplier	Species	Dilution	Incubation
Phosphopaxilin py118	primary	Invitrogen	Rabbit	1:200	Overnight at 4°C
Rac-GTP	primary	New-east biosciences	Mouse	1:1000	Overnight at room temperature
Rabbit--555	secondary	Invitrogen	Goat	1:400	Two hours at room temperature
Rabbit-647	secondary	Invitrogen	Goat	1:400	Two hours at room temperature
Mouse-488	secondary	Invitrogen	Goat	1:400	Two hours at room temperature
Mouse-555	secondary	Invitrogen	Goat	1:400	Two hours at room temperature

DAPI	-	Thermofisher	-	1:1000	With secondary antibody

Table 3: Primary and Secondary Antibodies

2.3.6 Morpholinos (MO)

Morpholinos were purchased from gene tools. 5 nanograms of the X-chef-1 MO (5'GTTTGTAACCTTCATTTTCCTCAGC 3') was injected per blastomere at the 8-cell stage to knockdown X-chef-1 in the neural crest. An equimolar concentration of a control morpholino (5'CCTCCTACCTCAGTTACAATTTA 3') was injected. The myo19 morpholino (5'TGGCTTTTGTCTTCTTGCTGGACAT3') was injected at a final amount of 5ng per blastomere into two dorso-vegetal blastomeres at the 16-cell stage to knockdown myosin light chain in the mesoderm.

2.3.7 Inhibitors

Rac-1 inhibitor NSC23766 (Tocris) was used for *in vitro* experiments at concentration of 100µM. For *in vitro* experiments, the Rac-1 inhibitor was dissolved in DMSO and added to the DFA solution in which explants were cultured in. Explants were left in the inhibitor for 2 hours prior to fixation for immunohistochemistry. The equivalent volume of DMSO was added to the DFA solution in which control explants were cultured in.

2.3.8 Polyacrylamide gels

Polyacrylamide gels were prepared as follows. Glass slides were coated overnight (ON) and at room temperature (RT) in a solution of Ethanol: Acetic Acid: PlusONE Bind-Silene® (GE 475Healthcare) added at a ratio of 14:1:1. For hydrophobic coating, glass coverslips were air dried and added to a solution of PlusONE Repel-Silene® ES 478(GE Healthcare) for 15 minutes at room temperature. Polyacrylamide mixes were then prepared as described. For stiff gels, a stiffness value of 150 pascals and for soft gels a stiffness value of approximately 50 pascals was chosen. These values were comparable to the stiffness measured in mesoderm *in vivo* in migratory and non-migratory embryos (Barriga et al.,2018). The required stiffness was obtained by adjusting the ratio of acrylamide to Bis- Acrylamide within the polyacrylamide mix. For stiff gels a mix containing 550 µl 7.6 mM HCl, 349.5 µl ddH2O, 0.5 484µl of N,N,N',N'-tetramethylethylenediamine (TEMED, Sigma), 20 µl bis-acrylamide, 75 µl of acrylamide was prepared For soft gels a mix containing 550 µl 7.6 mM HCl, 369.5 µl ddH2O, 0.5 µl of N,N,N',N'- tetramethylethylenediamine (TEMED, Sigma), 16 µl bis-acrylamide (BioRad), and 60 µl of acrylamide (BioRad) was prepared.. The polymerization reaction was initiated by adding 5 µl of10% Ammonium persulfate (APS, GE Healthcare). 12 microlitres of the polyacrylamide mix was placed on an adhesive slide, covered with a hydrophobic coverslip and allowed to polymerize for 25 min .Gels were washed for 10 min 3x times with 10 mM HEPES buffer. Fibronectin was covalently bound to polyacrylamide gels via a Sulfo-SANPAH mediated succinimide cross-linking reaction. Briefly, 1 mg of the cross-linker Sulfo-SANPAH (Thermo-Fisher 22589) reconstituted in 20 µl of DMSO (Thermo-Fisher), was added to 480 µl of 10 mM HEPES buffer. A drop of this mixture was added to the polyacrylamide gels, which were then subjected to UV irradiation for 5 minutes. UV irradiation is necessary to activate the cross linker. Activated gels were washed in HEPES buffer for 5 min, to discard the excess cross linker. Finally, activated gels were incubated with fibronectin (100 µg.ml-1) for two hours at room

temperature. Functionalised gels were washed with PBS and submerged in a petri dish containing DFA.

2.4 Analysis

2.4.1 *In vivo* migration

In vivo neural crest migration was studied by preforming *in situ* hybridisations against *Twist;* a marker of the neural crest, in stage 24 embryos. To evaluate the effect on migration, embryos were injected mRNA constructs or morpholinos on one side of the embryo. Where necessary embryos were coinjected with fluorescin dextran (Invitrogen) or rhodamine dextran (rdx) to act as a tracer. Following injection, embryos were allowed to develop to migratory stages, when they were fixed in order to conduct the *in-situ hybridization* protocol. Embryos were imaged on a Leica MZ FLIII stereomicroscope with a DCGC420 Leica camera with 3.4x zoom. The effect on neural crest migration was assessed through either computing the percentage of embryos exhibiting a defective migratory phenotype or by measuring the normalized migration stream length. The latter parameter was determined by measuring the length of the 2nd hyoid stream on the injected side of embryos and normalizing against the length of the embryo along the dorsal-ventral axis. As a control, the normalized migration distance was either measured in embryos injected with a control morpholino or in the uninjected side of embryos.

2.4.2 Single Cell Motility

To study single cell motility *in vitro*, neural crest explants were plated to plastic dishes and allowed to attach for half an hour. Individual cells which dispersed from cell explants were imaged with a DM550B Leica Microscope with a DFC 300FX Leica camera. Cells were imaged with a 10x magnification at a frame rate of 2 minutes. Cells were maintained at an ambient temperature of 18°C, during image acquisition. Individual cell nuclei were tracked using the manual tracking

plugin in image J. Obtained cell tracks were subsequently input to Chemotaxis plugin tool in ImageJ to compute cell velocity and directionality. Cells were tracked for at least an hour.

2.4.3 Dispersion

Cell explants were plated on a plastic dish and allowed to attach for half an hour, before imaging. NC explants were maintained at an ambient temperature of 18°C during image acquisition. Explants were imaged with a DM550B Leica Microscope and a DFC 300FX Leica camera for 6 hours, at a frame rate of 5 minutes, using a 10x objective. Cells within the explant were tracked using the cell nucleus. For a given time point, through marking the nuclei of all cells within an explant, a network of triangles known as a Delaunay Triangulation can be constructed. A Delaunay triangulation connects each cell within an explant with its closest neighbours. As such, it can be used measure the extent of cell dispersion. For each NC explant, the degree of cell dispersion was computed by quantifying the average triangle area between the nuclei of neighbouring cells using Delaunay triangulation (Carmona-Fontaine et al., 2011), using a 'Dispersion tool' plugin available on ImageJ.

2.4.4 Phosphopaxilin analysis

Cell matrix adhesion area and number was analyzed in phosphopaxilin immunostainings by thresholding the acquired images. Thresholding was kept constant for images obtained in the same experiment. The 'Analyze Particle' tool on ImageJ was used to quantify the total cell matrix adhesion area per cell and cell matrix adhesion number. Cell matrix adhesions located at leading edge of cells were analyzed. The leading edge was defined as the region, adjacent to free space, in which no yolk platelets of the cell body were present.

2.4.5 FAK-GFP analysis

Cell matrix adhesion dynamics were analysed in cells injected with a FAK-GFP construct. Cell matrix adhesion assembly and disassembly rates were quantified using the 'Focal Adhesion Analysis Server' developed by the Shawn Gomez Lab (Berginski and Gomez, 2013). Time lapse movies were acquired on an Olympus Fluoview FV1000 confocal microscope with a 63x objective with a frame rate of 6 secs.

2.4.6 Protrusion analysis

Protrusion dynamics were analysed from time lapse movies acquired on an Olympus Fluoview FV1000 confocal microscope or a Leica TCS SP8vis microscope with a 63x objective with a frame rate of 6 secs. Protrusions were defined as areas devoid of yolk platlets. Protrusions were tracked from their initial growth until their retraction. The maximum protrusion area over the lifetime of the protrusion was recorded, as well as the duration of protrusions.

2.4.7 Rac-GTP analysis

Rac-GTP immunostainings were imaged on an Olympus Fluoview FV1000 confocal microscope with 63X objective. Z stacks of 1µm were obtained. Images were then imported into imagej. A straight-line segment of 15µm was drawn from the leading edge towards the cell body and an intensity profile along this line segment was obtained. The intensities (mean grey values) measured at each point along the line segment were normalized by subtracting the of the intensity value of the immunostaining in the cell body.

2.4.8 Pak-gdb-GFP analysis

For Pak-gbd analysis, cells injected with the pak-gbd-GFP construct were imaged using a Leica TCS SP8vis microscope with a 63x objective. Z slices of 1µm were obtained during image acquisition. A maximum projection of the Z slices was obtained, and straight-line segment of 15µm was drawn from the leading edge towards the cell body. The mean grey value at the leading edge was normalized to the mean intensity value of the cytoplasm within the cell body.

2.4.9 Statistical analysis

GraphPad Prism was used to generate graphs and preform statistical analysis. The significance of results involving a comparison of percentages was assessed using contingency tables (CarmonaFontaine et al., 2008; Taillard et al., 2008). Two data sets were determined to be significantly different if $T>3.841$ ($\alpha = 0.05$,*), $T>6.635$ ($\alpha = 0.01$,**) or $T>10.83$ ($\alpha = 0.001$,***) Data sets were tested for normality using the Kolmogov-Smirnov test, d'Agostino and Pearson's test and were only considered to be normal if found to be so by two tests . Normally distributed data was analysed using an unpaired t-test (two tailed, unequal variances) or a one-way analysis of variance (ANOVA) test with a Dunnett's multiple comparison posttest. Data considered not be normally distributed was assessed using a Mann Whitney test or Kruskal-Wallis test.

3. Results

3.1 Investigating the functional role of X-chef-1 in NC migration

The conversion of the neural crest from a non-motile into a motile state involves interactions with the extracellular matrix via cell matrix adhesions (Alfandari., et al.,2003, Roycroft et al.2018). However, little remains known with regards to the constituent cell matrix proteins involved in regulating NC migration. The CAS-family proteins are signaling proteins that are recruited to cell matrix adhesions, where they regulate a range of cellular responses including cell migration (Klemke et al.,1998, Natarajan et al.,2006, Singh et al.,2008,). Interestingly, the mRNA of one CAS protein known as *X-chef-1,* was found to be specifically expressed in the neural crest prior to migration (Meek et al.,2004). In light of this study, we examined the subcellular localization of X-chef-1 in the neural crest and through loss of function experiments, we investigated the functional requirement of X-chef-1 during neural crest migration.

3.1.1 X-chef-1 localises to cell matrix adhesions

We first examined the subcellular localization of X-chef-1 in the neural crest. We generated a fusion protein containing *Xenopus* X-chef-1, upstream of the green fluorescent protein (GFP), hereafter called X-chef-1 -GFP. Embryos were injected with the mRNA of the fusion protein at the 8-cell stage. The neural crest was dissected and immunohistochemistry was performed against phospho-paxilin (Y118) to visualize cell matrix adhesions. Paxillin is a scaffolding protein which localizes to focal complexes and its phosphorylation on tyrosine 118 residue is necessary for the assembly of the focal adhesions (Zaidel-Bar et al., 2007b). Hence, it is a suitable marker to label early focal complexes and maturing adhesions. Our results show that X-chef-1 localizes to

the leading edge of neural crest cells, with a large degree of co-localization with cell matrix adhesion marker phosphopaxilin (fig 3.1A).

3.1.2 X-chef-1 is required for neural crest migration *in vivo*

In order to understand if X-chef-1 controls migration of the neural crest in *Xenopus Laevis*, we generated a knockdown of X-chef-1 by using a morpholino (X-chef-1 MO). First, we analyzed if X-chef-1 knockdown affected the migration of the neural crest *in vivo*, by preforming an *in-situ* hybridization against *Twist;* a marker of the neural crest. Whilst three well defined migratory neural crest streams are observed in control embryos, the majority of morpholino injected embryos did not form migratory streams (fig 3.2A). Furthermore, in X-chef-1 MO embryos which did form migratory streams, the effect on migration was assessed by measuring the length of the hyoid stream on the injected side and normalizing this to the length of the embryo along the dorso-ventral axis (fig3.2B). The results show a reduction in the normalized stream length upon the loss of function of X-chef-1, in comparison to embryos injected with a control morpholino(fig3.2C). The impairment in migration was observed in 80 percent of the embryos injected with the X-chef-1 MO (fig3.2D). Taken together, this indicates that X-chef-1 is required for neural crest migration *in vivo.*

To verify that the impairment in migratory stream formation resulted specifically from the loss of function of X-chef-1, as opposed to an off-target effect of morpholino injection, a rescue experiment was performed. As such, the X-chef-1 MO was co-injected with the mRNA of X-chef-1-GFP fusion construct. Notably, the chimeric full-length mRNA was designed such that it could not be targeted by the X-chef-1 morpholino. Whilst injection of the morpholino on its own, impaired the formation of migratory streams, this deficit could be rescued upon co-injection with

X-chef-1-GFP mRNA (Figure 3.3A). Analysis of both the percentage of embryos showing the migratory defect and also the relative length of migratory neural crest (NC) streams confirmed this rescue (Figure 3.3B and3.3C). Overall, this result suggests that X-chef-1 is necessary and sufficient of neural crest migration *in vivo*.

3.1.3 X-chef-1 is required for cell dispersion and motility *in vitro*

As the loss-of-function of X-chef-1 affected the migration of the neural crest *in vivo*, we next aimed to identify which aspects of the migration of the neural crest are controlled by X-chef-1. In order to do that, we performed *in vitro* culture of NC cells, as it is a more controlled system, where the different aspects of cell migration can be dissected. As cellular dispersion is necessary for the onset of neural crest migration, we first analyzed how X-chef-1 knockdown affected this process. To investigate the effect on dispersion, the neural crest was dissected at migratory stages and plated onto dishes coated with fibronectin. Overtime, the neural crest disperses in a radial manner (figure 3.4A). The degree of dispersion can be quantified by measuring the average Delaunay triangulation area, which provides a readout of the distance between neighbouring cells. After 6 hours, the average triangulation area in control explants was significantly greater than that observed in X-chef-1 MO explants (fig3.4B-C), suggesting that X-chef-1MO explants displayed an impairment in cell dispersion. To further examine the effect of X-chef-1 on cell motility, we analyzed the migration of single cells which dissociated from neural crest explants. The trajectory of individually migrating control and X-chef MO cells were tracked for the duration of an hour (figure 3.5A). Loss of X-chef-1 resulted in a uniform reduction in average cell velocity, with respect to control cells(figure3.5B). Furthermore, a directionality index was computed by normalizing the accumulated migratory distance against the Euclidian distance between the

starting and end point(figure3.5C). Perturbing the function of X-chef-1 resulted in a reduction in the degree of directionality during migration(figure3.5D). Hence, our results indicate that loss of X-chef-1 impairs neural crest dispersion and cell motility *in vitro.*

3.1.4 Discussion

In this chapter, we have investigated the role of the CAS family member X-chef-1*,* which was shown to be specifically expressed in the neural crest prior to and during migration (Meek et al.,2004). Through injection of an X-chef-GFP fusion construct, we observed that X-chef-1 preferentially localizes to paxillin positive cell matrix adhesions, consistent with its role as a cell matrix scaffolding protein.

Subsequently, using an X-chef-1 morpholino, we investigated, for the first time, the role of the Cass4 homologue in the migration of the neural crest. Unfortunately, we were unable to detect X-chef-1 through the use of commercially available Cass4 antibodies, hence we could not assess the efficiency of the knock down of the X-chef-1 morpholino by western blotting. In the absence of an antibody which recognizes endogenous X-chef-1, morpholino efficacy could have been tested by expressing a fluorescently tagged X-chef-1 construct and evaluating whether the morpholino knocks down expression of the X-chef-1 fusion construct, by preforming a western blot using an antibody specific to the fluorescent epitope. It is important to note however, that whilst this experiment would show that the morpholino recognizes the mRNA of the exogenous X-chef-1 construct, it would not assess whether or to what degree the endogenous protein is knocked down. Nevertheless, despite the need for further evaluation of morpholino efficacy, we were able to demonstrate that the effects on migratory stream formation, observed in X-chef-1 MO embryos, resulted specifically from the loss of function of X-chef-1 as opposed to an off-target

effect of the morpholino. Notably, the targeted injection of the X-chef-1 morpholino impaired the formation of migratory streams *in vivo*. The observed migratory deficit was able to be rescued, by co-injection of the morpholino with chimeric X-chef-1 full length mRNA.

As the loss-of-function of X-chef-1 impaired the migration of the neural crest *in vivo*, we sought to better understand how cell locomotion was affected, through further characterization *in vitro.*

In vitro, we observed an impairment of dispersion in X-chef-1 MO explants and a reduction in cell velocity and directionality during the migration of dissociated single cells. Our results are in part consistent with the results reported by the seminal paper, documenting the discovery of Cass4 (Singh et al.,2008). Indeed, a reduction in cell velocity was also observed in a subset of Cass4 siRNA cells (Singh et al.2008). However, the phenotype reported by Singh et al was more complex, with a subset of cells exhibiting an increase in cell velocity. It was proposed that in the subset of Cass4 siRNA cells that display a higher cell velocity, that Cass4 acts as dominant negative to oppose the action of other CAS proteins expressed. However, as a uniform reduction in cell velocity is observed upon the loss of function of X-chef-1 in our system and as current gene expression data suggests that other member of the CAS family are not expressed in the neural crest during migratory stages (Green et al.,2016, Pollet et al.,2005), we believe this is not the case in cephalic neural crest. Taken together, our results suggest that *X-chef-1* has prominent role in regulating neural crest migration. Furthermore, given that observed deficits in dispersion and cell motility in X-chef-1 MO cells are consistent with the phenotype of wildtype cells adhering to soft, mechanically non permissive substrates (Barriga et al.2018), our results could be suggestive of a potential role in rigidity sensing. In the following chapters, we will further investigate, the molecular mechanism by which X-chef-1 regulates neural crest migration and the potential role of X-chef-1 in regulating the cell's response to substrate stiffness.

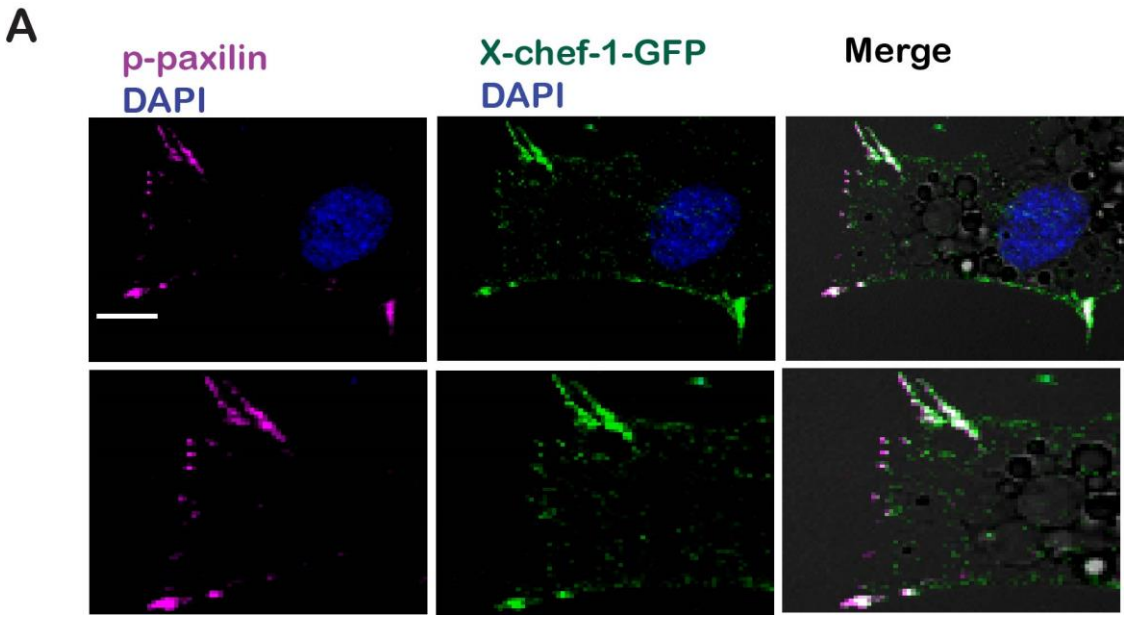

Figure 3.1: Subcellular localisation of X-chef-1 in the neural crest.

(A) Immunostaining for phosphopaxilin in explants injected with the X-chef-1 GFP construct. Scale bar represents 10µm.

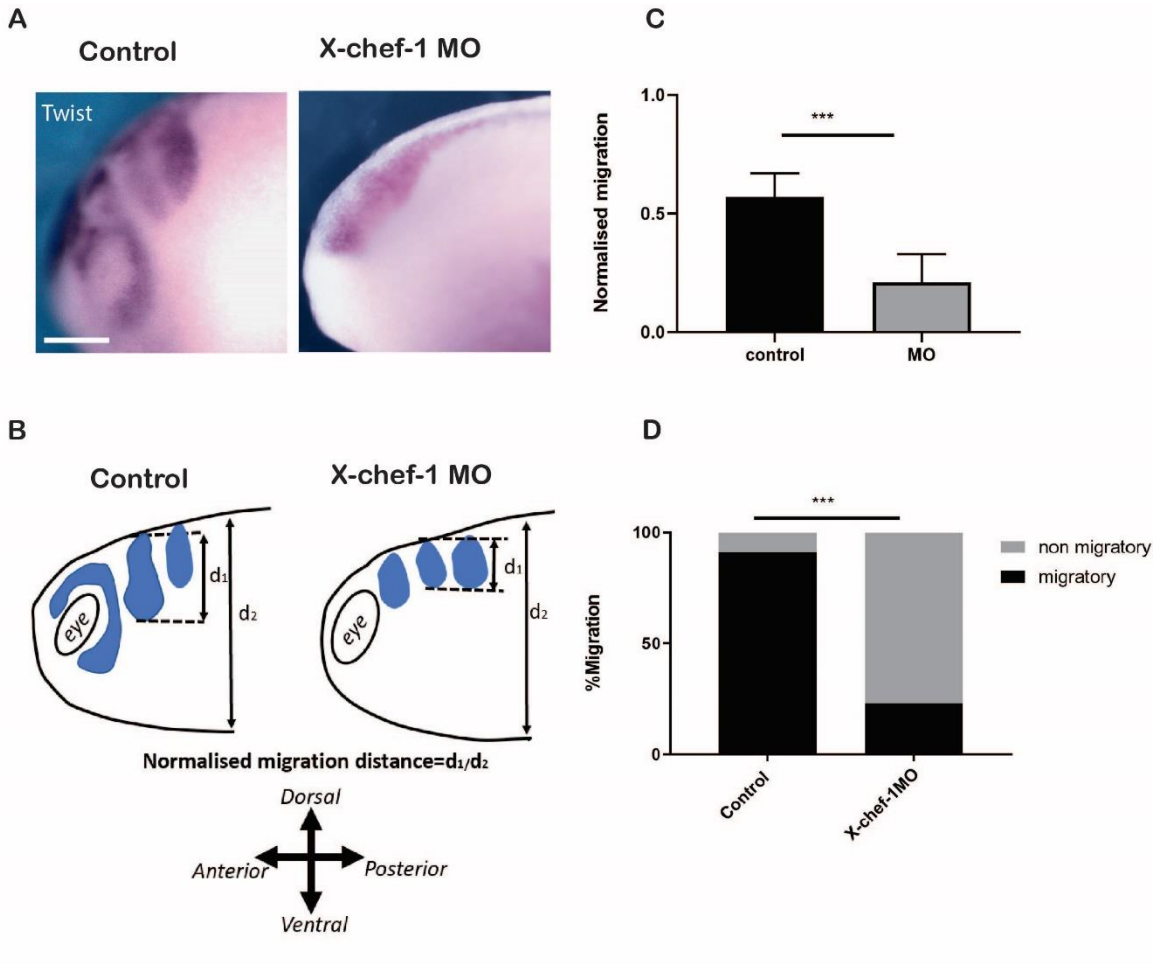

Figure 3.2: X-chef-1 is required for neural crest migration *in vivo*

(A)*In situ hybridization* of Twist in stage 24 embryos injected with control MO (left) and X-chef-1 MO (right). Scale bar represents 250µm (B) Schematic to demonstrate measurement of the normalized migration distance (C) normalized migration distance of the hyoid stream in the control (n=30), X-chef-1 MO (n=23) ;unpaired t-test *** P<0.001; Error bars represent mean and SEM (C) Percentage of embryos with inhibited migration in control (n=30) and X-chef-1 MO (n=45); Fishers exact test *** P<0.001

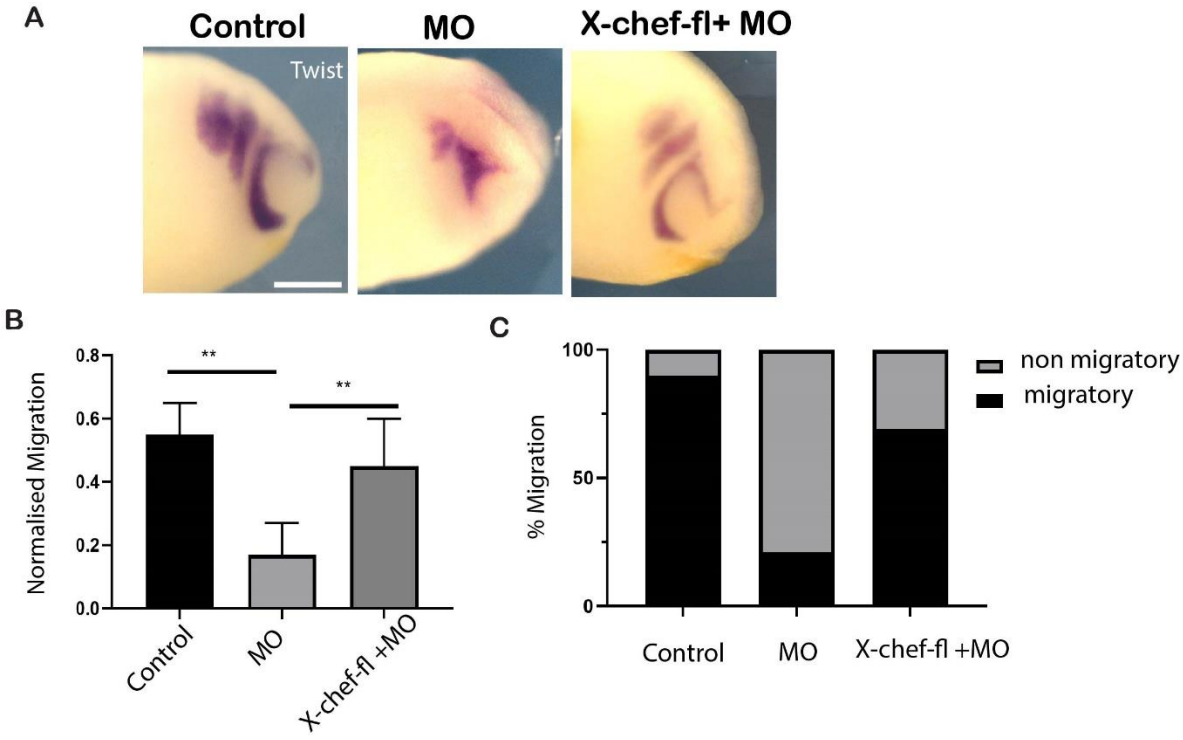

Figure 3.3: X-chef-1 full length mRNA rescues migration deficit resulting from morpholino

(A)*In situ* hybridization of *Twist* in stage 24 embryos injected with control MO (left), X-chef-1 MO (centre), X-chef-1 full length +MO (right). Scale bar represents 250µm. (B) normalized migration distance of the second hyoid stream in the control (n=20), X-chef-1 MO (n=20), X-chef-1 full length +MO(n=20); one way ANOVA with Dunnetts multiple comparisons ** P<0.01 .Error bars represent mean and SEM (C) Percentage of embryos with inhibited migration in control (n=20), X-chef-1 MO (n=20), X-chef-1 full length +MO(n=20).

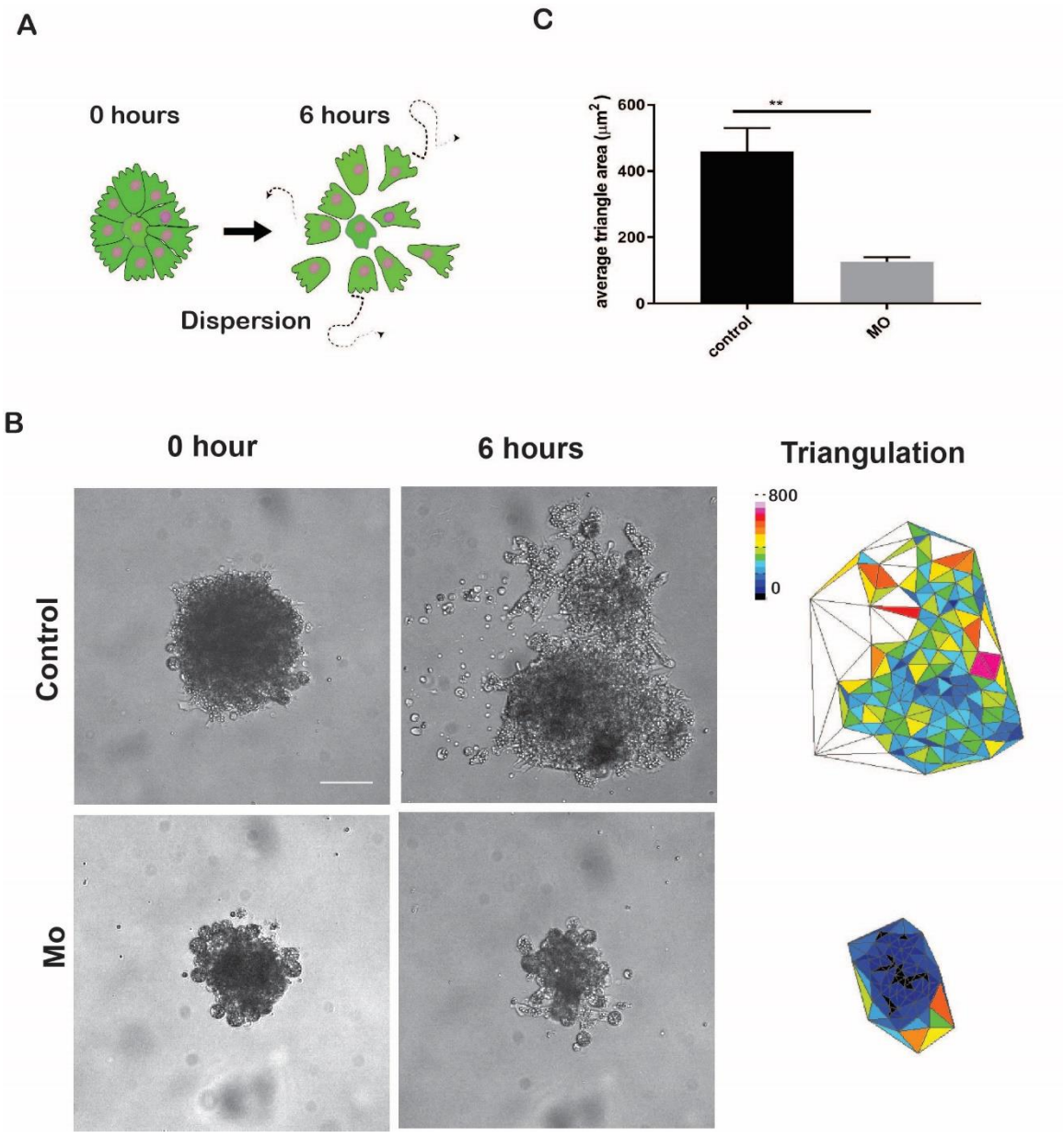

Figure 3.4: X-chef-1 is required for cell dispersion *in vitro*

(A) Schematic to depict a dispersion assay. (B) Brightfield of explants at zero hours (**left**) and 6 hours **(centre)** and visual representation of Delaunay triangulation in control and X-chef-1 Mo explants at 6 hours(**right**). (C)Dispersion analysis based on average Delaunay triangulation area at 6 hours for control (n=13) and X-chef1 Mo(n=10) explants; unpaired t-test **P>0.01. Error bars represent mean and SEM.

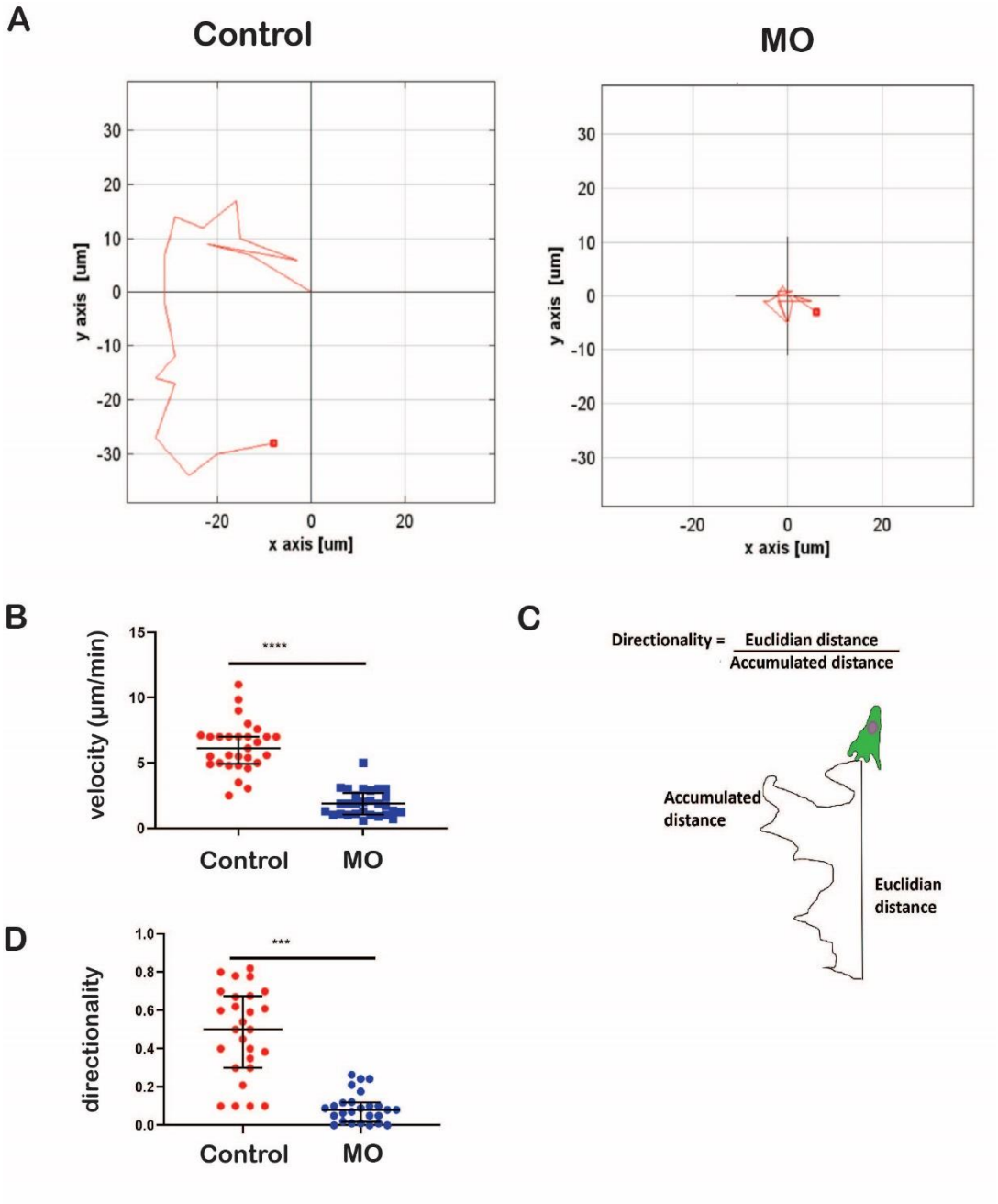

Figure3.5:X-chef-1 is required for cell motility *in vitro*

(A) Example trajectory of an individually migrating control (left) and MO cell (right) tracked for one hour(B) A box plot of single cell velocity in control (n=30) and MO cells(n=27) ; Mann Whitney t-test *** P<0.001; error bars represent median and interquartile range (C)A schematic to show calculation of cell directionality (D)Single cell directionality in control (n=30) and MO cells (n=27); Mann Whitney test *** P<0.001. Error bars represent median and interquartile range.

3.2. Elucidating the molecular mechanism of X-chef-1 dependent migration

Results in the previous section have alluded to a role of X-chef-1 in promoting the migration of the cephalic neural crest. We next set out to investigate the molecular mechanism by which X-chef-1 regulates neural crest migration. X-chef-1 contains a highly conserved N terminal SH3 domain and C terminus domain, which have been described to play a role in anchoring CAS proteins to cell matrix adhesions(Donato et al.,2010). Furthermore, X-chef-1 possesses a substrate domain with a series of 12 tyrosine (YxxP) motifs. Tyrosine phosphorylation of YxxP motifs within the substrate domain of p130cas and Nedd9 has been shown to be required for their signal transduction function (Zaidel-bar et al., 2005, Sharma et al.,2008 Sanz-Moreno et al.,2008. To elucidate the molecular mechanism by which X-chef-1 promotes migration, we designed a number of X-chef-1 constructs to delete or perturb the function of each of the aforementioned domains. In this section, we assessed the effects of each mutated domain on the migration of the neural crest *in vivo* and *in vitro.*

3.2.1 Loss of the SH3 and C terminus domains of X-chef-1 mildly impairs migration *in vivo* and cell motility *in vitro*

First, we sought to evaluate the role of the SH3 and C terminus domains of X-chef-1 in the neural crest, These domains have previously been described to have a joint function in cell matrix adhesion targeting, in other members of the CAS family of proteins, including P130cas and Nedd9 (Donato et al.,2010, Braniš et al.,2017). To investigate the role of SH3 and C terminus in targeting

to cell matrix adhesions, we designed two truncated X-chef-1 constructs, lacking amino acid residues 1-67(Δ-SH3) or lacking residues 653-853 (Δ-CT) (figure 3.6A). Furthermore, we designed a construct lacking both SH3 and C terminus domains (Δ/Δ). We then performed a phosphopaxilin immunofluorescence assay in neural crest explants expressing the truncated domain constructs. Notably Δ-SH3 and Δ-CT constructs displayed partial colocalization with phosphopaxilin cell matrix adhesions (figure3.6B). In comparison, in cells expressing the double truncated mutant, lacking both SH3 and C terminus domains, the Δ/ Δ construct showed a near complete exclusion from phosphopaxilin positive cell matrix adhesions. Hence, in agreement with previous findings (Donato et al.,2010), our results are suggestive of a dual requirement of the SH3 and C terminus domains in anchoring to cell matrix adhesions.

We next proceeded to investigate the function of the SH3 and C terminus domains on the migration of the neural crest *in vivo*. As such, Δ-SH3 and Δ-CT constructs were injected at the 8-cell stage and an *in-situ* hybridization was performed against *Twist* to label the migratory streams of the neural crest. Expression of both SH3 and CT deletion constructs in the neural crest resulted in a mild migratory deficit (figure 3.7A). In embryos injected with Δ-SH3 and Δ-CT constructs, a reduction in normalized stream length was observed on the injected side, with respect to the uninjected control side (figure3.7B). Hence, these results suggested that the Δ-SH3 and Δ-CT constructs function as dominant negatives within the neural crest.

To further probe the role of SH3 and C terminus domains in the neural crest, we examined the effect on cell dispersion and motility *in vitro*. 6 hours after plating *in vitro*, explants expressing the Δ-SH3 and Δ-CT constructs did not present any significant impairment in the degree of dispersion when compared to control neural crest explants, as assessed by a Delaunay triangulation (figure 3.8A-C). However, when the trajectory of dispersed single cells was tracked, whilst no significant difference was observed with regards to directionality of migration (figure3.8D), Δ-SH3 and Δ-CT

expressing cells did exhibit slower migration with respect to the control cells (figure3.8E). Taken together, the loss of the X-chef-1 SH3 and C terminus domains results in a mild reduction of migratory stream length *in vivo* and a reduction in the speed of migration *in vitro.*

3.2.2 Loss of tyrosine phosphorylation of the Xchef-1 substrate domain strongly impairs migration *in vivo* and dispersion and cell motility *in vitro*

Next, we sought to investigate the function of the X-chef-1 substrate domain (SD) in the neural crest. The X-chef-1 substrate domain spans from residues 67-389 and contains 12 tyrosine (Yxxp) motifs. To probe the functional role of tyrosine phosphorylation of the X-chef-1 substrate domain, we generated a phosphonull X-chef-1 fusion construct tagged to GFP (here after named Fxxp). In this construct, each tyrosine residue found within the 12 tyrosine motifs of the X-chef-1 substrate domain was mutated to a non phosphorylatable phenylalanine residue(fig3.9A-B). Notably, when immunofluorescence against phosphopaxillin was performed in neural crest explants expressing the Fxxp construct, the phosphonull construct was observed to colocalize with phosphopaxilin positive cell matrix adhesions (figure3.9C).

Using the phosphonull variant, we examined the role of tyrosine phosphorylation of X-chef-1 SD on the migration of the neural crest *in vivo*. When an *in-situ h*ybridization against *Twist* was performed in embryos injected with the mRNA of Fxxp construct, a severe impairment in migration was observed (figure3.10A). A large number of embryos did not form migratory streams at all on the injected side. In embryos which did form streams on the injected side, a significant reduction in the normalized length of the hyoid stream was observed, with respect to the control side (figure 3.10B).

To further characterize the migratory deficit, resulting from the expression of the phosphonull X-chef-1 construct, we examined cell behaviours *in vitro*, as described above. When we analyzed the extent of cellular dispersion in control and Fxxp expressing explants after 6 hours, we observed a reduction in the average Delaunay triangulation area in Fxxp expressing NC explants (fig3.11A-C). This result indicated that the loss of tyrosine phosphorylation of X-chef-1 substrate domain, impaired cell dispersion *in vitro*. To investigate the effect of tyrosine phosphorylation of X-chef-1 substrate domain on cell motility, we tracked the migratory trajectory of single cells which had dispersed from explants. Dissociated single cells expressing the Fxxp construct showed large reductions in both the velocity (figure 3.11D) and directionality(figure3.11E), comparable with the results observed in X-chef-1 MO cells. Hence, collectively our results suggest that tyrosine phosphorylation of the X-chef-1 substrate domain is required for formation of migratory streams *in vivo* and promotes cell dispersion and motility *in vitro.*

3.2.3 Discussion

In this section, we attempted to elucidate the molecular mechanism by which X-chef-1 promotes neural crest migration. As CAS proteins contain well-defined domains which facilitate interactions with a range of different proteins, we designed a number of mutated X-chef-1 constructs, with the aim of dissecting the role of each domain in different aspects of neural crest migration. As such, we designed truncated X-chef-1 constructs, lacking either the SH3 or CT domains. We furthermore designed a phosphonull construct, in which the global phosphorylation of tyrosine (Yxxp) motifs within the substrate domain was perturbed. We took the approach of perturbing tyrosine phosphorylation in the X-chef-1 substrate domain globally, rather than mutating individual tyrosine motifs. Our reasoning was based on a previous study in p130cas, where the

effect of introducing phosphonull mutations to individual vs. subsets of tyrosine motifs on wound healing migration was investigated (Shin et al.,2004). This study showed that mutating individual tyrosine residues did not have a significant effect on cell migration, suggesting a degree of redundancy in the function of the tyrosine of motifs. Mutating a larger subset of tyrosine motifs impaired the migration distance of cells to a greater extent, highlighting the importance of global tyrosine phosphorylation of the substrate domain in cell migration.

The SH3 and C-terminus domains have previously been described to have a joint function in targeting the protein to cell matirx adhesions. Consistent with observations in p130cas (Donato et al.,2010), we observed partial localisation of Δ-SH3 and Δ-CT constructs at paxillin positive cell matrix adhesions and a near complete exclusion from adhesive sites upon expression of the Δ/ Δ construct, lacking both SH3 and C-terminus domains. In the context of NC migration, expression of Δ-SH3 and Δ-CT constructs did not lead to any significant deficit in dispersion *in vitro*. However, injection of Δ-SH3 and Δ-CT constructs did result in a slight reduction in single cell speed *in vitro* and a mild reduction in the normalized migratory stream length in *vivo.* It is important to note that the full extent of the effect of the loss of the SH3 and C terminus domains on NC migration may be masked in the described results, as both deletion constructs were expressed in the presence of the endogenous X-chef-1 protein. Therefore, it is possible that the endogenous protein may compensate for any loss of function effect which may arise from the expression of Δ-SH3 and Δ-CT constructs. Hence, to further investigate the role of the SH3 and CT domains in the migration of the neural crest, deletion constructs should be expressed in NC cells injected with the X-chef-1 morpholino and further compared to cells co-injected with the X-chef-1 morpholino and full length X-chef-1 construct. Nevertheless, the observed reduction in the normalized migratory stream length and single cell speed could suggest that deletion of the cell matrix adhesion anchoring domains results in a delay in neural crest migration. Whilst the role of the

SH3 and CT domains have not been previously studied in the context of Cass4, this idea is in line with results observed in p130cas (Donato et al.,2010). Indeed, in p130cas-/- mouse embryonic fibroblasts reconstituted with p130cas Δ-CT and Δ-SH3 constructs, a reduction cell velocity was observed with respect to cells reconstituted with a full length p130cas construct (Donato et al.,2010). This impairment in cell motility, resulting from the p130cas mutants was attributed to the reduction in tyrosine phosphorylation substrate domain, as assessed though western blotting. Through their role in cell matrix adhesion anchoring, the SH3 and C terminus domains have been proposed to aid the physical extension of the substrate domain, allowing for increased accessibility for phosphorylation by Src (Sawada et al.,2006). Additionally, the protein- protein interactions of the SH3 and C terminus domains are also likely to promote motility. As described in section 1.34, FAK interacts with the SH3 domain of CAS proteins and the SH2 domain src kinase, thereby localizing CAS to cell matrix adhesions and activating src to phosphorylate the CAS substrate domain. As such, loss of the "FAK bridge" could indeed impair cell motility.

Regardless of whether and how, the SH3 and C terminus domains of X-chef-1 affect the tyrosine phosphorylation of the substrate domain, it is clear that substrate domain phosphorylation plays an important role in neural crest migration. Injection of the Fxxp construct resulted in a severe migratory deficit *in vivo*. *In vitro*, an impairment in both dispersion and single cell motility were observed, reminiscent of the phenotype observed in X-chef-1MO expressing cells. As such a strong effect is observed, upon the loss of function of tyrosine phosphorylation, in the following chapter we investigate the mechanism by which tyrosine phosphorylation promotes migration.

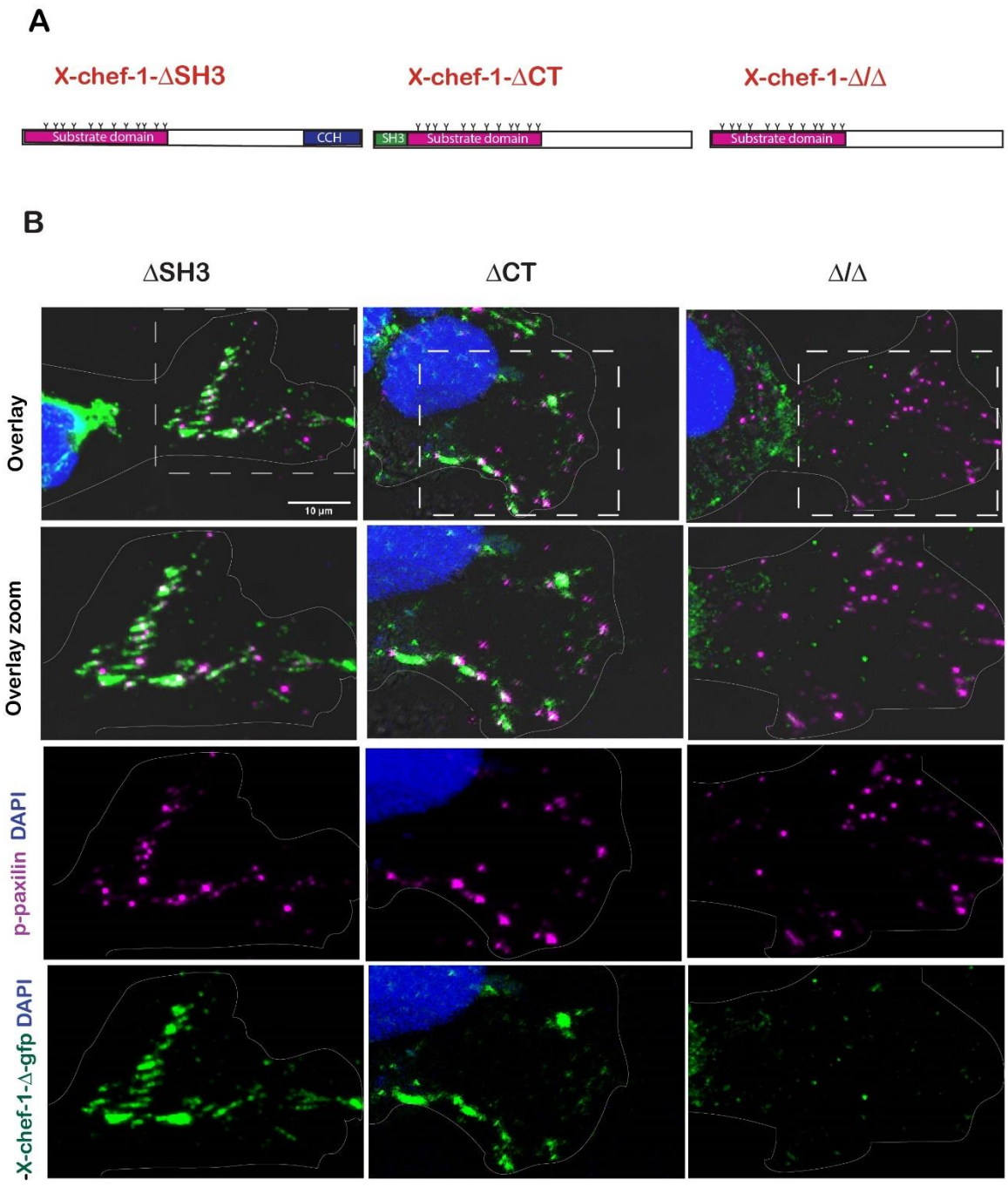

Figure 3.6: Design and subcellular localization of truncated X-chef-1 constructs

(A) Diagram to depict the design of X-chef-1 ΔSh3, ΔCT and Δ/Δ constructs (B) Immunostaining for phosphopaxilin in explants injected with the ΔSh3, ΔCT and Δ/Δ construct. Scale bar represents 10µm.

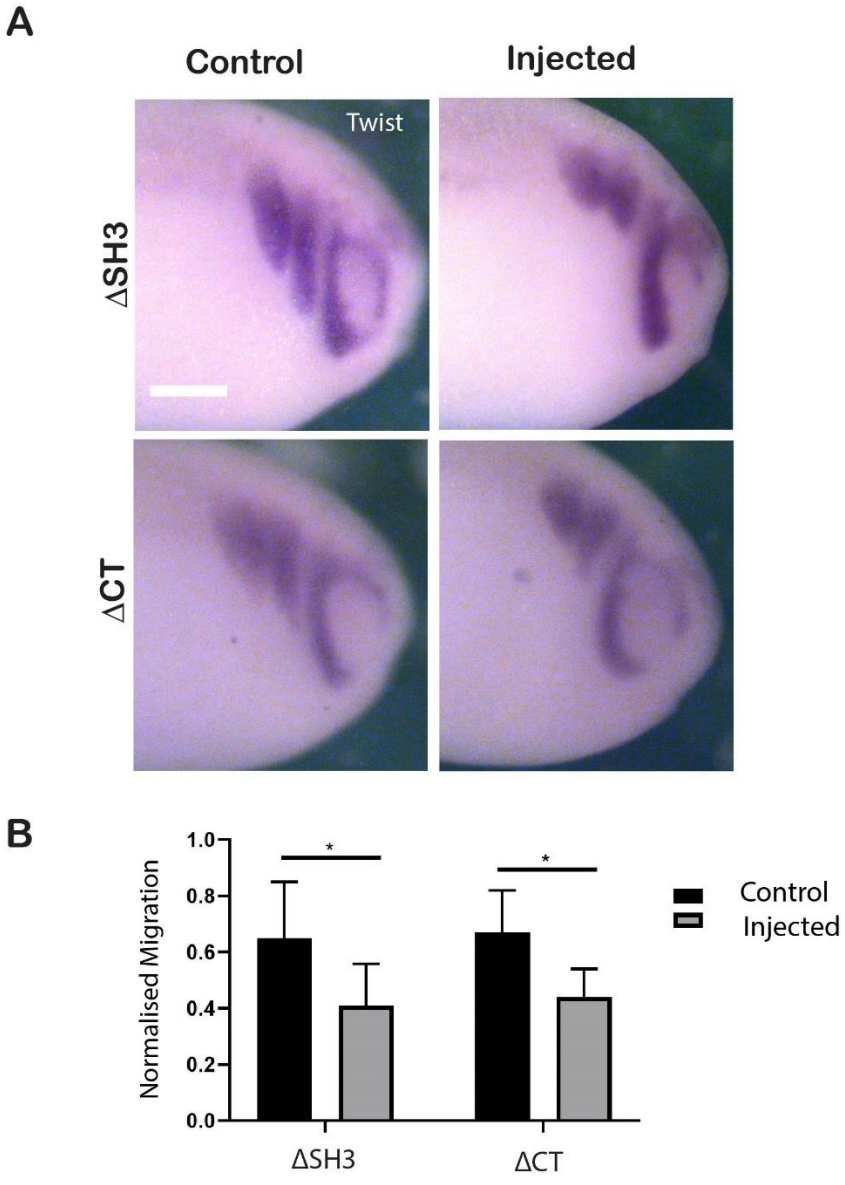
A
Control
Injected
Twist
ΔSH3
ΔCT
B
Normalised Migration
1.0
0.8
0.6
0.4
0.2
0.0
*
*
ΔSH3
ΔCT
Control
Injected

Figure 3.7: Loss of the SH3 and C terminus domains of X-chef-1 mildly impairs neural crest migration *in vivo*

(A) *In situ* hybridization of *Twist* in stage 24 embryos expressing ΔSh3 and ΔCT constructs. Control and injected sides are presented. Scale bar represents 250μm (B) normalized migration distance of the second hyoid stream in ΔSh3(n=17) and ΔCT (n=19) injected embryos; unpaired t-test* $P<0.05$. Error bars represent mean and SEM.

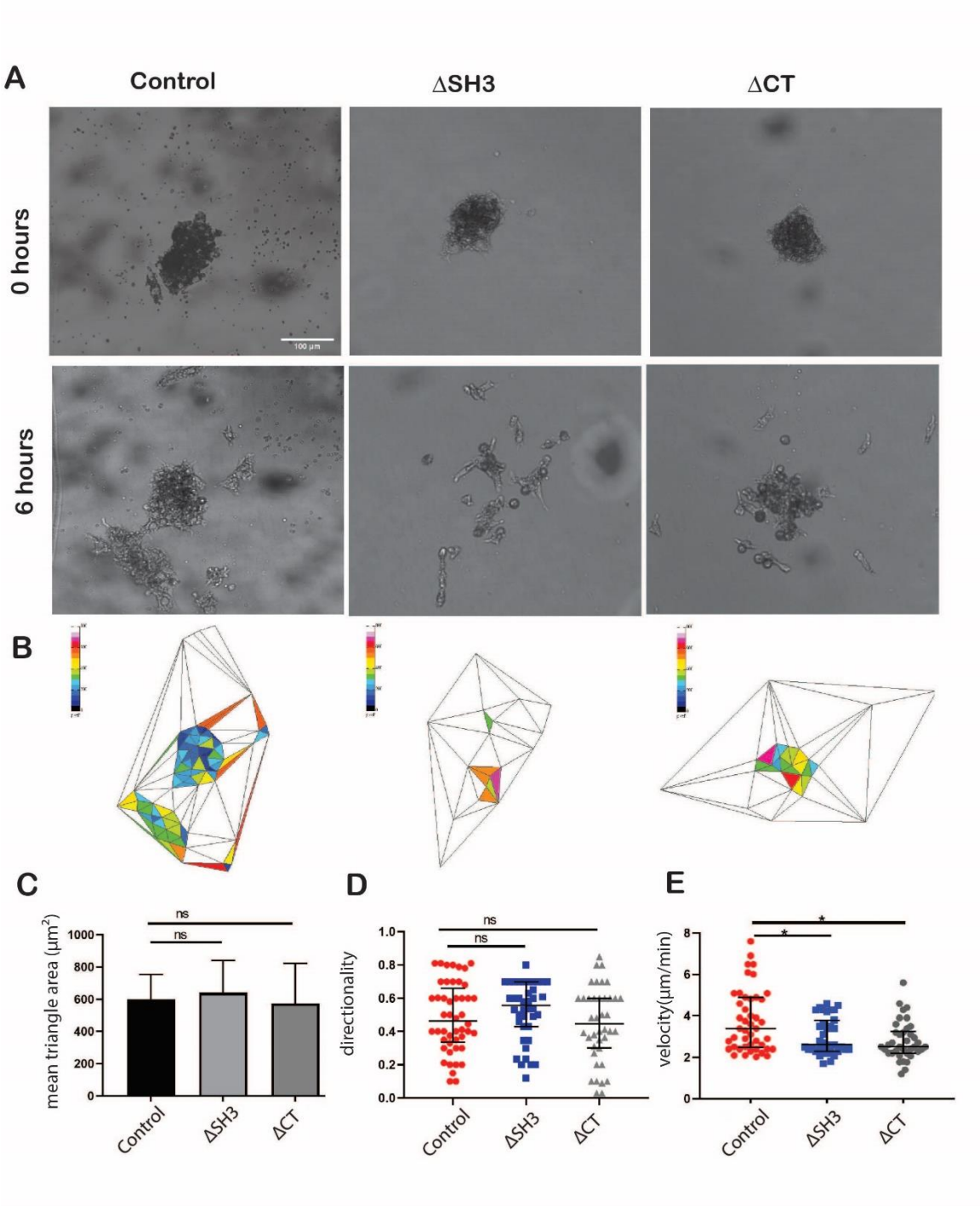
A
Control
ΔSH3
ΔCT
0 hours
6 hours
100 µm
B
C
mean triangle area (µm²)
1000
800
600
400
200
0
ns
ns
Control
ΔSH3
ΔCT
D
directionality
1.0
0.8
0.6
0.4
0.2
0.0
ns
ns
Control
ΔSH3
ΔCT
E
velocity(µm/min)
8
6
4
2
0
*
*
Control
ΔSH3
ΔCT

Figure 3.8: Loss of the SH3 and C terminus domains of X-chef-1 impairs cell motility but not dispersion *in vitro*

(A) Brightfield images of explants at zero hours (above) and 6 hours (below) of dispersion assay. Scale bar represents 100µm. (B)Visual representation of Delaunay triangulation in explants at 6 hours (C)Dispersion analysis based on average Delaunay triangulation area at 6 hours for control (n=17) and ΔSh3(n=15) and ΔCT (n=18) explants; unpaired t-test ns (D) single cell directionality in control (n=50) and ΔSh3(n=41) and ΔCT (n=43); Kruksal-Walis test with Dunn's multiple comparisons no significance ;error bars represent median and interquartile range (E) single cell velocity in control (n=50) and ΔSh3(n=41) and ΔCT (n=43); Kruksal-Walis test with Dunn's multiple comparisons * $P<0.05$; error bars represent median and interquartile range

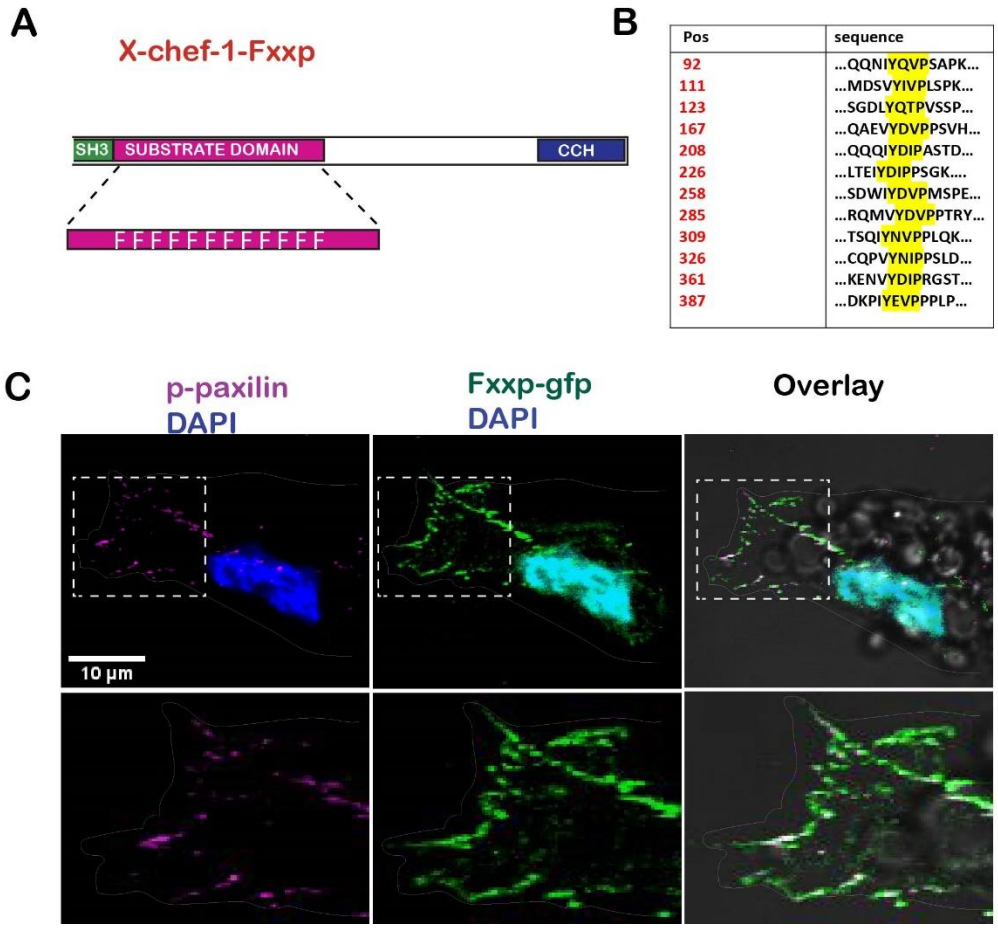

Figure 3.9: Design and subcellular localization of X-chef-1 Fxxp construct

(A)Diagram to depict X-chef-1 Fxxp construct (B) Table to indicate positions of tyrosine motifs which were mutated (C) Immunostaining for phosphopaxilin in explants injected with X-chef-1- FxxP. Scale bar represents 10µm.

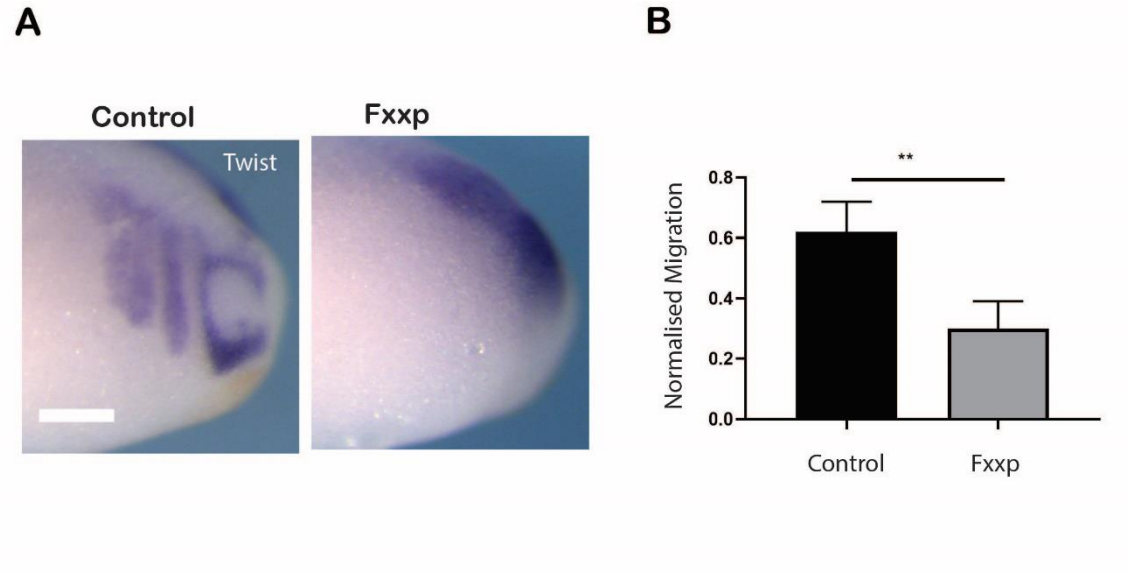

Figure 3.10: Loss of tyrosine phosphorylation of the Xchef-1 substrate domain impairs migration *in vivo*

(A) *In situ* hybridization of *Twist* in stage 24 control and Fxxp injected embryos. Scale bar represents 250µm (B)normalized migration distance of the second hyoid stream Fxxp injected embryos with respect to control side(n=20) ; unpaired t-test ** P<0.01 . Error bars represent mean and SEM.

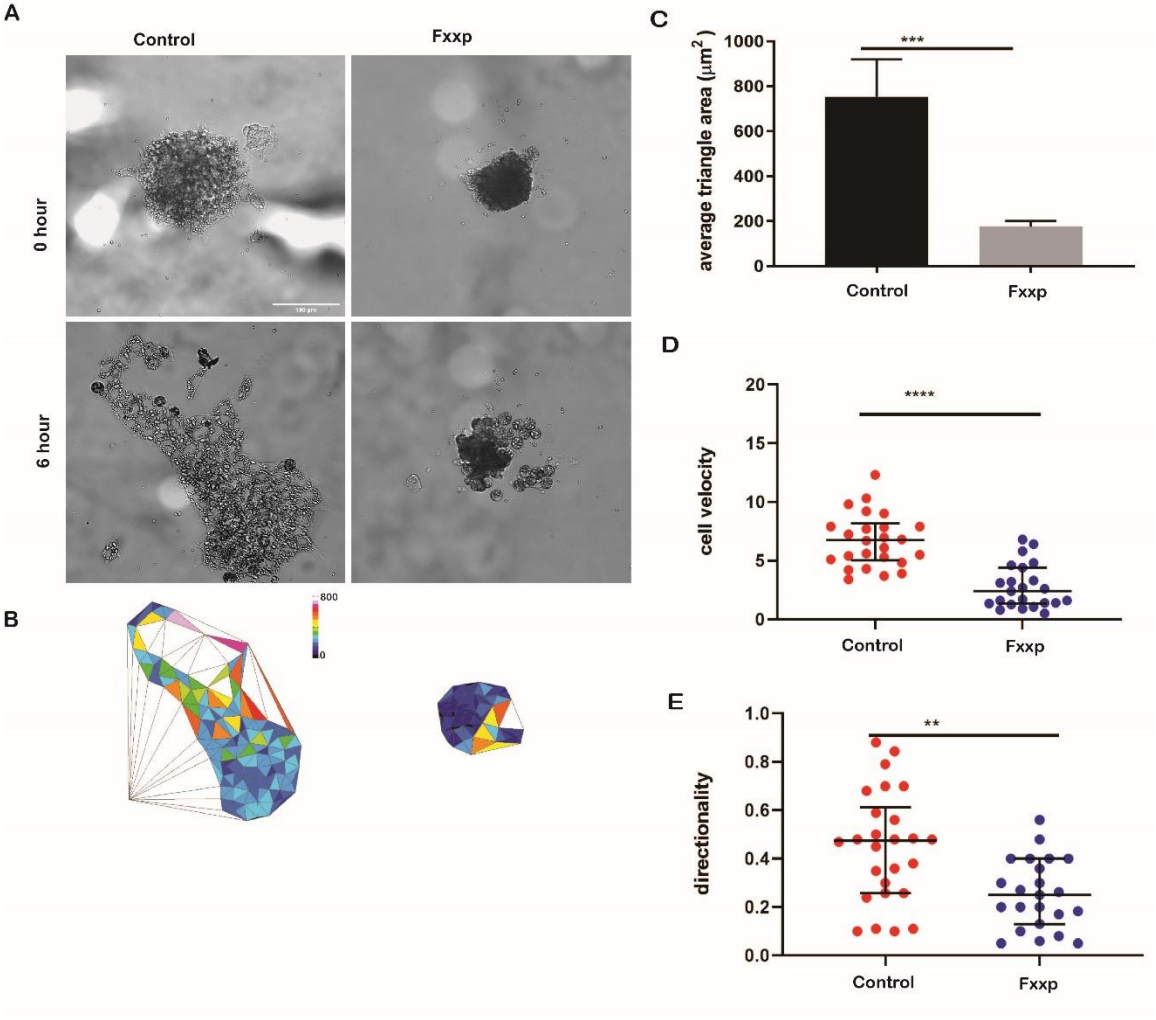

Figure 3.11: Loss of tyrosine phosphorylation of the Xchef-1 substrate domain impairs dispersion and cell motility *in vitro*

(A) Brightfield of control and X-chef-1 Fxxp explants at 0 and 6 hours. Scale bar represents 100μm (B) Visual representation of Delaunay triangulation in control and Fxxp explants at 6 hours(C)Dispersion analysis based on average Delaunay triangulation area at 6 hours for control (n=10) and Fxxp(n=10) explants unpaired t-test *** P<0.001. Error bars represent mean and SEM.(D)Single cell velocity in control (n=26) and Fxxp(n=23) cells. Mann Whitney test **** P<0.0001; error bars represent median and interquartile range (E)Single cell directionality in control (n=26) and Fxxp(n=23) cells. Mann Whitney test ** P<0.01; error bars represent median and interquartile range.

3.3 Identifying downstream targets of X-chef-1 that promote NC migration

Results in the previous section have highlighted the importance of tyrosine phosphorylation of the X-chef-1 substrate domain in the migration of the neural crest. One question which arises from this finding concerns the nature of the signaling cascades downstream of the X-chef-1 substrate domain, which promote the migration of the neural crest. To date, the function of the Cass4 substrate domain remains unknown. However, studies from other CAS family members, including p130cas and Nedd9 have shown that phosphorylated tyrosine motifs within the substrate domain can form binding sites for adaptor proteins (Klemke et al.,1998) which can subsequently recruit GDP-exchange factors to activate small G proteins (Ohashi et al.,1998), (Sanz-Moreno et al.,2008) (Kiyokawa et al.,1998). As a result, a front to rear polarity is established, through the regulation of actin polymerization and focal adhesion dynamics, which promotes cell migration. In line with this, tyrosine phosphorylation of the substrate domain of p130cas and Nedd9 has previously been reported to activate the small Rho GTPase, Rac-1(Zaidel-bar et al., 2005 , Sharma et al.,2008 Sanz-Moreno et al.,2008), which is also an established downstream effector of neural crest migration (Matthews et al.,2008). To further investigate the role of tyrosine phosphorylation of the X-chef-1 substrate domain, we examined the how cell polarity and the activity of downstream effectors of neural crest migration are affected in cells expressing an X-chef-1 phosphonull or an X-chef-1 phosphomimetic construct.

3.3.1 Loss of X-chef-1 tyrosine phosphorylation reduces size and number of cell matrix adhesions

The establishment of a front to rear polarity during mesenchymal migration is dependent on the formation cell- substrate adhesions at the leading edge of cells (Lauffenburger and Horwitz, 1996). As we observe that X-chef-1 colocalizes to paxillin positive cell matrx adhesions at the leading edge of the neural crest, we postulated that the impairment of cell migration upon the loss of function of X-chef-1 could be attributed to an effect on the formation of cell matrix adhesions. To test this idea, we injected embryos with X-chef-1 phosphonull construct (Fxxp) and performed an immuno against phosphopaxilin. In comparison with control neural crest cells, a reduction in the number and area of cell matrix adhesions was observed, in cells injected with the phosphonull substrate domain (SD) construct (fig3.12A-C), suggesting that tyrosine phosphorylation may be required for the formation of cell matrix adhesions during neural crest migration.

3.3.2 Loss of X-chef -1 SD tyrosine phosphorylation impairs cell matrix adhesion and lamellipodial dynamics

Given the observed effect on phosphopaxillin positive cell matrix adhesions, upon the loss of X-chef-1 SD tyrosine phosphorylation, we further investigated how cell matrix adhesion dynamics were affected using an exogenous focal adhesion kinase construct fused to GFP (FAK-GFP). Embryos were coinjected with a FAK-GFP construct and either the X-chef-1 morpholino or an untagged Fxxp construct. The neural crest was dissected and FAK-GFP expressing cells were imaged over time (figure 3.13A). Cell matrix adhesions at the leading edge in the morpholino or Fxxp injected cells were smaller in area (figure 3.13B), in confirmation with the results described

above. Furthermore, cell matrix adhesions in *X-chef-1* MO or Fxxp cells appeared to be more unstable. When the longevity of cell matrix adhesions was quantified, adhesions within *X-chef-1* MO and Fxxp expressing cells were significantly shorter in duration (figure3.13C-D). Whilst no significant difference was observed in the rates of adhesion assembly in *X-chef-1* MO or Fxxp cells with respect to the control (figure 3.13E), the disassembly rates of cell matrix adhesions in both *X-chef-1* MO and Fxxp cells were significantly greater (figure3.13F).

In addition to examining the effect on cell matrix adhesion dynamics, we further characterized the effect on protrusion dynamics upon the loss of function of X-chef-1(figure 3.14A). Notably, cells injected with the X-chef-1 MO or the phosphonull variant exhibited severe deficits in cell polarity and the majority of cells failed to form protrusions (figure 3.14B). In cells which were able to form protrusions they were smaller in area (fig3.14A, C) and shorter in duration (figure 3.14A,D) in X-*chef-1* MO or FxxP expressing cells. Hence, our results suggest that X-chef-1 SD phosphorylation is required for the establishment of a leading-edge polarity through regulating cell matrix adhesion and lamellipodial dynamics during neural crest migration.

3.3.3 Loss of X-chef-1 SD phosphorylation inhibits Rac-1 activation at leading edge

Due to the impairment of the front to rear cell polarity observed upon the loss of X-chef-1 SD tyrosine phosphorylation, we hypothesized that tyrosine phosphorylation of the X-chef-1 substrate domain could promote activation of the small rho GTPase Rac-1 at the leading edge during neural crest migration. To test this idea, we preformed immunofluorescence against Rac-GTP on neural crest explants *in vitro*. As an initial control, to validate the specificity of the antibody, we analyzed Rac-GTP fluorescence intensity in cells that were treated with Rac-1

inhibitor, NSC23766 (figure3.15A). NSC23766 is a small molecule inhibitor which inhibits Rac-1 activity, through interfering with Rac-GEF binding (Gao et al.,2004). Whilst Rac-GTP fluorescence intensity could be observed at the leading edge of control cells, it was almost undetectable in cells treated with the inhibitor (figure3.15A).

Having confirmed the specificity of the Rac-GTP antibody, we proceeded to preform immunofluorescence against Rac-GTP, upon the loss of function of X-chef-1. Immunofluorescence was performed on control, X-chef-1 MO and Fxxp expressing cells that were cultured on polyacrylamide gels with a stiffness of 150pascals, comparable to that of the migratory mesoderm *in vivo* (Barriga et al.,2018) (fig3.16A). The intensity profile of Rac-GTP immunofluorescence was analysed along a line segment, starting from the leading edge moving towards the cell body (fig3.16B). Furthermore, a ratio of protrusive to cytoplasmic immunofluorescence was also computed(fig3.16C) In cells injected with the X-chef-1 morpholino injected or Fxxp construct, a reduced fluorescence intensity was observed at the leading edge, with respect to control cells plated on stiff substrates. This suggested that tyrosine phosphorylation of the X-chef-1 substrate domain can promote Rac-1 activation at the leading edge of cells during neural crest migration (figure3.16A-C). In addition, to further investigate whether Rac-1 activation can being regulated by X-chef-1 in a substrate stiffness dependent manner (discussed further in the next section), we in parallel examined whether Rac-1 activity in the neural crest was dependent on the stiffness of the substrate which the cells adhere to . As such, we further analyzed levels of Rac-GTP immunofluorescence in control cells adhering to polyacrylamide gels with stiffness values of approximately 50 pascals, comparable to the stiffness measured in non-migratory mesoderm *in vivo* (Barriga et al.,2018). Similarly, to X-chef-1 deficient cells, lower levels of Rac-GTP fluorescence were observed in control cells adhering to soft substrates, in comparison to control cells plated on stiff substrates.

As an alternative method to assess the activity of Rac-1 within the neural crest, we made use of a live pak-gbd sensor (Stephenson et al.,2017). This sensor is an injectable mRNA probe, containing the GTPase binding domain(gbd) of an effector protein, known as pak, which specifically binds active conformation of Rac-1 (figure 3.17A). The gbd domain is fluorescently tagged, hence local increases in fluorescence intensity are observed when bound to active Rac-1. As a read out of active Rac-1 at the leading edge of cells, a ratio of protrusive to cytoplasmic GFP fluorescence was computed. The relative GFP fluorescence levels were lower in cells injected with the X-chef-1 MO or Fxxp compared to control cells, supporting previous results using the Rac-GTP antibody (figure3.17B-C). Furthermore, in a similar manner, control cells adhering to soft polyacrylamide substrates were also observed to have reduced GFP fluorescence levels. Hence, our results from two complementary approaches suggest that tyrosine phosphorylation of the X-chef-1 substrate domain promotes Rac-1 activation at the leading edge of the neural crest and that Rac-1 activation in the neural crest is dependent on the stiffness of the substrate to which cells adhere to.

3.3.4 Constitutive activation of X-chef-1 SD tyrosine phosphorylation increases cell matrix adhesion number, protrusion size and promotes Rac-1 activation

As the loss of tyrosine phosphorylation of the X-chef-1 substrate domain impaired cell polarity and Rac-1 activation at the leading edge, we sought to investigate the effect of constitutive tyrosine phosphorylation of X-chef-1 within the neural crest. To this end, we designed a phosphomimetic X-chef-1 construct (ExxP) in which all tyrosine residues found within the 12 tyrosine motifs of the X-chef-1 substrate domain were mutated to a phosphomimetic glutamate residue (fig3.18A). The Exxp was introduced into the neural crest via a targeted injection at the 8-cell stage and immunofluorescence against phosphopaxillin was performed in neural crest

explants. Similarly, to the phosphonull construct, the phosphomimetic variant localized preferentially to phosphopaxillin positive cell matrix adhesions (fig3.18B). When we analyzed the effect on the size and number of cell matrix adhesions, we observed that overexpression of the Exxp construct in the neural crest resulted in an increase in the number of cell matrix adhesions at the leading edge of the neural crest. (fig3.19A-B)

Next, we further questioned how constitutive tyrosine phosphorylation affected leading edge protrusions. Time lapse images of cellular protrusions in control and Exxp expressing cells were acquired (figure3.20A). Analysis of leading-edge protrusions revealed that protrusions were larger in area (fig 3.20B) in Exxp expressing cells with respect to the control. Finally, the observed effect on the size of leading-edge protrusions lead us to investigate how Rac-1 activity was affected in Exxp expressing cells. As such, we preformed immunohistochemistry against Rac-GTP in neural crest explants, similarly as described above. When we examined Rac-GTP immunofluorescence levels in cells expressing the phosphomimetic X-chef-1 variant, we observed an increase in Rac-GTP fluorescence intensity at the leading edge (fig 3.21A-C). Taken together, these results suggest that constitutive tyrosine phosphorylation of X-chef-1 substrate domain increases cell matrix adhesion number, protrusion size and promotes Rac-1 activation at the leading edge.

3.3.5 Discussion

In this section, we investigated how tyrosine phosphorylation of the X-chef-1 substrate domain promotes the migration of the neural crest. The substrate domain of CAS proteins contains a series of tyrosine (YxxP) motifs which when phosphorylated can trigger downstream signaling cascades that promote cell migration (Klemke et al.,1998, Ohashi et al.,1998) through the regulation of actin polymerization and focal adhesion dynamics. Making use of the phosphonull

(Fxxp) construct (introduced in section 3.2) and a phosphomimetic X-chef-1 variant, we examined how tyrosine phosphorylation affected cell polarity in the neural crest.

Expression of the Fxxp construct resulted in the formation of fewer cell matrix adhesions, which were smaller in area, consistent with the reported decrease in paxillin staining in Cass4 siRNA treated cells (Singh et al.2008). In addition to cell matrix adhesion formation,. our dynamic analysis using an exogenous FAK-GFP construct, indicated that loss of tyrosine phosphorylation affected the stability of cell matrix adhesions, with higher adhesion disassembly rates in treated cells .As FAK is present in both early focal complexes and later developing focal adhesions(Zaidel-bar et al.,2003), we are unable to determine whether the observed effect on adhesion disassembly rates, was reflective of an impairment on focal adhesion maturation *per se*. Further analysis of adhesion assembly and disassembly rates using a fluorescent reporter for zxyin, which is exclusively present in mature focal adhesions (Zaidel-bar et al., 2003) would shed greater light on this issue From acquired time lapse images, we also observed that fewer cells formed protrusions, which were smaller in area and shorter in duration. Consistent with its role in protrusion and adhesion formation (Ridley et al.,1992 ,Nobes et al.,1995), we observed a decrease in active Rac-1 at the leading edge of cells, through the use of an antibody detecting the active conformation of Rac-1 and an exogenous pak-gbd sensor. The described results were further reinforced by the phenotypes observed in cells expressing a phosphomimetic X-chef-1 variant. Overexpression of the phosphomimetic Exxp construct resulted in a greater number of cell matrix adhesions and larger membrane protrusions at the cell front. Furthermore, Exxp expressing cells displayed higher levels of Rac-GTP immunofluorescence at the leading edge. Hence, our results collectively suggest that X-chef-1 is an important regulator of cell polarity, through a possible activation of Rac-1.

Whilst our findings support a role for an X-chef-1/Rac-1 signaling axis in the establishment of a front to rear polarity during NC migration, further studies will be required. Importantly, it will be necessary to perform a rescue experiment in phosphonull cells ,utilizing a photoactivatable Rac-1 construct (Wu et al.,2009), to investigate whether the impairment of adhesion and protrusion formation are restored and whether a localized activation of Rac-1 is sufficient to promote NC migration. Furthermore, our results raise the question of how X-chef-1 could activate Rac-1. We discuss potential mechanisms of Rac-1 activation in greater length and propose further lines of investigation in section 4.3.

In addition to highlighting the potential function of an X-chef-1/Rac-1 mediated pathway during NC migration, the results in this chapter have also suggested that Rac-1 activity is dependent on substrate stiffness. Hence, in the following section, we will use our phosphomimetic construct to investigate whether X-chef-1 plays a role in the substrate stiffness dependent activation of Rac-1 within the neural crest.

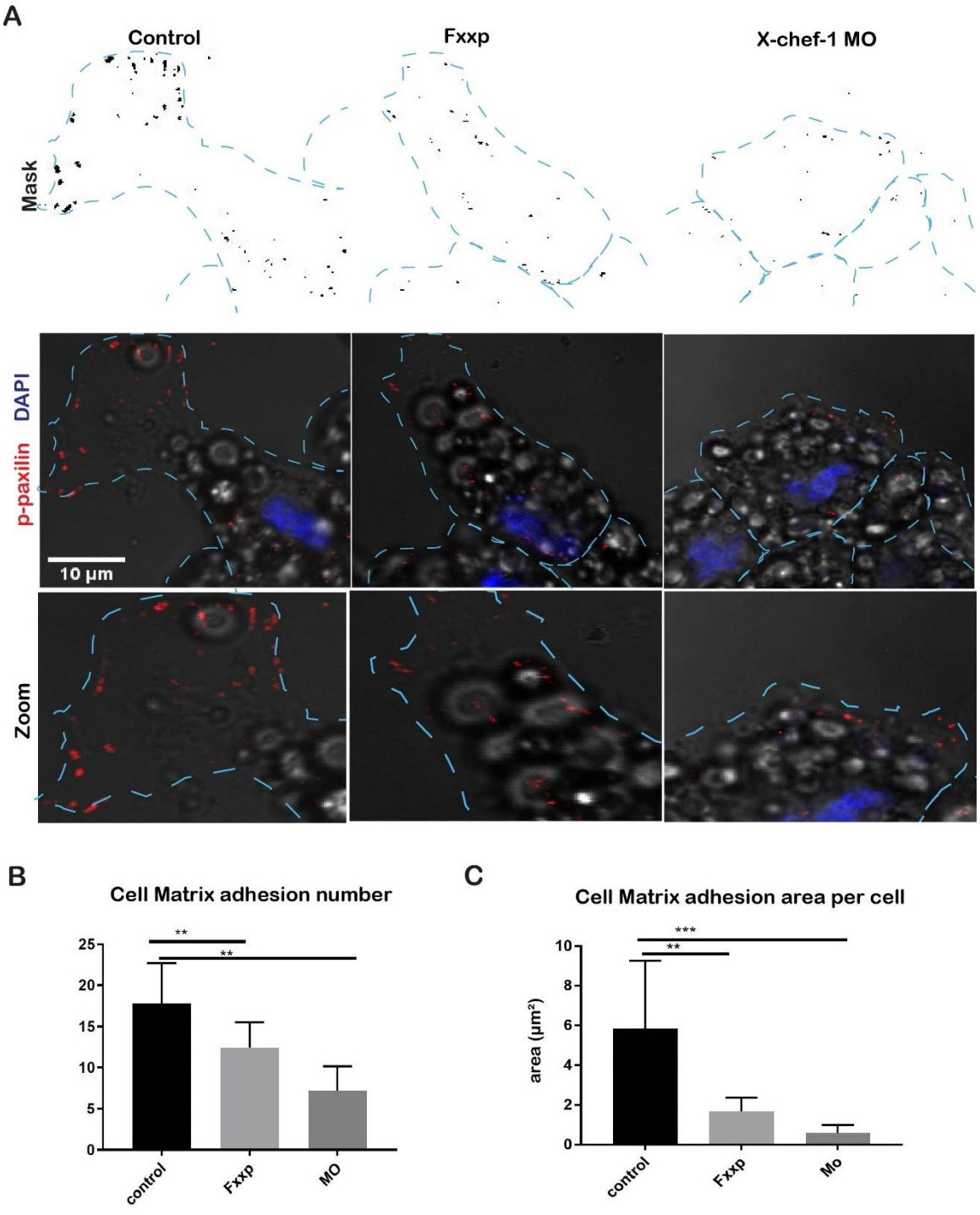
A
Control
Fxxp
X-chef-1 MO
Mask
DAPI
p-paxilin
10 µm
Zoom
B
Cell Matrix adhesion number
**
**
25
20
15
10
5
0
control
Fxxp
MO
C
Cell Matrix adhesion area per cell
***
**
area (µm²)
10
8
6
4
2
0
control
Fxxp
Mo

Figure 3.12: Loss of X-chef SD tyrosine phosphorylation reduces size and number of cell matrix adhesions

(A) Immunostaining for phosphopaxilin and DAPI in control Fxxp and MO cells (B) Number of cell matrix adhesions at the leading edge in control (n=12) Fxxp(n=12) and Mo (n=8) expressing cells; one way ANOVA with Dunnetts multiple comparisons **p<0.01 (C) cell matrix adhesion area per cell at the leading edge in control (n=12) Fxxp(n=12) and Mo (n=8) expressing cells; one way ANOVA with Dunnetts multiple comparisons **p<0.01 Error bars represent mean and standard deviation

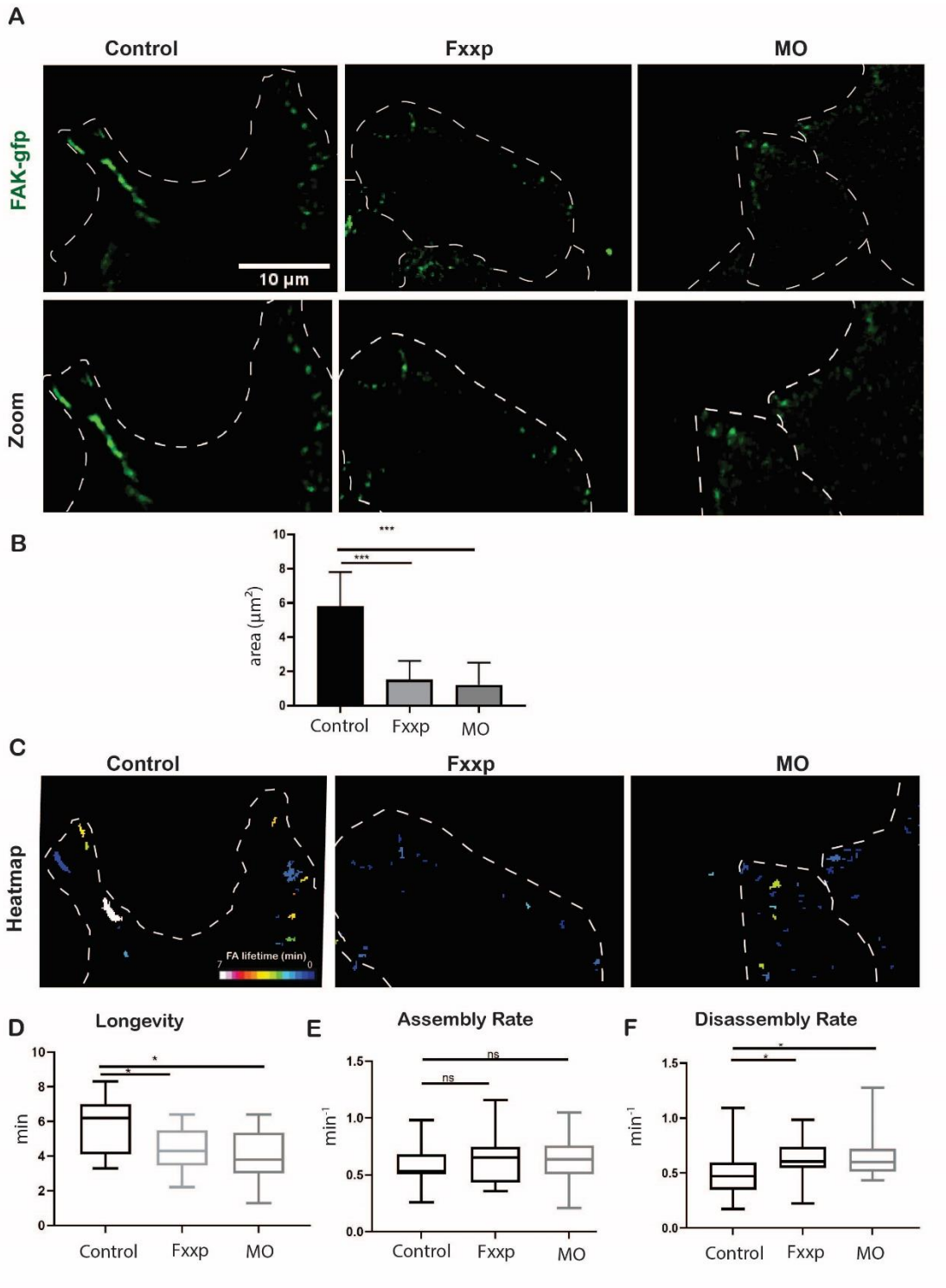
A
Control
Fxxp
MO
FAK-gfp
10 µm
Zoom
B
***
***
area (µm²)
Control
Fxxp
MO
C
Control
Fxxp
MO
Heatmap
FA lifetime (min)
D
Longevity
min
Control
Fxxp
MO
E
Assembly Rate
ns
ns
min⁻¹
Control
Fxxp
MO
F
Disassembly Rate
*
*
min⁻¹
Control
Fxxp
MO

Figure 3.13: Loss of X-chef SD tyrosine phosphorylation reduces cell matrix adhesion size and stability

(A) (above) still images of control, Fxxp and MO cells expressing FAK-GFP (below) zoom of control Fxxp and Mo cells expressing FAK-GFP (B) cell matrix adhesion area in control(n=20) Fxxp (n=17) X-chef-1 MO(n=14)cells ;one way ANOVA with Dunnetts multiple comparisons ***p<0.001 (C) Representative heatmaps of cell matrix adhesion longevity in control ,Fxxp and X-chef-1 MO cells (D) Cell matrix adhesion longevity in in control (n=20) Fxxp (n=17) X-chef-1 MO(n=14)cells * p<0.05 Kruksal-Walis test with Dunn's multiple comparisons (E) cell matrix adhesion assembly rate in control (n=20) Fxxp (n=17) X-chef-1 MO(n=14)cells ; ns p>0.05 Kruksal-Walis test with Dunn's multiple comparisons. Error bars represent min-max range and median (E) cell matrix adhesion disassembly rate in in control (n=20) Fxxp (n=17) X-chef-1 MO(n=14)cells expressing cells; * p<0.05 Kruksal-Walis test with Dunn's multiple comparisons. Error bars represent min-max range and median.

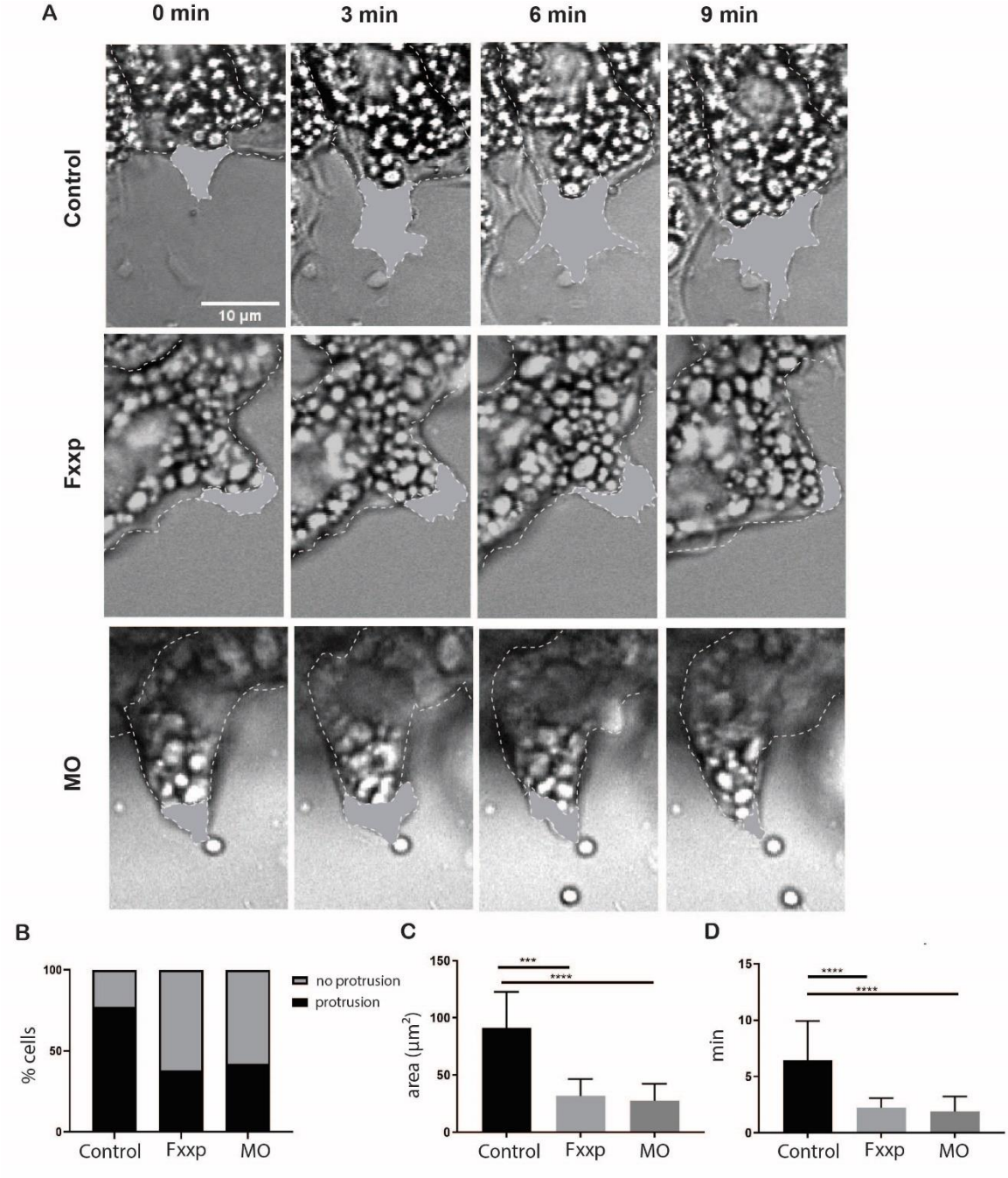
A
0 min
3 min
6 min
9 min
Control
Fxxp
MO
10 µm
B
% cells
100
50
0
no protrusion
protrusion
Control
Fxxp
MO
C
area (µm²)
150
100
50
0
***
****
Control
Fxxp
MO
D
min
15
10
5
0
****
****
Control
Fxxp
MO

Figure 3.14: Loss of X-chef SD tyrosine phosphorylation impairs formation and stability of protrusions

(A) Representative time lapse images to show the membrane protrusions 0, 3 6 and 9 mins after their formation in control, Fxxp and MO expressing cells. Membrane protrusions are defined as the region of the cell lacking yolk platelets and have been highlighted in grey. (B) Percentage of control (n=43) Fxxp (n=39), and X-chef-1 MO (n=41) forming protrusions in 15 minute time frame (C) Quantification of protrusion area in control (n=17) Fxxp (n=17), and X-chef-1 MO (n=17); unpaired t-test Error bars represent mean and standard deviation unpaired t-test *** P<0.001 (D).Quantification of duration of protrusions in control (n=17) Fxxp (n=17) and X-chef-1 MO expressing cells (n=17); unpaired t-test **** P<0.0001 Error bars represent mean and standard deviation.

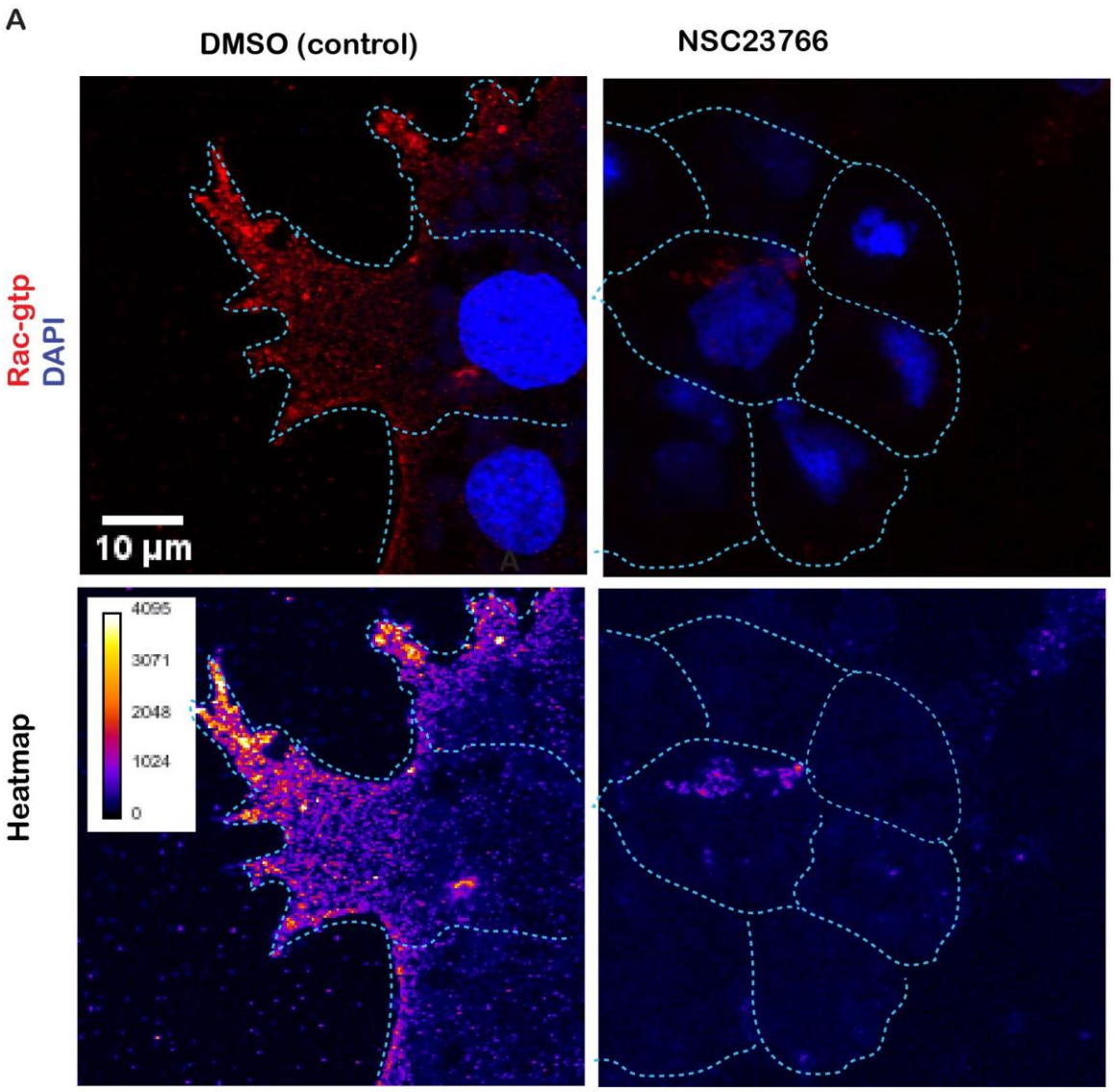

Figure 3.15: Validating the specificity of the Rac-GTP antibody (A)Representative images of Rac-GTP immunofluorescence in control and explants incubated with 100µm NSC23766.

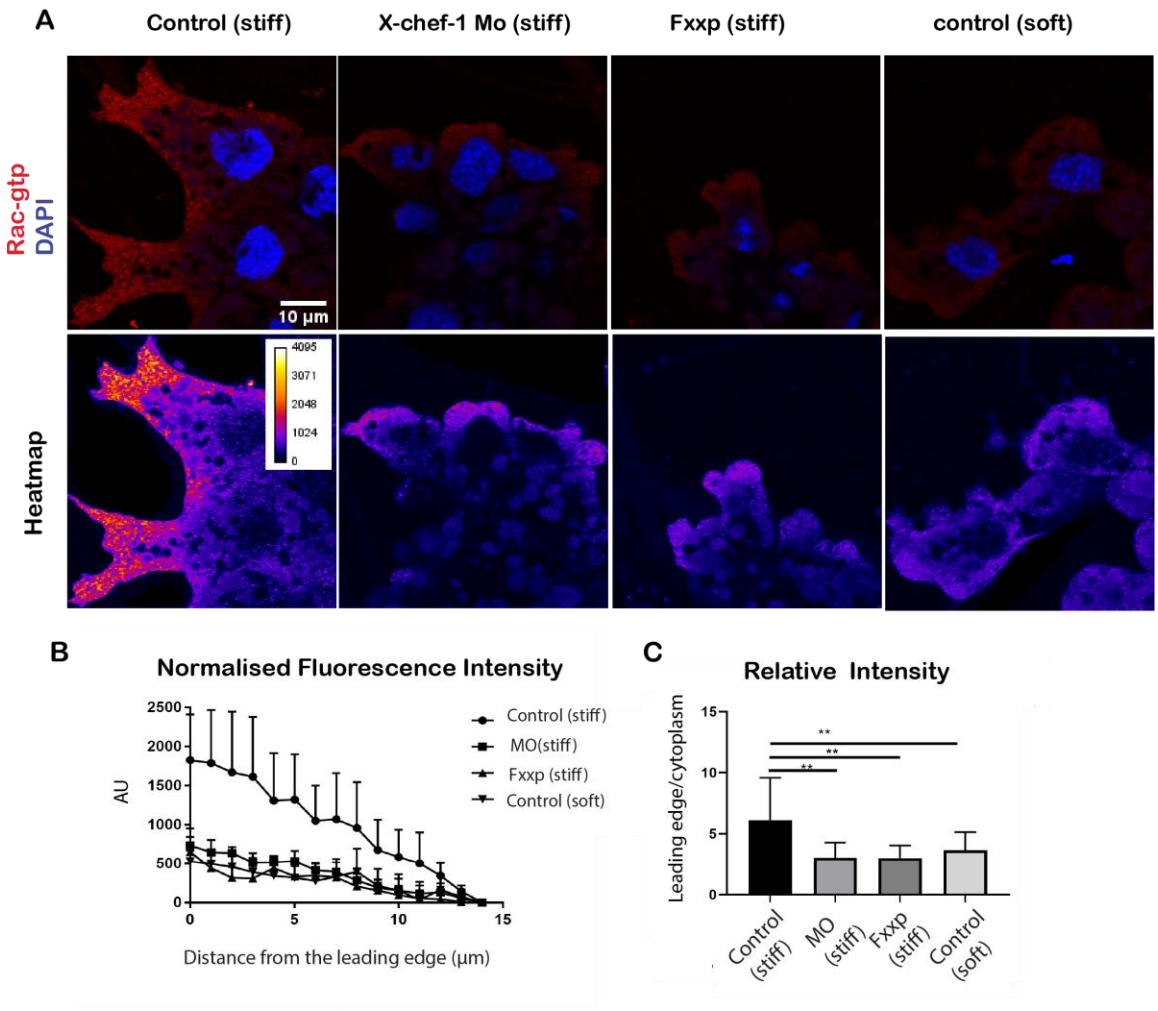

Figure 3.16: Loss of X-chef-1 SD phosphorylation reduces Rac-1 activation at leading edge (1)

(A)Representative images of Rac-GTP immunofluorescence (from left to right) of control, X-chef-1-MO and Fxxp cells plated on stiff substrates and control cells plated on soft polyacrylamide gels (B) Distribution of Rac-1 intensity from the leading edge to the cell body in X-chef-1 MO (n=16), Fxxp (n=15) ,control cells (n=20), plated on stiff substrates and control cells plated on soft substrates (n=15). Error bars represent mean and SEM (C) Relative Rac-GTP fluorescence intensity in protrusions normalized to the cytoplasm in in X-chef-1 MO (n=16), Fxxp (n=15) ,control cells (n=20) plated on stiff substrates and control cells plated on soft substrates (n=15).One way ANOVA with Dunnetts multiple comparsions** P<0.01. Error bars represent mean and SEM.

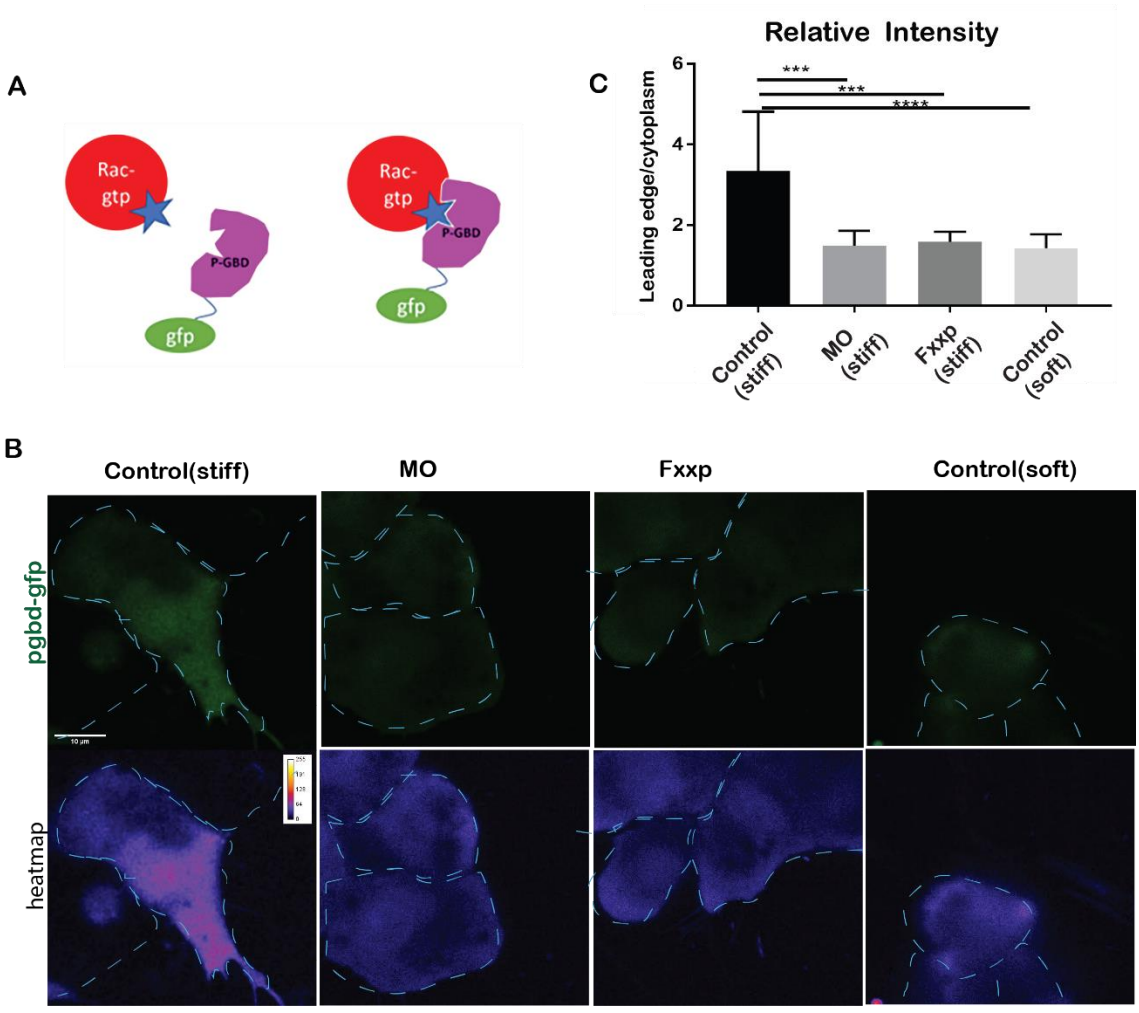

Figure 3.17: Loss of X-chef SD phosphorylation reduces Rac-1 activation at leading edge (2)

(A)Diagram to depict the mechanism of action of the pak-gbd sensor (B)Confocal projections (from left to right) of control, X-chef-1-MO and Fxxp cells plated on stiff substrates and control cells plated on soft polyacrylamide gels. Scale bar represents 10µm (c) Quantification of pak-gbd-GFP fluorescence intensity in protrusions normalized to the cytoplasm in control (n=20), X-chef-1 MO (n=16), Fxxp (n=15) cells plated on stiff substrates and control cells plated on soft substrates(n=11);one way ANOVA with Dunnetts multiple comparisons *** P<0.001 Error bars represent mean and standard deviation.

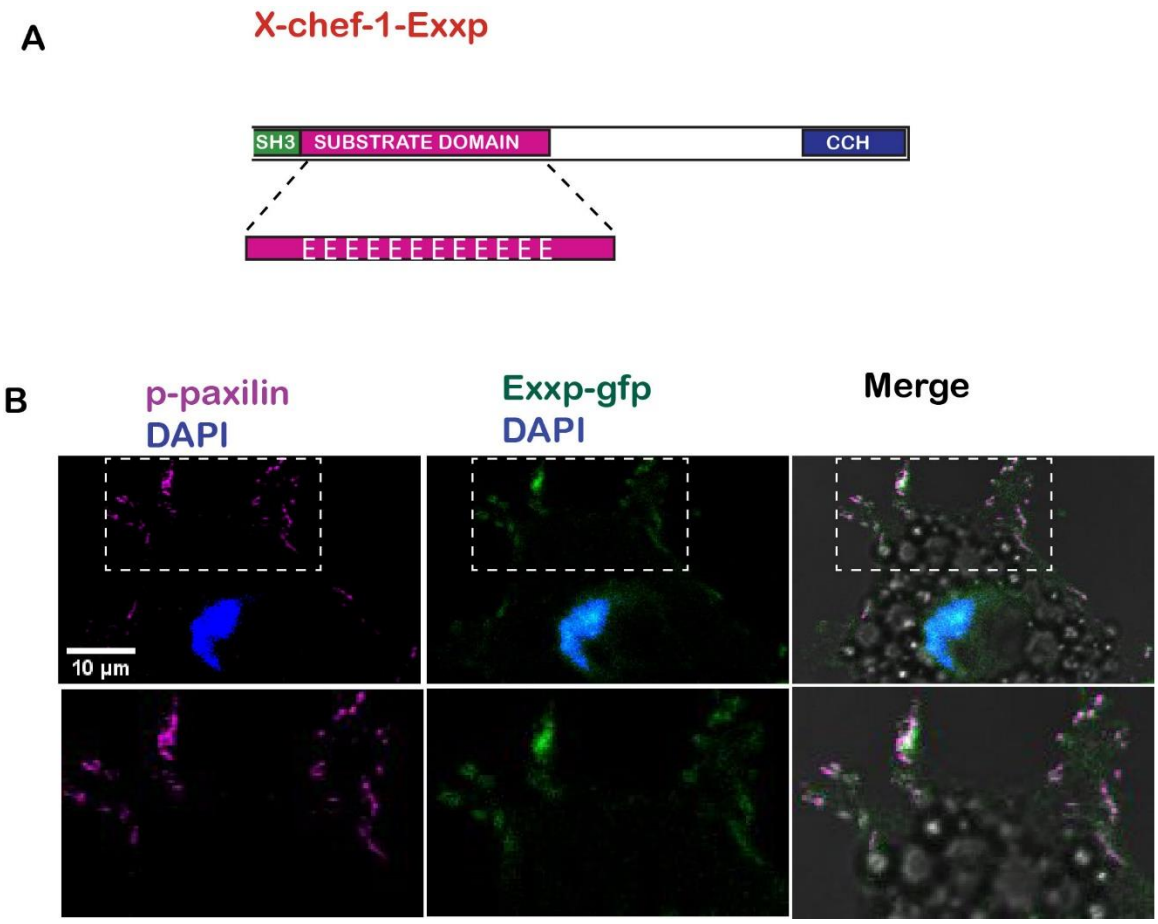

Figure 3.18: Design and localization of X-chef-1 phosphomimetic substrate domain construct

(A)Schematic of Exxp construct (B) Immunostaining for phosphopaxilin in explants injected with ExxP

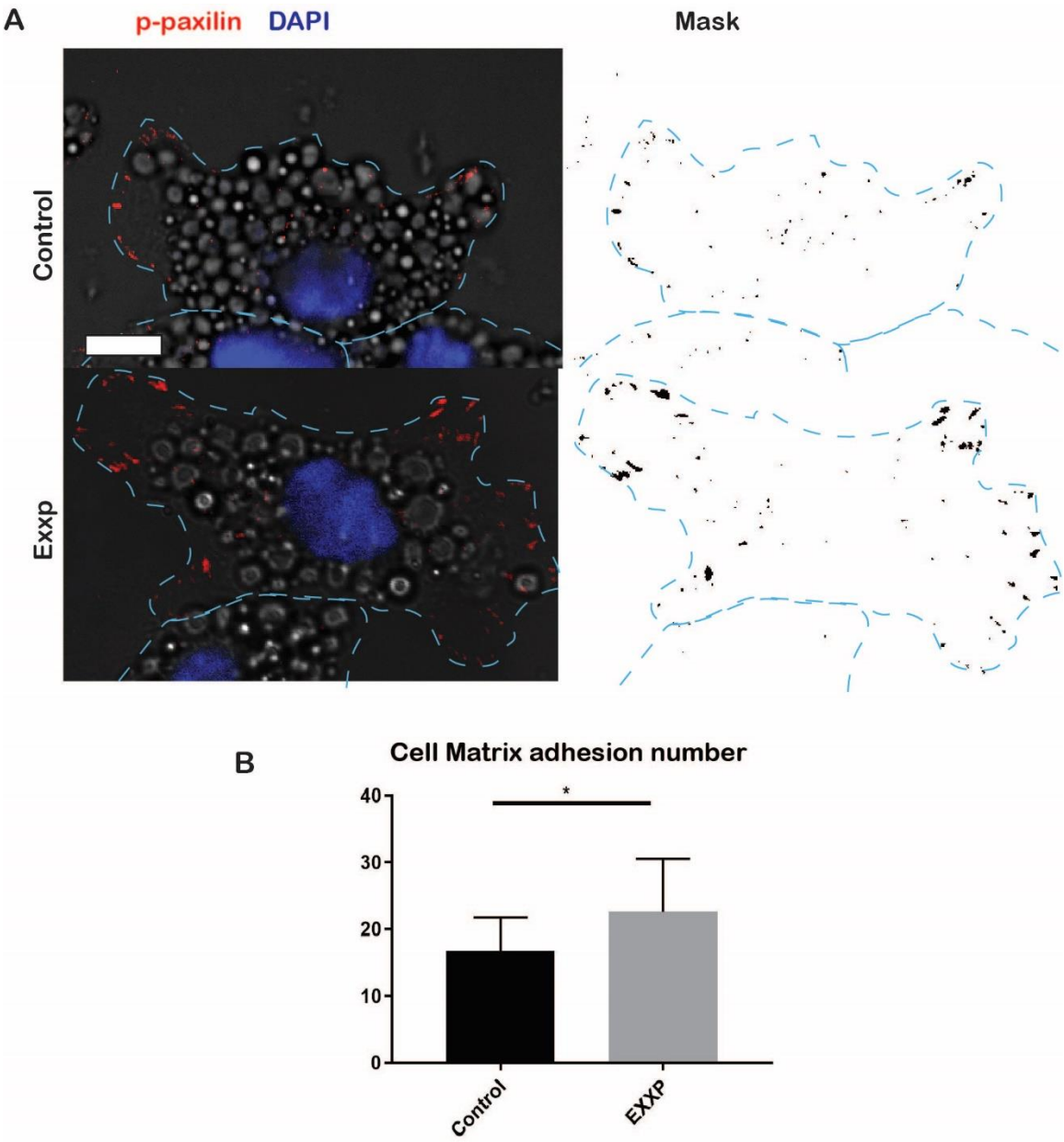

Figure 3.19: Constitutive activation of X-chef SD tyrosine phosphorylation results in an increased number of cell matrix adhesions at the leading edge

(A)Immunostaining for phosphopaxilin and DAPI in control and Exxp expressing cells. Scale bar represents 10µm (B) number of cell matrix adhesions at the leading edge in control (n=12) and Exxp(n=12) expressing cells; unpaired t-test*$p<0.05$. Error bars represent mean and standard deviation.

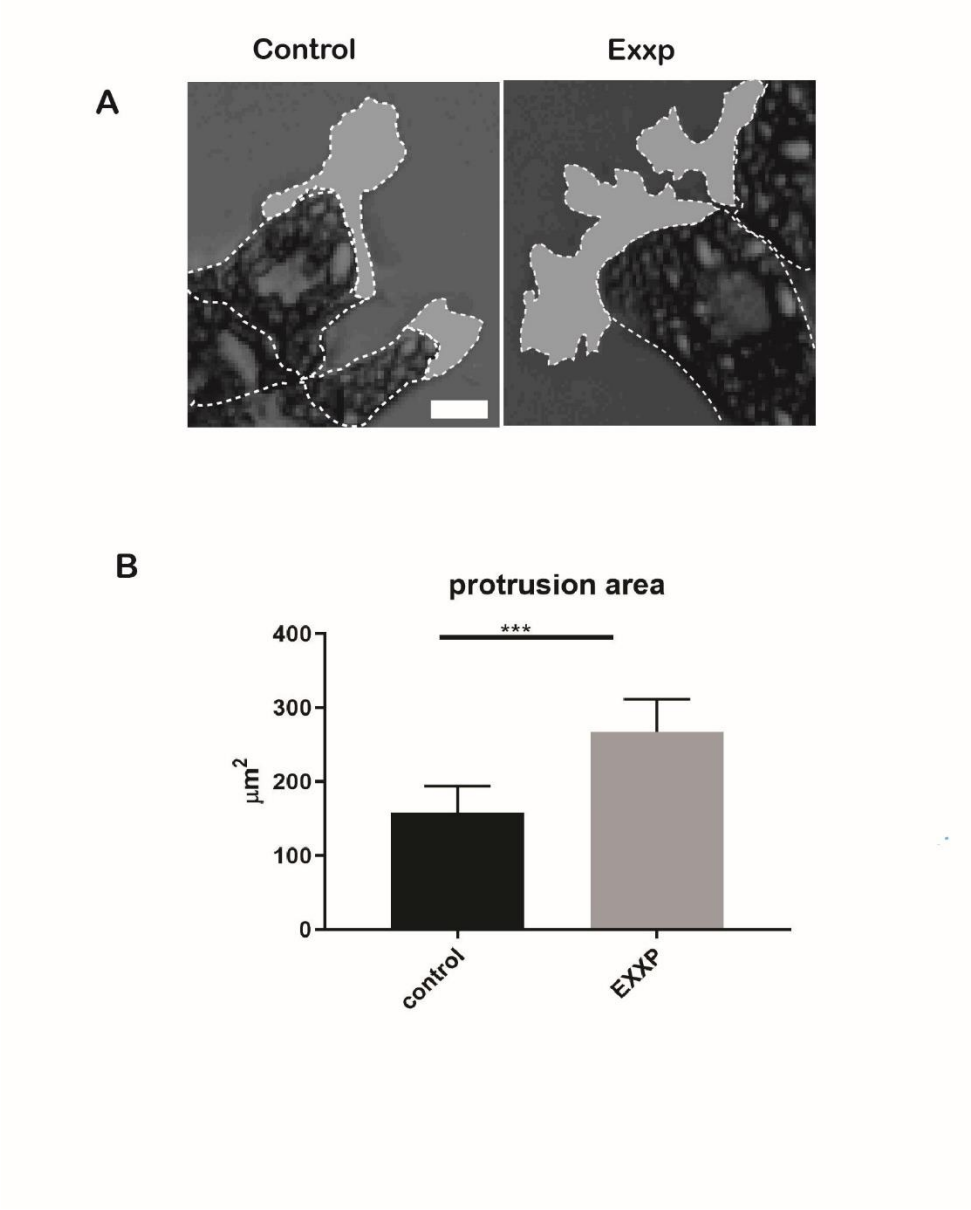

Figure 3.20: Constitutive activation of X-chef SD tyrosine phosphorylation results in an increase in the size of protrusions at the leading edge

(A)Images of leading-edge protrusions in control cells (left) and Exxp expressing cells (right) Shaded region indicates cell protrusions which is devoid of yolk platelets. Scale bar represents 10µm. (B) Quantification of protrusion area in control (n=17) and Exxp expressing cells (n=20); unpaired t-test *** P<0.001. Error bars represent mean and standard deviation.

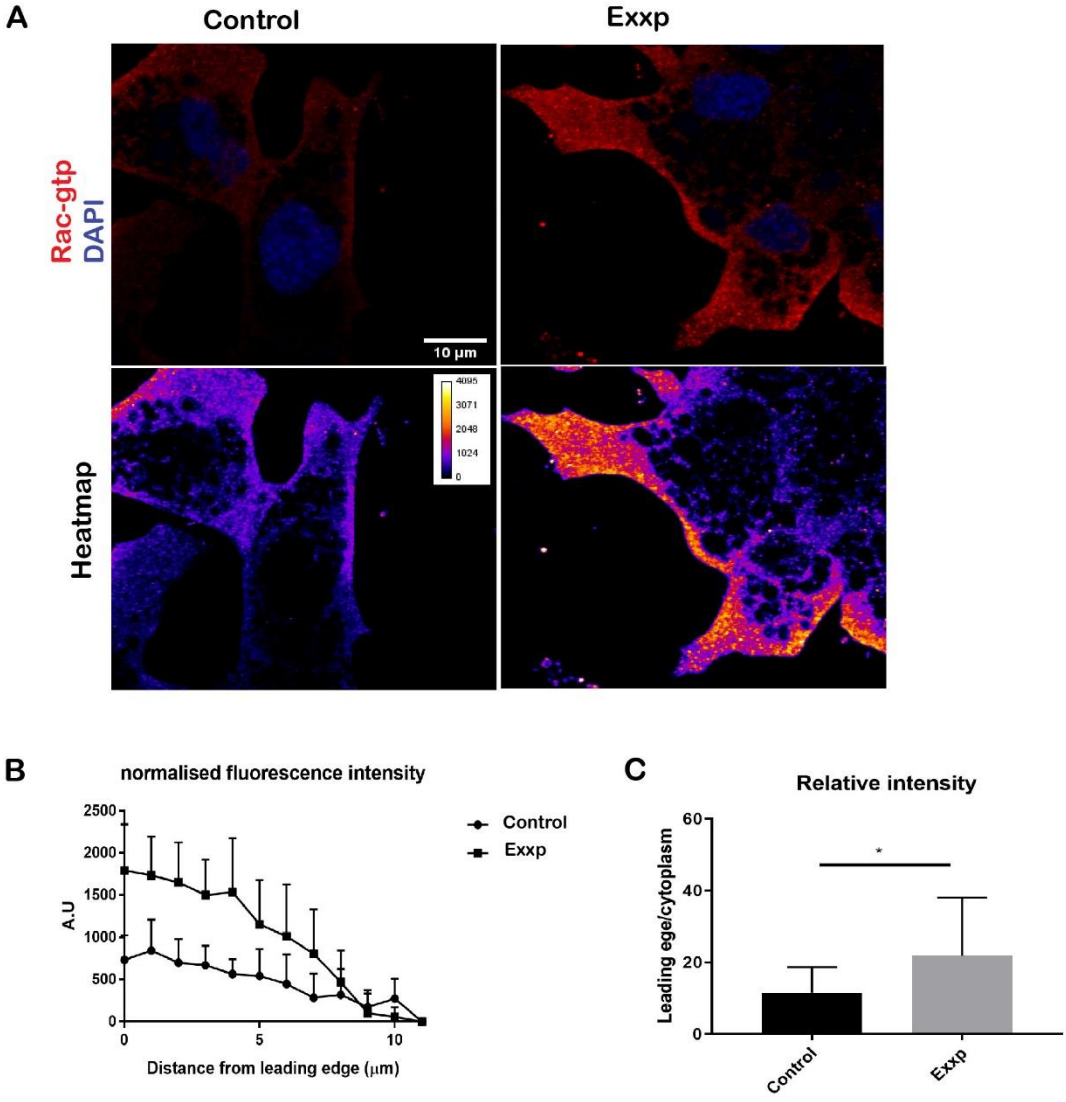

Figure 3.21: Constitutive activation of X-chef SD tyrosine phosphorylation promotes Rac-1 activation at the leading edge

(A)Representative images of Rac-GTP immunofluorescence in control and in Exxp expressing cells (B) Distribution of Rac-GTP intensity from the leading edge to the cell body in control (n=20) and Exxp (n=26) expressing cells (C) Relative Rac-GTP fluorescence intensity in protrusions normalized to the cytoplasm in control (n=20) and Exxp (n=26) expressing cell; unpaired t-test * $P<0.05$. Error bars represent mean and standard deviation.

3.4 Investigating the role of X-chef-1 in the response to substrate stiffness during NC migration

Results of the previous section have suggested that tyrosine phosphorylation of the X-chef-1 substrate domain can promote the establishment of cell polarity and Rac-1 activation during neural crest migration. Our findings described in section 3.3 have also indicated that Rac-1 activation in the neural crest is dependent on substrate stiffness. Given the previously described function of CAS proteins in mechanotransduction and rigidity sensing (Sawada et al.,2006, Kostic and Sheetz.,2006), in this chapter, we further investigated the role of X-chef-1 in the force dependent activation of downstream regulators of neural crest migration. As such, we tested whether expression of the X-chef-1 phosphomimetic construct can be used to promote cell spreading and migration through mechanically non permissive environments.

3.4.1 Expression of phosphomimetic construct leads to expansion of neural crest territory at pre migratory stages

Mechanical cues, specifically the stiffening of the substrate are required to trigger the onset of collective migration of the neural crest (Barriga et al.2018). Notably, whilst lowering the stiffness of the mesoderm, via mechanical and molecular perturbations, has been shown to inhibit migration of the neural crest, increasing the mesodermal stiffness has been shown to promote migration at pre migratory embryonic stages (Barriga et al.,2018). For this reason, we first investigated whether overexpression of the phosphomimetic SD X-chef-1 construct could trigger premature migration in younger non migratory embryos, with lower non permissive mesodermal

stiffness values. To this end, embryos were injected with the Exxp construct, fixed at pre-migratory stage 17 for an *in-situ* hybridization against *Slug,* a marker of the neural crest. Interestingly, a large expansion of the *Slug* expressing neural crest territory was observed on the injected side when compared to the uninjected side (figure3.22A). This effect was reminiscent of the phenotype observed in pre-migratory embryos, which had been subjected to the application of a sustained compressive force using the AFM, in order to increase mesodermal stiffness (figure 3.22B unpublished data.,Elias Barriga). In these embryos, a similar expansion in neural crest territory was observed. Hence, this finding was suggestive of a premature ectopic migration of the neural crest. To further investigate whether this resulted from an increased capacity of Exxp expressing neural crest to override mechanical cues from its substrate, we performed *in vitro* and *in vivo* rescue experiments.

3.4.2 Expression of phosphomimetic construct does not improve cell spreading/polarity on soft substrates *in vitro*

Firstly, to test if constitutive tyrosine phosphorylation could improve spreading and polarization of cells adhering to soft substrates, we cultured control cells and cells expressing the phosphomimetic construct on soft polyacrylamide gels (fig3.23A). To assess the degree of spreading in leading edge cells, the cell area was analyzed. Furthermore, as a readout of cell polarity, the circularity index of cells was quantified (a circularity index of 1 indicates a complete circle). No significant difference was observed with respect to the area and circularity of treated and control cells adhering to soft substrates (fig3.23B-C). These results suggest that constitutive tyrosine phosphorylation of the X-chef-1 substrate domain is unable to establish cell polarization in cells adhering to soft substrates *in vitro.*

3.4.3 Expression of phosphomimetic construct rescues migration of neural crest on softened mesoderm *in vivo*

Secondly, we investigated whether sustained tyrosine phosphorylation of the X-chef-1 substrate domain, could rescue neural crest migration *in vivo,* in embryos in which mesodermal stiffness has been lowered, via molecular manipulation. To reduce the stiffness of the mesoderm, we performed a targeted injection of a translation-blocking morpholino against myosin light chain 9 (*moyl9*-MO), at the 16-cell stage. This molecular perturbation has been previously been shown to lower the stiffness of the mesoderm as validated by iAFM measurements (Barriga et al.,2018). The decrease in substrate rigidity has been attributed to the reduction in the accumulation of mesodermal cells which express the *my19* morpholino. Importantly, this treatment resulted in the inhibition of neural crest migration (Barriga et al.,2018) as assessed through preforming an *in situ* hybridization. When we performed an in situ hybridisation against *Twist, in* embryos injected with the *myo19* MO, in agreement with Barriga et al., we observed a similar percentage of embryos injected with *myo19* MO, that displayed an impaired migratory phenotype (figure 3.24A), characterized by the absence of migratory streams. In an attempt to rescue migration *in vivo*, a subset of embryos were subjected to a double injection. These embryos were injected with the X-chef-1 phosphomimetic construct at the 8-cell stage to target the neural crest and with the my19-mo at the 16-cell stage to target the mesoderm. A significant number of embryos, subjected to a double injection, displayed a migratory phenotype, in comparison to embryos which were injected with the my19-mo alone (fig3.24A-B). This result suggests that constitutive phosphorylation of the X-chef-1 substrate domain may be able to rescue the inhibition of neural crest migration which manifests from a softening of its mesodermal substrate *in vivo*.

3.4.4 Discussion

The results in the previous chapter suggest a role for tyrosine phosphorylation of the X-chef-1 substrate in the establishment of a front to rear polarity to promote neural crest migration. In this chapter, we further investigated whether this mechanism was dependent on mechanical cues from the environment. The CAS family of proteins, in particular p130cas have been demonstrated to function as mechanosensors (Sawada et al.,2006, Kostic et al.,2006). In the case of p130cas, upon mechanical stimulation the substrate domain of p130cas has been shown to extend and become increasingly phosphorylated, leading to the activation downstream signaling molecules such as Rap-1 (Sawada et al.,2006). For this reason, we initially attempted to investigate whether tyrosine phosphorylation of the X-chef-1 substrate domain increased with increasing stiffness, using antibodies which recognize phosphorylated tyrosine residues with the substrate domain of CAS proteins (Fonseca et al.,2004). Unfortunately, we were unable to detect a signal in Xenopus lysates by western blotting. Therefore, we were unable to test a potential link between substrate stiffness and tyrosine phosphorylation. Further studies to investigate this possibility will require the design and production of phosphospecfic antibodies which recognize tyrosine motifs within the X-chef-1 substrate domain.

Although we were unable to test whether the phosphorylation status of the X-chef-1 substrate domain was related to substrate stiffness, we set out to investigate whether expression of a phosphomimetic X-chef-1 substrate domain vector could trigger premature migration in younger non migratory embryos, with lower non permissive mesodermal stiffness values. We observed that overexpression of the Exxp construct lead to the expansion of the neural crest territory in embryos at non migratory developmental stages. This could indeed be suggestive of an ectopic early migration of the neural crest, although it will be necessary to rule out other possibilities. One possibility is that constitutively active tyrosine phosphorylation could increase neural crest

proliferation leading to an expansion of neural crest. Indeed, p130cas has previously been reported to promote proliferation via the MAPK pathway (Cabodi et al.,2006). Whilst we did not observe an obvious increased incidence of cell proliferation *in vitro*, a Brdu assay must preformed to confirm this.

To further investigate whether constitutive tyrosine phosphorylation of the X-chef-1 substrate domain could override mechanical cues from the substrate, we performed *in vitro* and *in vivo* rescue experiments on cells adhering to mechanically non permissive substrates. *In vitro*, we evaluated whether constitutive tyrosine phosphorylation could improve spreading and polarization in cells plated on to soft poly acrylamide gels. I*n vivo* we assessed whether expression of a phosphomimetic construct could rescue NC migration in embryos in which mesodermal stiffness had been lowered via a targeted injection of *myo19* MO, a myosin light chain inhibitor. While the myosin light chain plays a crucial role in mediating cellular contractility, the decrease in mesodermal rigidity, in treated embryos is not believed to manifest directly from a reduction of contractile material properties of mesoderm. In fact, it has been suggested that actomyosin contractility has little direct contribution to the increase in mesodermal stiffness immediately prior to and during the stages at which the neural crest migrates. Barriga et al provided evidence to support this idea, through experiments involving the application of blebbistatin to pre migratory embryos and incubation in blebbistatin until the onset of NC migration (Barriga et al.,2018). When embryos were incubated with blebbistatin for a duration of 4 hours, no effect on mesoderm rigidity or neural crest migration was observed, despite a clear reduction in the degree of myosin phosphorylation. However, when blebbistatin was applied to embryos from an earlier developmental stage, for a total incubation period of 10 hours, mesoderm stiffness was reduced, and neural crest migration was impaired. It was hypothesized that the temporal difference in observed effects is likely to be due to the fact that myosin activity is required for the migration of

mesodermal cells during convergent extension, which commences at earlier gastrula stages. As such the apparent decrease in rigidity as a result of myosin inhibition, has been suggested to arise indirectly from a reduction in the degree of mesodermal cell accumulation, which is driven by convergent extension. In agreement with this idea, a reduction in the in mesodermal cell density was observed in embryos which were injected with a *myo19* morpholino. Thus, through *in vitro* and *in vivo* studies, we characterized the effect of sustained X-chef-1 tyrosine phosphorylation on the behavior of cells, adhering to compliant substrates.

The results of the described rescue experiments were somewhat puzzling. Although expression of the phosphomimetic construct was unable to rescue cell spreading on soft poly acrylamide gels *in vitro*, a rescue of migration was observed *in vivo* in embryos in which mesodermal stiffness has been lowered via myo19 MO injection. Whilst these two rescue experiments were performed to assess different parameters, the observed results may demonstrate a potential discrepancy. For this reason, further experimentation is required. Crucially, it will be important to perform *in vivo* experiments in which phosphonull expressing neural crest are grafted into host embryos injected with a myo19 morpholino in the mesoderm. This will eliminate the possibility of a rescue of migration by a non-cell autonomous affect. Furthermore, the described *in vitro* rescue experiment should be conducted on gels within a range of mechanically non permissive stiffness values, to investigate whether differences in the degree of cell polarization between control and treated explants are observed at intermediate stiffness intervals. Our results could also be suggestive of differences in cell behaviors on 2D planar substrates vs complex 3D microenvironments. Whilst this possibility could have been further investigated by preforming supplementary 3D *in vitro* studies, we were unable to pursue this line of research as an optimal 3D culture system for the *Xenopus* NC is yet to be identified. Nevertheless, the potential implications of dimensionality during the migration of the neural crest are discussed at length later in section 4.5.

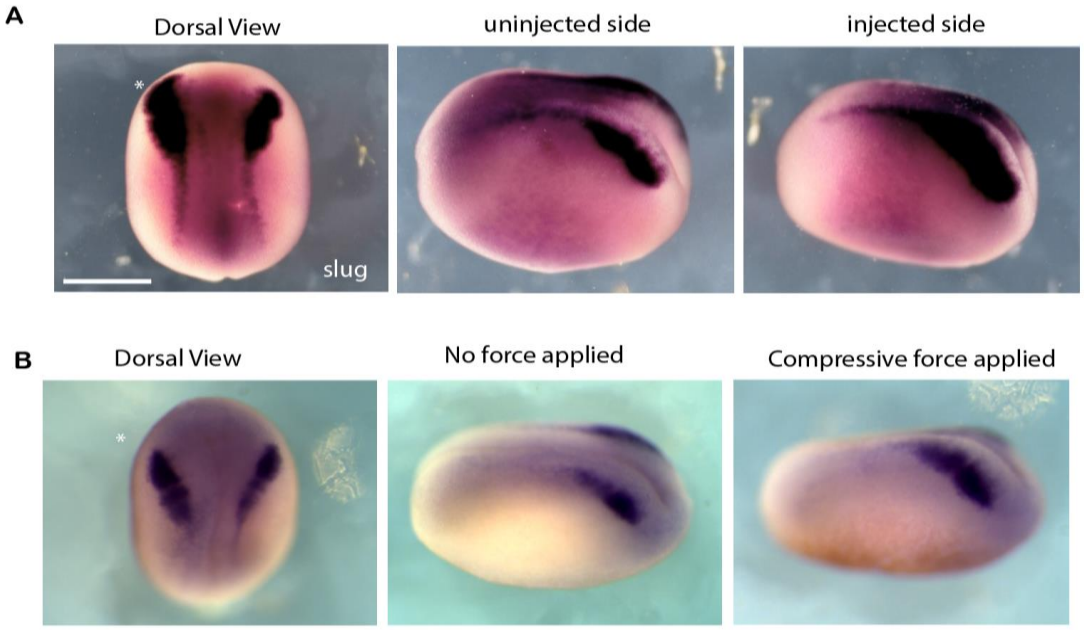

Figure 3.22: Expression of phosphomimetic construct leads to expansion of neural crest territory at pre migratory stages

(A)In situ hybridization against *slug* of a stage 17 embryo injected with Exxp mRNA (left) dorsal view, Asterix indicates injected side ; (center) lateral view of uninjected side; (right) lateral view on injected side (B)*In situ* hybridization against *slug* of a stage 17 embryo in which a sustained compressive force using the AFM was applied to one side, to increase mesodermal stiffness. (left) dorsal view, Asterix indicates compressed side; (center) lateral view of side with no force applied; (right) lateral view of side with compressive force applied.

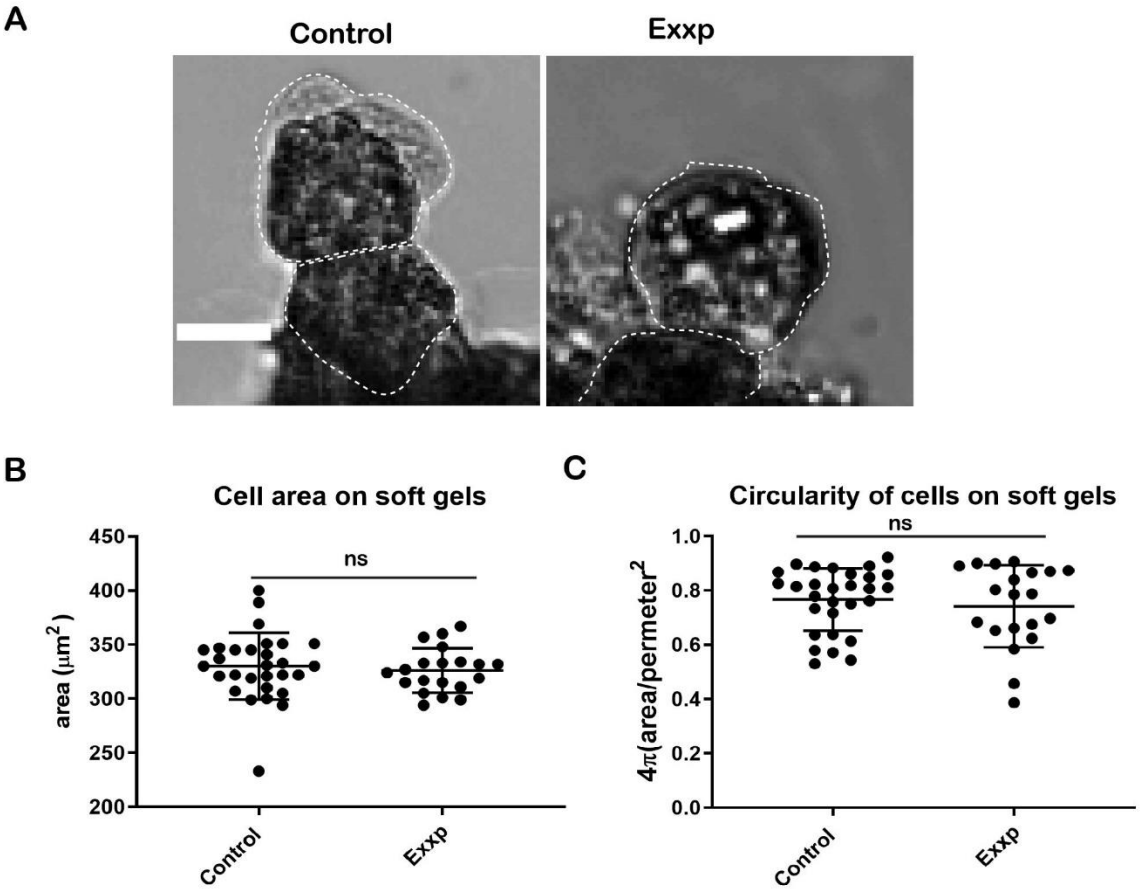

Figure 3.23: Expression of phosphomimetic construct does not improve cell spreading/polarity on soft substrates *in vitro*

(A)Brightfield images of control cells (left) or Exxp expressing cells (right) adhering to soft polyacrylamide gels in vitro. Dashed lines indicate cell perimeter. Scale bar represents 10μm. (B)average cell area of control (n=30) and Exxp expressing cells(n=25) adhering to soft substrates; n.s P>0.05 Mann Whitney test; error bars represent median and interquartile range. (C) Circularity index analysis of control (n=30) and Exxp expressing cells (n=25) adhering to soft substrates ; Mann Whitney test; error bars represent median and interquartile range.

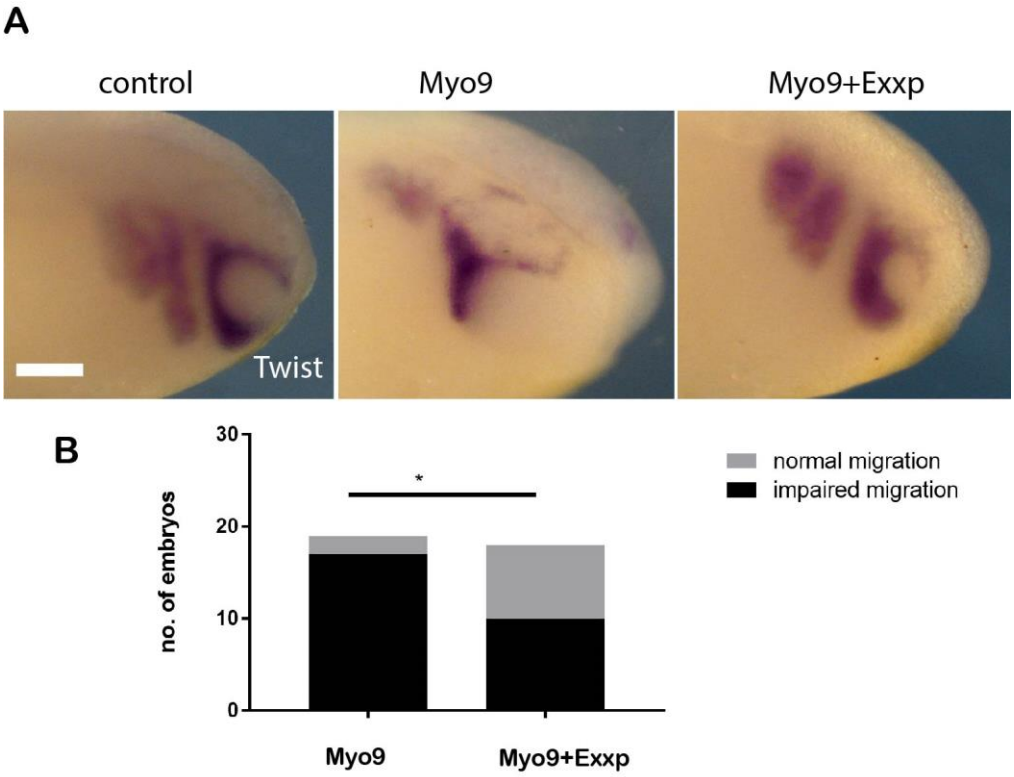

Figure 3.24: Expression of phosphomimetic construct rescues migration of neural crest on softened mesoderm *in vivo*

(A) *In situ* hybridization of *Twist* in stage 24 embryos, injected with myo19 morpholino targeting the mesoderm (left) or co-injected with myo19 targeting the mesoderm and Exxp targeting the neural crest (right). Scale bar represents 250µm. (B) number of embryos with inhibited migration in myo19 injected (n=20) or Myo19+Exxp injected embryos (n=18,); Fisher's exact test * $p<0.05$

4. Discussion

4.1 Summary of Results and Working Model

Cell matrix adhesions are required for the migration of the cephalic neural crest in *Xenopus laevis,* to transform cells from a non-motile to a motile state (Alfandari., et al.,2003, Roycroft et al.2018). However, little is known regarding the composition of these adhesions and how they regulate the collective migration of the neural crest. In this thesis, we have investigated the role of one CAS family member, X-chef-1 which was shown to be specifically expressed in the neural crest prior to and during migration (Meek et al.,2004). Our results show that X-chef-1 localised to cell-matrix adhesions in the neural crest. We observed that the loss of function of X-chef-1, though the injection of a morpholino impairs cell migration *in vivo* and dispersion and cell motility *in vitro.*

When we further investigated the molecular mechanism by which X- chef-1 regulates migration, through the targeted expression of X-chef-1 dominant negative constructs, we observed that the loss of tyrosine phosphorylation of the X-chef-1 substrate domain (SD) led to the strongest impairment of neural crest migration Loss of tyrosine phosphorylation inhibited migratory stream formation *in vivo* and cell motility and dispersion *in vitro*. We further observed that loss of tyrosine phosphorylation affected the stability size and number of cell matrix adhesions, in addition to the stability and size of lamellipodial protrusions. Loss of tyrosine phosphorylation further reduced levels of active Rac-1 at the leading edge of neural crest. On the contrary, expression of a phosphomimetic substrate domain construct increased the number of cell matrix adhesions, the size and duration of protrusions and the levels of active Rac-1 at the leading edge.

Finally, to begin to study the potential role of X-chef-1 in the response to mechanical cues from the substrate, we examined whether constitutive tyrosine phosphorylation could promote migration through mechanically non permissive environments. Our results also show that constitutive tyrosine phosphorylation of X-chef-1 substrate domain in the neural crest results in

an expansion of neural crest territory in pre- migratory embryos and a rescue of migration in embryos in which mesodermal stiffness has been lowered via a targeted injection of a myosin light chain inhibitor.

Taken together, the work discussed in this thesis represents one of the first functional studies to investigate the role of Cass4 in migration. On the basis of the described results, we propose the following working model (figure 4.1). Prior to migration, X- chef-1 begins to be expressed in the neural crest. On the onset of expression, X-chef-1 localises to cell matrix adhesions in the neural crest and is subsequently phosphorylated in tyrosine motifs within its substrate domain by Src kinases. Phosphorylated tyrosine motifs act as docking sites for adaptor proteins which lead to the activation of downstream signaling effectors of neural crest migration, such as Rac-1. This promotes the formation and stabilization of cell matrix adhesions and protrusions at the leading edge, resulting in an establishment of a front to rear cell polarity. The establishment of a leading-edge polarity thereby facilitates the onset of neural crest migration. Given that the stiffening of the mesoderm is a pre-requisite to trigger the migration of the neural crest, we hypothesize that this mechanism could be dependent on mechanical cues from the environment. However, further work will be required to confirm this.

4.2 The role of X-chef-1 in neural crest migration

In this thesis, we investigate, for the first time, the role of a CAS protein, in the migration of the cephalic neural crest of *Xenopus laevis.* Previously, however, the role of CAS family protein Nedd9,

in the migration of trunk neural crest in chick was investigated (Aquino et al.,2009, Liu et al.,2017). Notably, neural crest cells electroporated with a Nedd9 siRNA construct displayed deficits delamination from the neural tube and an overall impairment in migration (Aquino et al.,2009). As cell dispersion is a hallmark of delamination, these results are consistent with our *in vitro* data. However, contrary to our data Nedd9 was described to localize predominantly to the cytoplasm in neural crest explants, as opposed to cell-matrix adhesions. This distinction gives rise to an interesting possibility of whether CAS proteins employ differential mechanisms to regulate migration in trunk vs cephalic neural crest. Due to its suitability for high resolution *in vivo* live imaging, allowing for the visualization of both the cephalic and trunk neural crest, it would be more appropriate to address this question in the chick embryo. In this context, the subcellular localization of CAS proteins as well as the functional role of each CAS domain during NC migration should be analysed in greater depth, in the trunk vs cephalic neural crest. Given that the trunk and cranial neural crest exhibit strikingly different modes of migration (Li et al.,2019) (stochastic individual migration vs directed collective migration), it is indeed possible that CAS proteins utilize distinct strategies in each NC subpopulation to promote cell motility.

4.3 The role of X-chef-1 in Rac-1 activation

Cell polarity is regulated by the activity of small GTPases, namely Rac-1, RhoA and Cdc42. In the host lab, it has previously been shown that Cdc42 has no effect on neural crest migration (Matthews et al.,2008). As we observed that X-chef-1 preferentially localizes to cell matrix adhesions at the cell front and loss of function of X-chef-1 resulted in defects of cell spreading and in the formation of focal complexes, we examined the effect of tyrosine phosphorylation of the

X-chef-1 substrate domain on Rac-1 activation. Through the use of immunohistochemistry and pak-gdb sensors, we observe that tyrosine phosphorylation of X-chef-1 promotes Rac-1 activation at the leading edge. However, how X-chef-1 activates Rac-1 at the leading edge during neural crest migration remains unclear.

It is possible that the activation of Rac-1 could occur as a direct consequence of the tyrosine phosphorylation of the X-chef-1 substrate domain. Indeed, phosphorylated tyrosine motifs within the substrate domain CAS proteins can lead to the recruitment of nucleotide exchange factors such as Dock3 and Dock180 (Zaidel-bar et al.2005, Sanz-Moreno et al.,2008), which in turn can activate Rac-1. To investigate whether an X-chef-1-Dock-Rac-1 pathway could regulate collective migration, it will first be necessary to conduct *in situ* hybridization experiments to identify Dock GEF's which are expressed within the neural crest, upon the onset of migration. Currently, no information is available regarding the expression patterns of Dock GEFS in the neural crest at migratory and pre-migratory stages. Interestingly, however, the mRNA of *Dock180* is expressed in the pharyngeal arches at post migratory stages (Epting et al.2015), making it a potential candidate for further investigation. Following identification of Dock proteins expressed in the neural crest, knock down studies should be performed to investigate the effect on migration and Rac-1 activation, upon the loss of function of the GEF in question. It is anticipated that the loss of function of a GEF, functioning within an X-chef-1/Rac-1 axis, would phencopy the loss of tyrosine phosphorylation of the X-chef-1 substrate domain. Finally, the described functional experiments should be supplemented by co-immunoprecipitation assays to determine whether X-chef-1 and Rac-1 form a complex with the candidate GEF. Taken together, these studies would help to establish whether the CAS-Dock-Rac-1 signaling pathway, described for p130cas and Nedd9, is also conserved in Cass4.

Whilst a direct activation of Rac-1 via tyrosine phosphorylation of the X-chef-1 substrate domain is possible, tyrosine phosphorylation of the substrate domain of CAS proteins can lead to the recruitment and activation of a number of other downstream effectors. Hence, it's possible that observed effects can be due to an indirect activation of Rac-1. One potential downstream target of X-chef-1 which requires further investigation is Rap-1. Indeed, expression of an isoform of Rap-1 was observed in the neural crest at pre-migratory stages (rap1b Expression [Xenopus] - Xenbase Gene Catalog, 2021). Furthermore, tyrosine phosphorylation of the substrate domain of p130cas and Nedd9 has been reported to activate Rap-1 (Sakakibara et al 2002, Sawada et al.,2006). Mechanistically, Rap-1 has been reported to regulate cell polarity, through effects on integrin activation (Caron et al.,2000), as well as adhesion turnover (Altemeier et al.,2012). Moreover, Rap-1 has further been described as a mediator of cell spreading (Arthur et al.,2004). In line with this, pull down assays in cells transfected with dominant negative or constitutively active Rap-1 constructs have suggested that Rac-1 can be activated by Rap-1(Maillet et al.2003, Arthur et al.2004). Hence, in a similar manner, it is possible that X-chef-1 can promote an indirect activation of Rac-1 through regulating Rap-1 activity. This possibility could be investigated further by examining the degree of Rac-1 activation, upon the loss of function of Rap-1 in the neural crest. Furthermore, through expressing a constitutively active Rap-1 construct in cells injected with phosphonull X-chef-1 variant, it would be necessary to evaluate whether Rap-1 expression is sufficient to rescue the activation of Rac-1 during NC migration. Whilst a role for Rap-1 in the X-chef-1 signaling axis is based on mere speculation, it is important to consider that X-chef-1 may affect the activation status of multiple downstream polarity effectors during NC migration.

Another possibility is that X-chef-1 functions to ensure the correct localization of downstream effectors such as Rac-1. The study described in section 4.2, examining the role of homologous protein Nedd9 in the migration of the chick neural crest, also reported a role for the CAS protein

in the establishment of a front to rear polarity (Liu et al.,2017), consistent with our findings. It was proposed that Nedd9 promoted a front to rear polarity in the trunk neural crest, by regulating the asymmetric distribution of active RhoA, through its association with Rhogap DLC1. Notably, loss of function of Nedd9 did not affect RhoA levels, but rather its localization. Whilst, an altered distribution of Rac-1 upon the loss of function of X-chef-1 was not observed through immunohistochemistry or through the use of a pak-gdp sensor, it is possible that these methods are not sensitive enough to detect such changes. Examination of the localization and total activation of Rac-1 in X-chef-1 deficient cells , through the use of more sensitive techniques, such as a Rac-1 FRET sensor (Itoh et al.,2002) may provide more information. Nevertheless, such a mechanism is unlikely to involve Rhogap DLC1 as the mRNA of DLC1 is expressed in the neuroectoderm and neural plate and not in the neural crest prior to or during migration (Zhang et al.,2017).

4.4 The role of X-chef-1 in EMT

Whilst we have investigated the role of X-chef-1 in the activation of Rac-1 at the leading edge, the function of X-chef-1 in the process of EMT remains to be studied. However, preliminary immunohistochemistry experiments, performed in X-chef-1 MO cells, revealed an increase of E cadherin fluorescence levels in the neural crest (unpublished data) suggesting a role for X-chef-1 in E-cadherin regulation, consistent with previous studies in Cass4 (Li et al.,2016), p130cas and Nedd9(Tikhmyamova et al.,2011). These findings elude to a central role for X-chef-1 in coordinating the cross talk between cell-substrate and cell- cell adhesions during EMT. An important question which arises from this result is how X-chef-1 regulates E-cadherin expression.

One possibility is that X-chef-1 regulates E-cadherin expression on the transcriptional level. This hypothesis could be addressed by preforming qPCR to assess E-cadherin transcript levels, upon the loss of function of X-chef-1. Another possibility is that X-chef-1 regulates E-cadherin, at the post translational level, through promoting its degradation or recycling. Analysis of E-cadherin dynamics at cell- cell junctions upon the loss of function of X-chef-1 would shed more light on this matter.

Given its potential role in EMT programme, prior to neural crest migration, a further question concerns what lies upstream of X-chef-1. Interestingly, *Twist*, a master regulator of EMT and migration of the neural crest (Barriga et al,2013) has also been shown to upregulate the expression of CAS proteins during EMT in other systems (Yang et al.,2012). Analysis of X-chef-1 transcript levels upon the loss of function of *Twist* using qPCR, will help to determine whether this is the case in the neural crest. Given that both *Twist* and X-chef-1 negatively regulate of E-cadherin expression in the neural crest, it is tempting to speculate that Twist could, in part, downregulate E-cadherin levels by promoting transcription of X-chef-1. This idea could be investigated through the implementation of further epistasis experiments, examining whether expression of X-chef-1 can rescue the impairment of NC migration and increased junctional E-cadherin levels, observed upon the loss of function of *Twist.*

4.5 The role of X-chef-1 in the response to mechanical cues

The results discussed above suggest a role for tyrosine phosphorylation of the X-chef-1 substrate in the establishment of a front to rear polarity to promote neural crest migration. In this thesis, we further sought to investigate whether tyrosine phosphorylation of the X-chef-1 substrate

domain promoted polarity acquisition and migration in a substrate stiffness dependent manner. This is the first study to investigate the mechanical activation of substrate domain of CAS protein, aside from p130cas. Due to technical limitations, we could not directly test how substrate stiffness impacts upon the phosphorylation status of X-chef-1. Future attempts to address this, will require the design of phosphospecfic antibodies for tyrosine motifs within the X-chef-1 substrate domain. Using these tools, a direct read out of how substrate rigidity affects the degree of X-chef-1 tyrosine phosphorylation in the neural crest can be obtained, by immunohistochemistry and western blotting . Nevertheless, whilst we were unable to test whether the phosphorylation status of the X-chef-1 substrate domain was dependent on substrate stiffness, we were able to investigate whether expression of a phosphomimetic X-chef-1 substrate domain vector could promote cell spreading and migration through mechanically non permissive environments. Although expression of the phosphomimetic construct was unable to rescue cell spreading on soft poly acrylamide gels *in vitro*, a rescue of migration was observed in embryos in which mesodermal stiffness has been lowered via a targeted injection of a myosin light chain inhibitor. Whilst these two rescue experiments have been used to evaluate different parameters, the observed results may demonstrate a potential discrepancy.

It is possible that the discrepancy between *in vitro* and *in vivo* rescue experiments may result from differences between the 2D and 3D microenvironment. Mechanistically, the function of CAS proteins in mechanotransduction relies on the extension of the substrate domain, in response to mechanical force, to reveal tyrosine residues which become phosphorylated and form binding sites for adaptor proteins (Sawada et al.,2006). On 2D polyacrylamide substrates forces exerted in the XY plane on cell matrix adhesions may be insufficient to unfold the X-chef-1 substrate domain to reveal constitutively active tyrosine phosphorylation. Hence due to steric hindrance/spatial constraints, adaptor proteins cannot access the phosphomimetic tyrosine

motifs of the X-chef-1 substrate domain. In contrast in a 3D *Xenopus* embryo, cell matrix adhesions experience forces from several orientations and sources (e.g. shearing from epidermis) and it is possible that forces experienced by cell matrix adhesions in 3D may be sufficient to unfold the substrate domain.

In addition to the differences in the magnitude and orientation of forces exerted on the neural crest, cell matrix adhesion localization and composition also differ in 2D vs 3D microenvironments. In a 2D environment focal adhesions form only in the XY plane. However, in a 3D environment, focal adhesions localise can along the height of cells and tissues (Beningo et al.,2004). Furthermore, studies suggest that cell- matrix adhesion composition may differ in 2D vs 3D environments. For example, it has been reported that a_5 β_1 integrin, one of the primary components of cell matrix adhesion in the CNC neural crest (Alfandari et al.,2003) is expressed to a higher degree in 3D focal adhesions than in 2D (Cukierman et al.2001). In contrast integrin $\alpha_v\beta_3$, is highly expressed in 2D environments and absent in 3D. Hence, it is possible that such differences in cell matrix adhesions could alter signal transduction pathways in cells occupying 3D environments. To investigate the effect of dimensionality on the cellular responses elicited in the neural crest, it will be necessary to analyse the subcellular localization, composition and molecular dynamics of cell matrix adhesions, as well as the effects on the activation of downstream polarity effectors ,in cells cultured in 2D vs 3D environments. This analysis should be further supplemented with functional studies to determine the impact of dimensionality on the migratory response of the neural crest, through careful examination of cell motility parameters including velocity and directionality. Furthermore, to investigate whether X-chef-1 plays a differential role in migratory neural crest, occupying 2D vs 3D environments, the described experiments should be carried out, upon the loss and gain of function of function of X-chef-1. Given that other CAS

proteins have been observed to have distinct effects on 2D vs 3D cell migration (Zhong et al.,2012), this line of research indeed warrants further investigation.

Whilst 3D *in vitro* studies would provide a greater insight into the role of X-chef-1 in NC migration, and a potential explanation to the discrepancy observed in rescue experiments on mechanically non permissive substrates (described in section 3.4.1 and 3.4.2) ,we were unable to conduct such studies as a suitable 3D culture system for the *Xenopus* NC is yet to be identified. One potential possibility would involve culturing cells in 3D matrices or scaffolds. Indeed, a 3D Matrigel culture system has been established for the quail neural crest (Ramos-Hryb., et al., 2013). However, as Matrigel is comprised primarily of ECM proteins laminin, nidogen, collagen, (Kleinman and Martin,2005) it would not be an appropriate choice for the culture of the *Xenopus* NC, which utilizes fibronectin to migrate (Alfandari et al.,2003). Furthermore, Matrigel has been reported to exhibit lot to lot variations with respect to its mechanical properties, including elastic modulus (Soofi et al.,2009). As such, it may not be the most suitable option to investigate the effects of substrate stiffness on the migratory response of the neural crest. Future efforts to establish a 3D culture system for the migratory neural crest should focus on the optimization of culture conditions on fibronectin-based 3D synthetic hydrogels with fine- tuned mechanical properties (Trujilo et al.2020).

4.6 The role of X-chef-1 in the response to chemical cues

Whilst culturing cells on a 3D system would help to dissect the role of dimensionality during neural crest migration, it would alone be insufficient to recapitulate the complexity of an *in vivo* environment. *In vivo*, cells are required to coordinate their response to multiple inputs from their

surroundings. In addition to mechanical cues from the substrate, the neural crest must respond to chemical cues from its environment and it is possible that this is mediated by X-chef-1. For example, as discussed in section 1.45, the SDF-1 plays a role in the polarization of leader cells in the towards the chemoattractant, to promote directional migration (Theveneau et al.,2010). Whilst the neural crest was not exposed to a source of SDF-1 in the *in vitro* rescue experiment, described in section 3.42, migratory stream formation observed the *in vivo* rescue experiment (section 3.43) would have been in the presence of the chemoattractant. Hence, once possible explanation of this result is that X-chef-1 is mediating cell polarization and/or migration in response to SDF-1, in mechanically non permissive environments. This idea could be tested by performing a chemotaxis assay on complaint substrates *in vitro*, by positioning a heparin bead, coated in SDF-1, in the vicinity of a neural crest explant.

In addition to attractive cues, inhibitory cues, such as Semaphorins, are expressed in the surrounding tissue and prevent the neural crest from invading the adjacent territory. Semaphorin3A signaling has been proposed to do so through inhibition of Rac-1 and through impairment of cell polarity and cell- matrix adhesion formation in the neural crest (Bajanca et al.,2019). However, the mechanistic link between Semaphorin signaling and Rac-1 inactivation remains unclear. In this regard, it would be interesting to investigate whether X-chef-1 may act downstream of sema3A in this process. It is tempting to speculate that Semaphorin signaling may inhibit Rac-1 activation through regulating the phosphorylation status of the X-chef-1 substrate domain. Indeed, Semaphorin signaling has been shown to lead to alterations in the phosphorylation status of key tyrosine residues within substrate domains of CAS proteins (Perez-Branguli et al.,2016). Furthermore, our results have suggested that overexpression of the phosphomimetic X-chef-1 variant in the pre-migratory neural crest can lead to a pre-mature expansion of the NC territory into non permissive regions, in which inhibitory Sema3A/3F

molecules are expressed (Bajanca et al.,2019). This could imply that constitutive tyrosine phosphorylation of X-chef-1 can enable the neural crest to override inhibitory Semaphorin cues. To investigate a possible link between Semaphorin signaling and X-chef-1 tyrosine phosphorylation, NC explants overexpressing the phosphomimetic construct should be cultured in the presence of a Semaphorin source *in vitro*. More precisely, this experiment could be carried out through the creation of a dual substrate, containing a defined region coated with fibronectin, in which the neural crest are plated and a distinct region containing fibronectin and purified Semaphorin, as previously described (Bajanca et al.,2019). Under these conditions, it would be interesting to examine whether constitutive tyrosine phosphorylation of X-chef-1 could provide cells with an enhanced capacity to invade the Semaphorin coated region. Furthermore, examination of Rac-1 levels in control vs Exxp expressing cells adhering to Semaphorin coated substrates, will also provide greater insight into whether constitutive tyrosine phosphorylation of X-chef-1 can rescue cell polarity deficits which arise from Semaphorin signaling. It should be noted that whilst we postulate a potential link between X-chef-1 and Semaphorin signaling, we do not exclude the possibility that X-chef-1 may function in concert with other chemical signaling cues that regulate NC migration. Indeed, cross talk between eph/ ephrin signaling and CAS proteins in other systems has also been reported (Foo et al.,2006). Hence, future studies should focus on investigating the role of X-chef-1 in coordinating the cell's response to chemical cues, as well as mechanical cues, to obtain a more wholistic perspective on the function of Cass4 during collective migration.

4.7 Concluding remarks

In conclusion, this thesis proposes that X-chef-1 is required for neural crest migration. Through tyrosine phosphorylation of its substrate domain, X-chef-1 promotes Rac-1 activation at the leading edge of neural crest to promote an establishment of a front to rear polarity. Taken together, this thesis presents a novel body of work of the role of a largely understudied CAS family in promoting collective cell migration. Our results also set up the framework for further investigation into the role of X-chef-1 in rigidity sensing. Whilst the role of this cell-matrix adhesion protein was studied in a developmental context, the impact of this study extends far beyond development. Given that Cass4 mRNA expression in both lung adenocarcinoma and lung squamous carcinoma tissues is upregulated (Miao et al.,2012), our results may have important implications for cancer cell migration and invasion.

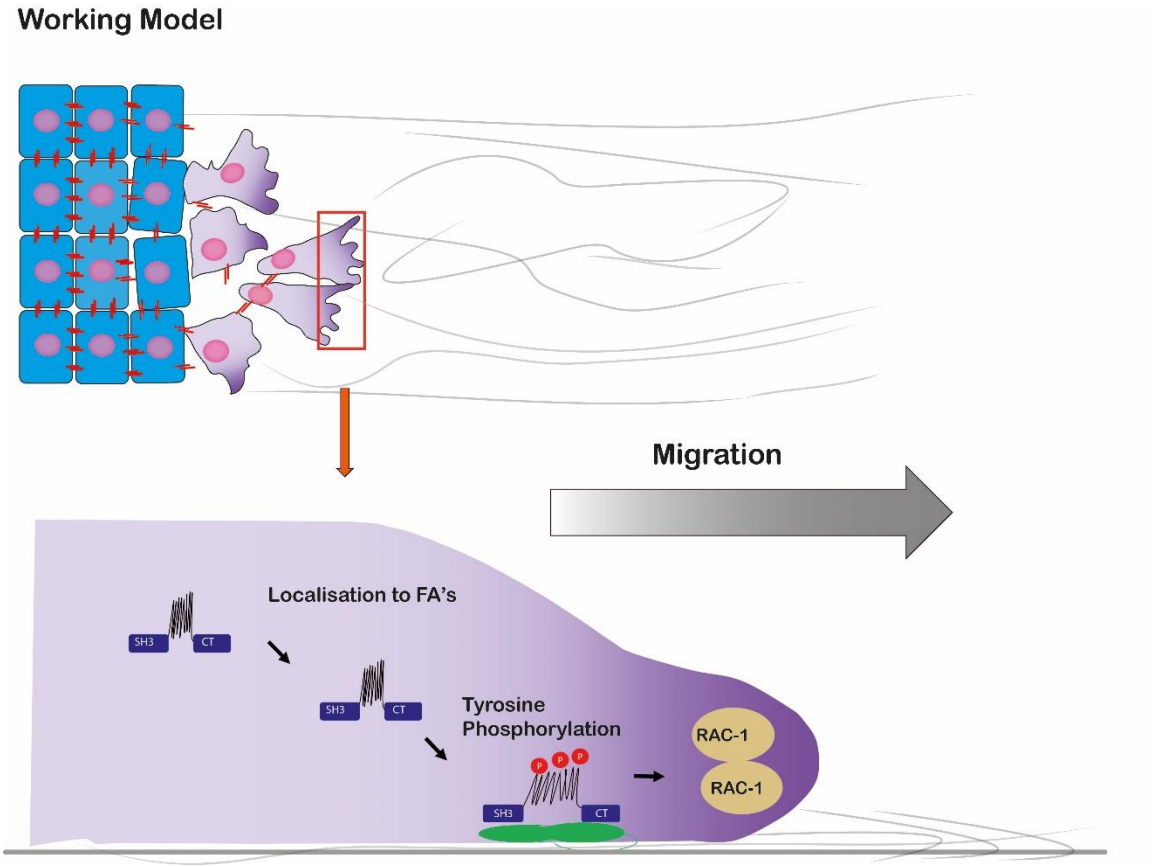

Figure 4.1: Working model of X-chef-1 dependent migration

(Above) Upon the onset of NC migration, leader cells (purple) establish a front to rear polarity and move in a dorso-ventral direction. (Below) X-chef-1 localises to cell matrix adhesions (green) at the front of leader cells and is phosphorylated in tyrosine motifs within its substrate domain. Tyrosine phosphorylation promotes activation of downstream effectors of neural crest migration such as Rac-1 at the leading edge. As a result, this enhances the formation and stabilization of cell matrix adhesions and protrusions, leading to an establishment of a front to rear cell polarity. In this way X-chef-1 promotes the migration of the cephalic neural crest in *Xenopus Laevis*.

5. References

Alexandropoulos, K., & Baltimore, D. (1996). Coordinate activation of c-Src by SH3-and SH2-binding sites on a novel, p130(Cas)-related protein, Sin. *Genes and Development*, *10*(11), 1341–1355.

Alexandrova, A. Y., Arnold, K., Schaub, S., Vasiliev, J. M., Meister, J. J., Bershadsky, A. D., & Verkhovsky, A. B. (2008). Comparative dynamics of retrograde actin flow and focal adhesions: Formation of nascent adhesions triggers transition from fast to slow flow. *PLoS ONE*, *3*(9), 3234.

Alfandari, D., Cousin, H., Gaultier, A., Hoffstrom, B. G., & DeSimone, D. W. (2003). Integrin α5β1 supports the migration of Xenopus cranial neural crest on fibronectin. *Developmental Biology*, *260*(2), 449–464.

Alfandari, D., Cousin, H., Gaultier, A., Smith, K., White, J. M., Darribère, T., & DeSimone, D. W. (2001). Xenopus ADAM 13 is a metalloprotease required for cranial neural crest-cell migration. *Current Biology*, *11*(12), 918–930.

Altemeier, W. A., Schlesinger, S. Y., Buell, C. A., Parks, W. C., & Chen, P. (2012). Syndecan-1 controls cell migration by activating rap1 to regulate focal adhesion disassembly. *Journal of Cell Science*, *125*(21), 5188–5195.

Ananthakrishnan, R., & Ehrlicher, A. (2007). The forces behind cell movement. *International Journal of Biological Sciences* (Vol. 3, Issue 5). 303-317

Anthis, N. J., Wegener, K. L., Ye, F., Kim, C., Goult, B. T., Lowe, E. D., Vakonakis, I., Bate, N., Critchley, D. R., Ginsberg, M. H., & Campbell, I. D. (2009). The structure of an integrin/talin complex reveals the basis of inside-out signal transduction. *EMBO Journal*, *28*(22). 3623-3632

Aquino, J. B., Lallemend, F., Marmigère, F., Adameyko, I. I., Golemis, E. A., & Ernfors, P. (2009). The retinoic acid inducible Cas-family signaling protein Nedd9 regulates neural crest cell migration by modulating adhesion and actin dynamics. *Neuroscience*, *162*(4), 1106–1119.

Arthur, W. T., Quilliam, L. A., & Cooper, J. A. (2004). Rap1 promotes cell spreading by localizing Rac guanine nucleotide exchange factors. *Journal of Cell Biology*, *167*(1). 111-122

Askari, J. A., Buckley, P. A., Mould, A. P., & Humphries, M. J. (2009). Linking integrin conformation to function. *Journal of Cell Science* (Vol. 122, Issue 2, pp. 165–170).

Astier, A., Manié, S. N., Avraham, H., Hirai, H., Law, S. F., Zhang, Y., Golemis, E. A., Fu, Y., Druker, B. J., Haghayeghi, N., Freedman, A. S., & Avraham, S. (1997). The related adhesion focal tyrosine kinase differentially phosphorylates p130(Cas) and the Cas-like protein, p105(HEF1). *Journal of Biological Chemistry*, *272*(32), 19719–19724.

Aybar, M. J., Nieto, M. A., & Mayor, R. (2003). Snail precedes Slug in the genetic cascade required for the specification and migration of the Xenopus neural crest. *Development* (Vol. 130, Issue 3). 483-494

Bahm, I., Barriga, E. H., Frolov, A., Theveneau, E., Frankel, P., & Mayor, R. (2017). PDGF controls contact inhibition of locomotion by regulating N-cadherin during neural crest migration. *Development (Cambridge)*, *144*(13), 2456–2468.

Bajanca, F., Gouignard, N., Colle, C., Parsons, M., Mayor, R., & Theveneau, E. (2019). In vivo topology converts competition for cell-matrix adhesion into directional migration. *Nature Communications*, *10*(1).

Ballestrem, C., Hinz, B., Imhof, B. A., & Wehrle-Haller, B. (2001). Marching at the front and dragging behind: Differential αVβ3-integrin turnover regulates focal adhesion behavior. *Journal of Cell Biology*, *155*(7), 1319–1332.

Barriga, E. H., Franze, K., Charras, G., & Mayor, R. (2018). Tissue stiffening coordinates morphogenesis by triggering collective cell migration in vivo. *Nature*, *554*(7693). 523-527

Barriga, E., Maxwell, P., Reyes, A. and Mayor, R., 2013. The hypoxia factor Hif-1α controls neural crest chemotaxis and epithelial to mesenchymal transition. *The Journal of Cell Biology*, 201(5), pp.759-776.

Bear, J. E., Svitkina, T. M., Krause, M., Schafer, D. A., Loureiro, J. J., Strasser, G. A., Maly, I. V., Chaga, O. Y., Cooper, J. A., Borisy, G. G., & Gertler, F. B. (2002). Antagonism between Ena/VASP proteins and actin filament capping regulates fibroblast motility. *Cell*, *109*(4). 509-521

Beningo, K. A., Dembo, M., & Wang, Y. L. (2004). Responses of fibroblasts to anchorage of dorsal extracellular matrix receptors. *Proceedings of the National Academy of Sciences of the United States of America*, *101*(52), 18024–18029.

Berginski, M. E., & Gomez, S. M. (2013). The Focal Adhesion Analysis Server: a web tool for analyzing focal adhesion dynamics. *F1000Research*, *2*, 68.

Berndt, J. D., Clay, M. R., Langenberg, T., & Halloran, M. C. (2008). Rho-kinase and myosin II affect dynamic neural crest cell behaviors during epithelial to mesenchymal transition in vivo. *Developmental Biology*, *324*(2), 236–244.

Braniš, J., Pataki, C., Spörrer, M., Gerum, R. C., Mainka, A., Cermak, V., Goldmann, W. H., Fabry, B., Brabek, J., & Rosel, D. (2017). The role of focal adhesion anchoring domains of CAS in mechanotransduction. *Scientific Reports*, *7*(1), 1–12.

Burridge, K., & Mangeat, P. (1984). An interaction between vinculin and talin. *Nature*, *308*(5961). 744-746

Cabodi, S., Tinnirello, A., Di Stefano, P., Bisarò, B., Ambrosino, E., Castellano, I., Sapino, A., Arisio, R., Cavallo, F., Forni, G., Glukhova, M., Silengo, L., Altruda, F., Turco, E., Tarone, G., & Defilippi, P. (2006). p130Cas as a new regulator of mammary epithelial cell proliferation, survival, and HER2-Neu oncogene- dependent breast tumorigenesis. *Cancer Research*, *66*(9). 4672-4680

Calderwood, D. A., Yan, B., De Pereda, J. M., Alvarez, B. G., Fujioka, Y., Liddington, R. C., & Ginsberg, M. H. (2002). The phosphotyrosine binding-like domain of talin activates integrins. *Journal of Biological Chemistry*, *277*(24). 21749-21758

Carl, T. F., Dufton, C., Hanken, J., & Klymkowsky, M. W. (1999). Inhibition of neural crest migration in Xenopus using antisense slug RNA. *Developmental Biology*, *213*(1). 101-115

Carmona-Fontaine, C., Matthews, H. K., Kuriyama, S., Moreno, M., Dunn, G. A., Parsons, M., Stern, C. D., & Mayor, R. (2008). Contact inhibition of locomotion in vivo controls neural crest directional migration. *Nature*, *456*(7224), 957–961.

Carmona-Fontaine, C., Theveneau, E., Tzekou, A., Tada, M., Woods, M., Page, K. M., Parsons, M., Lambris, J. D., & Mayor, R. (2011). Complement Fragment C3a Controls Mutual Cell Attraction during Collective Cell Migration. *Developmental Cell*, *21*(6), 1026–1037.

Carmona-Fontaine, M. L., Barnes, C. P., Couzin, C. P., & Mayor, I. D. (2014). Directional Collective Cell Migration Emerges as a Property of Cell Interactions. *PLoS ONE*, *9*(9),

Caron, E., Self, A. J., & Hall, A. (2000). The GTPase rap1 controls functional activation of macrophage integrin αMβ2 by LPS and other inflammatory mediators. *Current Biology*, *10*(16), 974–978.

Chaffer, C. L., Thompson, E. W., & Williams, E. D. (2007). Mesenchymal to epithelial transition in development and disease. *Cells Tissues Organs*, *185*(1–3), 7–19.

Chan, C. E., & Odde, D. J. (2008). Traction dynamics of filopodia on compliant substrates. *Science*, *322*(5908), 1687–1691.

Cheung, M., Chaboissier, M. C., Mynett, A., Hirst, E., Schedl, A., & Briscoe, J. (2005). The transcriptional control of trunk neural crest induction, survival, and delamination. *Developmental Cell*, *8*(2). 179–192

Choi, C. K., Vicente-Manzanares, M., Zareno, J., Whitmore, L. A., Mogilner, A., & Horwitz, A. R. (2008). Actin and α-actinin orchestrate the assembly and maturation of nascent adhesions in a myosin II motor-independent manner. *Nature Cell Biology*, 10(9). 1039-1050

Choquet, D., Felsenfeld, D. P., & Sheetz, M. P. (1997). Extracellular matrix rigidity causes strengthening of integrin- cytoskeleton linkages. *Cell*, *88*(1). 39-48

Clay, M. R., & Halloran, M. C. (2010). Control of neural crest cell behavior and migration: Insights from live imaging. *Cell Adhesion and Migration*, *4*(4), 586–594.

Cooper, L., Shen, T. and Guan, J.,(2003). Regulation of Focal Adhesion Kinase by Its Amino-Terminal Domain through an Autoinhibitory Interaction. *Molecular and Cellular Biology*, 23(22), pp.8030-8041.

Cukierman, E., Pankov, R., Stevens, D. R., & Yamada, K. M. (2001). Taking cell-matrix adhesions to the third dimension. *Science*, *294*(5547), 1708–1712.

Dady, A., Blavet, C., & Duband, J.-L. (2012). Timing and kinetics of E- to N-cadherin switch during neurulation in the avian embryo. *Developmental Dynamics*, *241*(8), 1333–1349.

Damm, E. W., & Clements, W. K. (2017). Pdgf signalling guides neural crest contribution to the haematopoietic stem cell specification niche. *Nature Cell Biology*, *19*(5), 457–467.

Davy, A., & Soriano, P. (2007). Ephrin-B2 forward signaling regulates somite patterning and neural crest cell development. *Developmental Biology*, *304*(1), 182–193.

del Barrio, M. G., & Nieto, M. A. (2002). Overexpression of Snail family members highlights their ability to promote chick neural crest formation. *Development* (Vol. 129, Issue 7). 1583-1593

Del Rio, A., Perez-Jimenez, R., Liu, R., Roca-Cusachs, P., Fernandez, J. M., & Sheetz, M. P. (2009). Stretching single talin rod molecules activates vinculin binding. *Science*, *323*(5914). 638-641

Donato, D. M., Ryzhova, L. M., Meenderink, L. M., Kaverina, I., & Hanks, S. K. (2010). Dynamics and mechanism of p130Cas localization to focal adhesions. *Journal of Biological Chemistry*, *285*(27), 20769–20779.

Duband JL. Neural Crest Delamination and Migration: Integrating Regulations of Cell Interactions, Locomotion, Survival and Fate. (2013) In: Madame Curie Bioscience Database [Internet]. Austin (TX): Landes Bioscience; 2000-2013.

Duband, J. L. (2006). Neural crest delamination and migration: Integrating regulations of ceil interactions, locomotion, survival and fate. *Advances in Experimental Medicine and Biology* (Vol. 589). 45-77

Duband, J. L. (2010). Diversity in the molecular and cellular strategies of epithelium-to-mesenchyme transitions: Insights from the neural crest. *Cell Adhesion and Migration*, *4*(3), 458–482.

Dubash, A. D., Menold, M. M., Samson, T., Boulter, E., García-Mata, R., Doughman, R., & Burridge, K. (2009). Chapter 1 Focal Adhesions: New Angles on an Old Structure. In *International Review of Cell and Molecular Biology* (Vol. 277, Issue C, pp. 1–65). Academic Press.

Eberhart, J. K., He, X., Swartz, M. E., Yan, Y. L., Song, H., Boling, T. C., Kunerth, A. K., Walker, M. B., Kimmel, C. B., & Postlethwait, J. H. (2008). MicroRNA Mirn140 modulates Pdgf signaling during palatogenesis. *Nature Genetics*, *40*(3), 290–298.

Ehrlicher, A. J., Nakamura, F., Hartwig, J. H., Weitz, D. A., & Stossel, T. P. (2011). Mechanical strain in actin networks regulates FilGAP and integrin binding to filamin A. *Nature*, *478*(7368), 260–263.

Epting, D., Slanchev, K., Boehlke, C., Hoff, S., Loges, N. T., Yasunaga, T., Indorf, L., Nestel, S., Lienkamp, S. S., Omran, H., Wolfgang Kuehn, E., Ronneberger, O., Walz, G., & Kramer-Zucker, A. (2015). The Rac1 regulator ELMO controls basal body migration and docking in multiciliated cells through interaction with Ezrin. *Development (Cambridge)*, *142*(1). 174-184

Etienne-Manneville, S. (2014). Neighborly relations during collective migration. *Current Opinion in Cell Biology* (Vol. 30, Issue 1). 51-59

Ezratty, E. J., Bertaux, C., Marcantonio, E. E., & Gundersen, G. G. (2009). Clathrin mediates integrin endocytosis for focal adhesion disassembly in migrating cells. *Journal of Cell Biology*, *187*(5), 733–747.

Ezratty, E. J., Partridge, M. A., & Gundersen, G. G. (2005). Microtubule-induced focal adhesion disassembly is mediated by dynamin and focal adhesion kinase. *Nature Cell Biology*, *7*(6), 581–590.

Faix, J., Breitsprecher, D., Stradal, T. E. B., & Rottner, K. (2009). Filopodia: Complex models for simple rods. *International Journal of Biochemistry and Cell Biology* (Vol. 41, Issues 8–9). 1656-1664

Fashena, S. J., Einarson, M. B., O'Neill, G. M., Patriotis, C., & Golemis, E. A. (2002). Dissection of HEF1-dependent functions in motility and transcriptional regulation. *Journal of Cell Science*, *115*(1). 99-111

Fonseca, P., 2004. Regulation and localization of CAS substrate domain tyrosine phosphorylation. *Cellular Signalling*, 16(5), pp.621-629.

Foo, S. S., Turner, C. J., Adams, S., Compagni, A., Aubyn, D., Kogata, N., Lindblom, P., Shani, M., Zicha, D., & Adams, R. H. (2006). Ephrin-B2 controls cell motility and adhesion during blood-vessel-wall assembly. *Cell*, *124*(1). 163-171

Friedl, P., & Gilmour, D. (2009). Collective cell migration in morphogenesis, regeneration and cancer. *Nature Reviews Molecular Cell Biology* (Vol. 10, Issue 7). 445-457

Friedl, P., & Wolf, K. (2010). Plasticity of cell migration: A multiscale tuning model. *Journal of Cell Biology*, *188*(1), 11–19.

Galbraith, C. G., Yamada, K. M., & Sheetz, M. P. (2002). The relationship between force and focal complex development. *Journal of Cell Biology*, *159*(4), 695–705.

Gammill, L. S., Gonzalez, C., & Bronner-Fraser, M. (2007). Neuropilin 2/semaphorin 3F signaling is essential for cranial neural crest migration and trigeminal ganglion condensation. *Developmental Neurobiology*, *67*(1), 47–56.

Gans, C., & Northcutt, R. G. (1983). Neural crest and the origin of vertebrates: A new head. *Science* (Vol. 220, Issue 4594, pp. 268–274).

Gao, Y., Dickerson, J., Guo, F., Zheng, J. and Zheng, Y., 2004. Rational design and characterization of a Rac GTPase-specific small molecule inhibitor. Proceedings of the National Academy of Sciences, 101(20), pp.7618-7623.

Garcia-Guzman, M., Dolfi, F., Russello, M., & Vuori, K. (1999). Cell adhesion regulates the interaction between the docking protein p130(Cas) and the 14-3-3 proteins. *Journal of Biological Chemistry*, *274*(9), 5762–5768.

Gardiner, E. M., Pestonjamasp, K. N., Bohl, B. P., Chamberlain, C., Hahn, K. M., & Bokoch, G. M. (2002). Spatial and temporal analysis of Rac activation during live neutrophil chemotaxis. *Current Biology*, *12*(23), 2029–2034.

Garton, A. J., Burnham, M. R., Bouton, A. H., & Tonks, N. K. (1997). Association of PTP-PEST with the SH3 domain of p130(cas); A novel mechanism of protein tyrosine phosphatase substrate recognition. *Oncogene*, *15*(8), 877–885.

Geiger, B., & Bershadsky, A. (2001). Assembly and mechanosensory function of focal contacts. *Current Opinion in Cell Biology* (Vol. 13, Issue 5, pp. 584–592).

Geiger, B., Spatz, J. P., & Bershadsky, A. D. (2009). Environmental sensing through focal adhesions. In *Nature Reviews Molecular Cell Biology* (Vol. 10, Issue 1, pp. 21–33).

Giovannone, D., Reyes, M., Reyes, R., Correa, L., Martinez, D., Ra, H., Gomez, G., Kaiser, J., Ma, L., Stein, M. P., & De Bellard, M. E. (2012). Slits affect the timely migration of neural crest cells via robo receptor. *Developmental Dynamics*, *241*(8), 1274–1288.

Gittes, F., Mickey, B., Nettleton, J., & Howard, J. (1993). Flexural rigidity of microtubules and actin filaments measured from thermal fluctuations in shape. *Journal of Cell Biology*, *120*(4). 923-934

Grashoff, C., Hoffman, B. D., Brenner, M. D., Zhou, R., Parsons, M., Yang, M. T., McLean, M. A., Sligar, S. G., Chen, C. S., Ha, T., & Schwartz, M. A. (2010). Measuring mechanical tension across vinculin reveals regulation of focal adhesion dynamics. *Nature*, *466*(7303).263-266

Green, Y. S., Kwon, S., & Christian, J. L. (2016). Expression pattern of bcar3, a downstream target of Gata2, and its binding partner, bcar1, during Xenopus development. *Gene Expression Patterns*, *20*(1). 55-62

Haas, P., & Gilmour, D. (2006). Chemokine Signaling Mediates Self-Organizing Tissue Migration in the Zebrafish Lateral Line. *Developmental Cell*, *10*(5), 673–680.

Hall, A. (2009). The cytoskeleton and cancer. *Cancer and Metastasis Reviews* (Vol. 28, Issues 1–2, pp. 5–14).

Harland, R. M. (1991). In situ hybridization: an improved whole-mount method for Xenopus embryos. *Methods in Cell Biology*, *36*. 685–695

His, W. (1868). Untersuchungen über die erste Anlage des Wirbeltierleibes: die erste Entwickelung des Hühnchens im Ei. *Vogel FCW:Leipzig*, 237 p.

Ho, L., Symes, K., Yordán, C., Gudas, L. J., & Mercola, M. (1994). Localization of PDGF A and PDGFRα mRNA in Xenopus embryos suggests signalling from neural ectoderm and pharyngeal endoderm to neural crest cells. *Mechanisms of Development*, *48*(3), 165–174.

Honda, H., Oda, H., Nakamoto, T., Honda, Z. I., Sakai, R., Suzuki, T., Saito, T., Nakamura, K., Nakao, K., Ishikawa, T., Katsuki, M., Yazaki, Y., & Hirai, H. (1998). Cardiovascular anomaly, impaired actin bundling and resistance to Src- induced transformation in mice lacking p130(Cas). *Nature Genetics*, *19*(4), 361–365.

Horwitz, R., & Webb, D. (2003). Cell migration. In *Current biology : CB* (Vol. 13, Issue 19, pp. R756–R759).

Hotulainen, P., & Lappalainen, P. (2006). Stress fibers are generated by two distinct actin assembly mechanisms in motile cells. *Journal of Cell Biology*, *173*(3). 383-394

Hutchins, E. J., & Bronner, M. E. (2018). Draxin acts as a molecular rheostat of canonical Wnt signaling to control cranial neural crest EMT. *Journal of Cell Biology*, *217*(10). 3683-3697

Ishino, M., Ohba, T., Sasaki, H., & Sasaki, T. (1995). Molecular cloning of a cDNA encoding a phosphoprotein, Efs, which contains a Src homology 3 domain and associates with Fyn. *Oncogene*, *11*(11). 2331–8.

Itoh, R. E., Kurokawa, K., Ohba, Y., Yoshizaki, H., Mochizuki, N., & Matsuda, M. (2002). Activation of Rac and Cdc42 Video Imaged by Fluorescent Resonance Energy Transfer-Based Single-Molecule Probes in the Membrane of Living Cells. *Molecular and Cellular Biology*, *22*(18), 6582–6591.

Janssen, H., & Marynen, P. (2006). Interaction partners for human ZNF384/CIZ/NMP4 - Zyxin as a mediator for p130CAS signaling? *Experimental Cell Research*, *312*(7). 1194-1204

Jia, L., Cheng, L., & Raper, J. (2005). Slit/Robo signaling is necessary to confine early neural crest cells to the ventral migratory pathway in the trunk. *Developmental Biology*, *282*(2), 411–421.

Jiang, G., Giannone, G., Critchley, D. R., Fukumoto, E., & Sheet, M. P. (2003). Two-piconewton slip bond between fibronectin and the cytoskeleton depends on talin. *Nature*, *424*(6946), 334–337.

Johnson, R. P., & Craig, S. W. (1995). F-actin binding site masked by the intramolecular association of vinculin head and tail domains. *Nature* (Vol. 373, Issue 6511). 261-264

Kaibuchi, K., Kuroda, S., & Amano, M. (1999). Regulation of the Cytoskeleton and Cell Adhesion by the Rho Family GTPases in Mammalian Cells. *Annual Review of Biochemistry*, *68*(1), 459–486.

Kang, Y., & Massagué, J. (2004). Epithelial-mesenchymal transitions: Twist in development and metastasis. *Cell* (Vol. 118, Issue 3, pp. 277–279).

Katsumi, A., Naoe, T., Matsushita, T., Kaibuchi, K., & Schwartz, M. A. (2005). Integrin activation and matrix binding mediate cellular responses to mechanical stretch. *Journal of Biological Chemistry*, *280*(17), 16546–16549.

Kaverina, I., Krylyshkina, O., & Small, J. V. (1999). Microtubule targeting of substrate contacts promotes their relaxation and dissociation. *Journal of Cell Biology*, *146*(5), 1033–1043.

Kim, M., Carman, C. V., & Springer, T. A. (2003). Bidirectional transmembrane signaling by cytoplasmic domain separation in integrins. *Science*, *301*(5640). 1720-1725

Kirby, M. L., & Hutson, M. R. (2010). Factors controlling cardiac neural crest cell migration. In *Cell Adhesion and Migration* (Vol. 4, Issue 4). 609-621

Kirsch, K. H., Georgescu, M. M., & Hanafusa, H. (1998). Direct binding of p130(Cas) to the guanine nucleotide exchange factor C3G. *Journal of Biological Chemistry*, *273*(40), 25673–25679.

Kiyokawa, E., Hashimoto, Y., Kobayashi, S., Sugimura, H., Kurata, T., & Matsuda, M. (1998). Activation of Rac1 by a Crk SH3-binding protein, DOCK180. *Genes and Development*, *12*(21), 3331–3336.

Klemke, R. L., Leng, J., Molander, R., Brooks, P. C., Vuori, K., & Cheresh, D. A. (1998). CAS/Crk coupling serves as a "molecular switch" for induction of cell migration. *Journal of Cell Biology*, *140*(4), 961–972.

Kleinman, H. and Martin, G., 2005. Matrigel: Basement membrane matrix with biological activity. Seminars in Cancer Biology, 15(5), pp.378-386.

Koestner, U., Shnitsar, I., Linnemannstöns, K., Hufton, A. L., & Borchers, A. (2008). Semaphorin and neuropilin expression during early morphogenesis of *Xenopus laevis*. *Developmental Dynamics*, *237*(12), 3853–3863.

Kostic, A., & Sheetz, M. P. (2006). Fibronectin rigidity response through Fyn and p130Cas recruitment to the leading edge. *Molecular Biology of the Cell*, *17*(6), 2684–2695.

Krylyshkina, O., Kaverina, I., Kranewitter, W., Steffen, W., Alonso, M. C., Cross, R. A., & Small, J. V. (2002). Modulation of substrate adhesion dynamics via microtubule targeting requires kinesin-1. *Journal of Cell Biology*, *156*(2), 349–359.

LaBonne, C. and Bronner-Fraser, M., 2000. Snail-Related Transcriptional Repressors Are Required in Xenopus for both the Induction of the Neural Crest and Its Subsequent Migration. Developmental Biology, 221(1), pp.195-205.

LaBonne, C., & Bronner-Fraser, M. (1998). Neural crest induction in Xenopus: Evidence for a two-signal model. *Development*, *125*(13).

Lai, F. P. L., Szczodrak, M., Block, J., Faix, J., Breitsprecher, D., Mannherz, H. G., Stradal, T. E. B., Dunn, G. A., Small, J. V., & Rottner, K. (2008). Arp2/3 complex interactions and actin network turnover in lamellipodia. *EMBO Journal*, *27*(7). 982-992

Lämmermann, T., & Sixt, M. (2009). Mechanical modes of "amoeboid" cell migration. *Current Opinion in Cell Biology* (Vol. 21, Issue 5, pp. 636–644).

Larue, L., & Bellacosa, A. (2005). Epithelial-mesenchymal transition in development and cancer: Role of phosphatidylinositol 3' kinase/AKT pathways. *Oncogene* (Vol. 24, Issue 50). 7443-7454.

Lauffenburger, D. A., & Horwitz, A. F. (1996). Cell migration: A physically integrated molecular process. *Cell* (Vol. 84, Issue 3, pp. 359–369).

Law, S. F., Estojak, J., Wang, B., Mysliwiec, T., Kruh, G., & Golemis, E. A. (1996). Human enhancer of filamentation 1, a novel p130cas-like docking protein, associates with focal adhesion kinase and induces pseudohyphal growth in Saccharomyces cerevisiae. *Molecular and Cellular Biology*, *16*(7), 3327–3337.

Law, S. F., Zhang, Y. Z., Fashena, S. J., Toby, G., Estojak, J., & Golemis, E. A. (1999). Dimerization of the docking/adaptor protein HEF1 via a carboxy-terminal helix-loop-helix domain. *Experimental Cell Research*, *252*(1), 224–235.

Le Douarin, N. and Kalcheim, C. (1999) The Neural Crest. 2nd edn. Cambridge: Cambridge University Press (Developmental and Cell Biology Series

Lecaudey, V., & Gilmour, D. (2006). Organizing moving groups during morphogenesis. *Current Opinion in Cell Biology* (Vol. 18, Issue 1, pp. 102–107).

Li, A., Zhang, W., Xia, H., Miao, Y., Zhou, H., Zhang, X., Dong, Q., Li, Q., Qiu, X., & Wang, E. (2016). Overexpression of CASS4 promotes invasion in non-small cell lung cancer by activating the AKT signaling pathway and inhibiting E-cadherin expression. *Tumor Biology*, *37*(11). 15157–15164

Li, Y., Vieceli, F., Gonzalez, W., Li, A., Tang, W., Lois, C. and Bronner, M., 2019. In Vivo Quantitative Imaging Provides Insights into Trunk Neural Crest Migration. *Cell Reports*, 26(6), pp.1489-1500.e3.

Liu, J. A., Rao, Y., Cheung, M. P. L., Hui, M. N., Wu, M. H., Chan, L. K., Ng, I. O. L., Niu, B., Cheah, K. S. E., Sharma, R., Hodgson, L., & Cheung, M. (2017). Asymmetric localization of DLC1 defines avian trunk neural crest polarity for directional delamination and migration. *Nature Communications*, *8*(1).

Liu, S., Thomas, S. M., Woodside, D. G., Rose, D. M., Klosses, W. B., Pfaff, M., & Ginsberg, M. H. (1999). Binding of paxillin to α4 integrins modifies integrin-dependent biological responses. *Nature*, *402*(6762), 676–681.

Luo, T., Matsuo-Takasaki, M., Thomas, M. L., Weeks, D. L., & Sargent, T. D. (2002). Transcription factor AP-2 is an essential and direct regulator of epidermal development in Xenopus. *Developmental Biology*, *245*(1), 136–144.

MacHacek, M., Hodgson, L., Welch, C., Elliott, H., Pertz, O., Nalbant, P., Abell, A., Johnson, G. L., Hahn, K. M., & Danuser, G. (2009). Coordination of Rho GTPase activities during cell protrusion. *Nature*, *461*(7260). 99-103

Maillet, M., Robert, S. J., Cacquevel, M., Gastineau, M., Vivien, D., Bertoglio, J., Zugaza, J. L., Fischmeister, R., & Lezoualc'h, F. (2003). Crosstalk between Rap1 and Rac regulates secretion of sAPPα. *Nature Cell Biology*, *5*(7). 633–639

Mancilla, A., & Mayor, R. (1996). Neural crest formation in Xenopus laevis: Mechanisms of Xslug induction. *Developmental Biology*, *177*(2). 580-589

Marchant, L., Linker, C., Ruiz, P., Guerrero, N., & Mayor, R. (1998). The inductive properties of mesoderm suggest that the neural crest cells are specified by a BMP gradient. *Developmental Biology*, *198*(2). 319-329

Margadant, C., Kreft, M., Zambruno, G., & Sonnenberg, A. (2013). Kindlin-1 Regulates Integrin Dynamics and Adhesion Turnover. *PLoS ONE*, *8*(6)

Matthews, H. K., Marchant, L., Carmona-Fontaine, C., Kuriyama, S., Larraín, J., Holt, M. R., Parsons, M., & Mayor, R. (2008). Directional migration of neural crest cells in vivo is regulated by Syndecan-4/Rac1 and non-canonical Wnt signaling/RhoA. *Development*, *135*(10), 1771–1780.

Mayor, R., & Etienne-Manneville, S. (2016). The front and rear of collective cell migration. *Nature Reviews Molecular Cell Biology* (Vol. 17, Issue 2). 97-109

Mayor, R., Guerrero, N., Young, R. M., Gomez-Skarmeta, J. L., & Cuellar, C. (2000). A novel function for the Xslug gene: Control of dorsal mesendoderm development by repressing BMP-4. *Mechanisms of Development*, *97*(1–2), 47–56.

McLennan, R., & Kulesa, P. M. (2007). In vivo analysis reveals a critical role for neuropilin-1 in cranial neural crest cell migration in chick. *Developmental Biology*, *301*(1), 227–239.

McLennan, R., Schumacher, L. J., Morrison, J. A., Teddy, J. M., Ridenour, D. A., Box, A. C., Semerad, C. L., Li, H., McDowell, W., Kay, D., Maini, P. K., Baker, R. E., & Kulesa, P. M. (2015). VEGF signals induce trailblazer cell identity that drives neural crest migration. *Developmental Biology*, *407*(1), 12–25.

McLennan, R., Teddy, J. M., Kasemeier-Kulesa, J. C., Romine, M. H., & Kulesa, P. M. (2010). Vascular endothelial growth factor (VEGF) regulates cranial neural crest migration in vivo. *Developmental Biology*, *339*(1), 114–125.

Meek, L. M., Hayata, T., Shin, Y. C., Evinger, A. J., & Cho, K. W. Y. (2004). Cloning and expression of an SH3 domain-containing protein (Xchef-1), a novel downstream target of activin/nodal signaling. *Gene Expression Patterns*, *4*(6). 719-724

Mellor, H. (2010). The role of formins in filopodia formation. *Biochimica et Biophysica Acta - Molecular Cell Research* (Vol. 1803, Issue 2). 191-200

Mellott, D. O., & Burke, R. D. (2008). Divergent roles for Eph and ephrin in avian cranial neural crest. *BMC Developmental Biology*, *8*, 56.

Miao, Y., Wang, L., Liu, Y., Li, A. L., Liu, S. L., Cao, H. Y., Zhang, X. P., Jiang, G. Y., Liu, D., & Wang, E. H. (2013). Overexpression and cytoplasmic accumulation of Hepl is associated with clinicopathological parameters and poor prognosis in non-small cell lung cancer. *Tumor Biology*, *34*(1), 107–114.

Miki, H., Suetsugu, S., & Takenawa, T. (1998). WAVE, a novel WASP-family protein involved in actin reorganization induced by Rac. *EMBO Journal*, *17*(23). 6932-6941

Minegishi, M., Tachibana, K., Sato, T., Iwata, S., Nojima, Y. and Morimoto, C., 1996. Structure and function of Cas-L, a 105-kD Crk-associated substrate-related protein that is involved in beta 1 integrin-mediated signaling in lymphocytes. *The Journal of Experimental Medicine*, 184(4), pp.1365-1375.

Montell, D. J., Yoon, W. H., & Starz-Gaiano, M. (2012). Group choreography: Mechanisms orchestrating the collective movement of border cells. *Nature Reviews Molecular Cell Biology* (Vol. 13, Issue 10). 631-645

Moore, R., Theveneau, E., Pozzi, S., Alexandre, P., Richardson, J., Merks, A., Parsons, M., Kashef, J., Linker, C., & Mayor, R. (2013). Par3 controls neural crest migration by promoting microtubule catastrophe during contact inhibition of locomotion. *Development (Cambridge)*, *140*(23), 4763–4775.

Nabeshima, K. (1999) 'Cohort migration of carcinoma cells: Differentiated colorectal carcinoma cells move as coherent cell clusters or sheets', *Histology and Histopathology*. Histol Histopathol, pp. 1183–1197.

Nakamoto, T., Yamagata, T., Sakai, R., Ogawa, S., Honda, H., Ueno, H., Hirano, N., Yazaki, Y., & Hirai, H. (2000). CIZ, a Zinc Finger Protein That Interacts with p130cas and Activates the Expression of Matrix Metalloproteinases. *Molecular and Cellular Biology*, *20*(5), 1649–1658.

Natarajan, M., Stewart, J. E., Golemis, E. A., Pugacheva, E. N., Alexandropoulos, K., Cox, B. D., Wang, W., Grammer, J. R., & Gladson, C. L. (2006). HEF1 is a necessary and specific downstream effector of FAK that promotes the migration of glioblastoma cells. *Oncogene*, *25*(12), 1721–1732.

Nguyen, V. H., Schmid, B., Trout, J., Connors, S. A., Ekker, M., & Mullins, M. C. (1998). Ventral and lateral regions of the zebrafish gastrula, including the Neural crest progenitors, are established by a bmp2b/swirl pathway of genes. *Developmental Biology*, *199*(1). 93-110

Nichols, D. H. (1981). Neural crest formation in the head of the mouse embryo as observed using a new histological technique. In *J. Embryol. exp. Morph* (Vol. 64). 105-120.

Nichols, D. H. (1987). Ultrastructure of neural crest formation in the midbrain/rostral hindbrain and preotic hindbrain regions of the mouse embryo. *American Journal of Anatomy*, *179*(2), 143–154.

Niediek, V., Born, S., Hampe, N., Kirchgeßner, N., Merkel, R., & Hoffmann, B. (2012). Cyclic stretch induces reorientation of cells in a Src family kinase- and p130Cas-dependent manner. *European Journal of Cell Biology*, *91*(2), 118–128.

Nieto, M. A., Huang, R. Y. Y. J., Jackson, R. A. A., & Thiery, J. P. P. (2016). EMT: 2016. *Cell* (Vol. 166, Issue 1). 21-45

Nieto, M. A., Sargent, M. G., Wilkinson, D. G., & Cooke, J. (1994). Control of cell behavior during vertebrate development by Slug, a zinc finger gene. *Science*, *264*(5160), 835–839.

Nobes, C. D., & Hall, A. (1995). Rho, Rac, and Cdc42 GTPases regulate the assembly of multimolecular focal complexes associated with actin stress fibers, lamellipodia, and filopodia. *Cell*, *81*(1). 53-62

Oakes, P. W., & Gardel, M. L. (2014). Stressing the limits of focal adhesion mechanosensitivity. *Current Opinion in Cell Biology* (Vol. 30, Issue 1, pp. 68–73).

Ohashi, Y., Tachibana, K., Kamiguchi, K., Fujita, H., & Morimoto, C. (1998). T cell receptor-mediated tyrosine phosphorylation of Cas-L, a 105-kDa Crk-associated substrate-related protein, and its association of Crk and C3G. *Journal of Biological Chemistry*, *273*(11), 6446–6451.

Olesnicky Killian, E. C., Birkholz, D. A., & Artinger, K. B. (2009). A role for chemokine signaling in neural crest cell migration and craniofacial development. *Developmental Biology*, *333*(1), 161–172.

Otey, C. A., Pavalko, F. M., & Burridge, K. (1990). An interaction between α-actinin land the β1 integrin subunit in vitro. *Journal of Cell Biology*, *111*(2). 721-729

Pankov, R., Cukierman, E., Katz, B. Z., Matsumoto, K., Lin, D. C., Lin, S., Hahn, C., & Yamada, K. M. (2000). Integrin dynamics and matrix assembly: Tensin-dependent translocation of α5β1 integrins promotes early fibronectin fibrillogenesis. *Journal of Cell Biology*, *148*(5), 1075–1090.

Pellicena, P., & Miller, W. T. (2001). Processive Phosphorylation of p130Cas by Src Depends on SH3-Polyproline Interactions. *Journal of Biological Chemistry*, *276*(30), 28190–28196.

Perez-Branguli, F., Zagar, Y., Shanley, D. K., Graef, I. A., Chédotal, A., & Mitchell, K. J. (2016). Reverse signaling by semaphorin-6A regulates cellular aggregation and neuronal morphology. *PLoS ONE*, *11*(7).

Pertz, O., Hodgson, L., Klemke, R. L., & Hahn, K. M. (2006). Spatiotemporal dynamics of RhoA activity in migrating cells. *Nature*, *440*(7087). 1069-1072

Pollet, N., Muncke, N., Verbeek, B., Li, Y., Fenger, U., Delius, H., & Niehrs, C. (2005). An atlas of differential gene expression during early Xenopus embryogenesis. *Mechanisms of Development*, *122*(3). 365-439

Pratt, S. J., Epple, H., Ward, M., Feng, Y., Braga, V. M., & Longmore, G. D. (2005). The LIM protein Ajuba influences p130Cas localization and Rac1 activity during cell migration. *Journal of Cell Biology*, *168*(5), 813–824.

Puklin-Faucher, E., Gao, M., Schulten, K., & Vogel, V. (2006). How the headpiece hinge angle is opened: New insights into the dynamics of integrin activation. *Journal of Cell Biology*, *175*(2). 349-360

Rabadán, M. A., Herrera, A., Fanlo, L., Usieto, S., Carmona-Fontaine, C., Barriga, E. H., Mayor, R., Pons, S., & Martí, E. (2016). Delamination of neural crest cells requires transient and reversible Wnt inhibition mediated by Dact1/2. *Development (Cambridge)*, *143*(12), 2194–2205.

Ramos-Hryb, A., Da-Costa, M., Trentin, A. and Calloni, G., 2013. Matrigel supports neural, melanocytic and chondrogenic differentiation of trunk neural crest cells. The International Journal of Developmental Biology, 57(11-12), pp.885-890.

Rap1b Expression [Xenopus] - Xenbase Gene Catalog. 2021 [online] Available at: <http://www.xenbase.org/gene/expression.do?method=displayGenePageExpression&geneId=479036&objId=479036> [Accessed 20 January 2021].

Reinhart-King, C. A., Dembo, M., & Hammer, D. A. (2005). The dynamics and mechanics of endothelial cell spreading. *Biophysical Journal*, *89*(1), 676–689.

Ren, X. D., Kiosses, W. B., Sieg, D. J., Otey, C. A., Schlaepfer, D. D., & Schwartz, M. A. (2000). Focal adhesion kinase suppresses Rho activity to promote focal adhesion. *Journal of Cell Science*, *113*(20).

Ridley, A. J. (2001). Rho GTPases and cell migration. *Journal of Cell Science*, *114*(15).2713-2722

Ridley, A. J., Paterson, H. F., Johnston, C. L., Diekmann, D., & Hall, A. (1992). The small GTP-binding protein rac regulates growth factor-induced membrane ruffling. *Cell*, *70*(3). 401-410

Ridley, A. J., Schwartz, M. A., Burridge, K., Firtel, R. A., Ginsberg, M. H., Borisy, G., Parsons, J. T., & Horwitz, A. R. (2003). Cell Migration: Integrating Signals from Front to Back. In *Science* (Vol. 302, Issue 5651, pp. 1704–1709).

Riveline, D., Zamir, E., Balaban, N. Q., Schwarz, U. S., Ishizaki, T., Narumiya, S., Kam, Z., Geiger, B., & Bershadsky, A. D. (2001). Focal Contacts as Mechanosensors: Externally Applied Local Mechanical Force Induces Growth of Focal Contacts by an mDia1-dependent and ROCK-independent Mechanism. *The Journal of Cell Biology* (Vol. 153, Issue 6). 1175-1186.

Rogers, C. D., Saxena, A., & Bronner, M. E. (2013). Sip1 mediates an E-cadherin-to-N-cadherin switch during cranial neural crest EMT. *Journal of Cell Biology*, *203*(5). 835-847.

Romero, S., Le Clainche, C., Didry, D., Egile, C., Pantaloni, D., & Carlier, M. F. (2004). Formin is a processive motor that requires profilin to accelerate actin assembly and associated ATP hydrolysis. *Cell*, *119*(3). 419-429

Rooney, C., White, G., Nazgiewicz, A., Woodcock, S. A., Anderson, K. I., Ballestrem, C., & Malliri, A. (2010). The Rac activator STEF (Tiam2) regulates cell migration by microtubule-mediated focal adhesion disassembly. *EMBO Reports*, *11*(4), 292–298.

Rørth, P. (2007). Collective guidance of collective cell migration. *Trends in Cell Biology*, *17*(12), 575–579.

Rørth, P. (2009). Collective Cell Migration. *Annual Review of Cell and Developmental Biology*, *25*(1), 407–429

Rottner, K., Hall, A., & Small, J. V. (1999). Interplay between Rac and Rho in the control of substrate contact dynamics. *Current Biology*, *9*(12). 640-S1

Roycroft, A. and Mayor, R., 2015. Molecular basis of contact inhibition of locomotion. *Cellular and Molecular Life Sciences*, 73(6), pp.1119-1130.

Roycroft, A., Szabó, A., Bahm, I., Daly, L., Charras, G., Parsons, M., & Mayor Correspondence, R. (2018). Redistribution of Adhesive Forces through Src/FAK Drives Contact Inhibition of Locomotion in Neural Crest. *Developmental Cell*, *45*, 565–579.

Ruest, P. J., Shin, N.-Y., Polte, T. R., Zhang, X., & Hanks, S. K. (2001). Mechanisms of CAS Substrate Domain Tyrosine Phosphorylation by FAK and Src. *Molecular and Cellular Biology*, *21*(22). 7641-7652

Rush, J., Moritz, A., Lee, K. A., Guo, A., Goss, V. L., Spek, E. J., Zhang, H., Zha, X. M., Polakiewicz, R. D., & Comb, M. J. (2005). Immunoaffinity profiling of tyrosine phosphorylation in cancer cells. *Nature Biotechnology*, *23*(1), 94–101.

Sadaghiani, B., & Thiébaud, C. H. (1987). Neural crest development in the Xenopus laevis embryo, studied by interspecific transplantation and scanning electron microscopy. *Developmental Biology*, *124*(1), 91–110.

Sakai, R., Iwamatsu, A., Hirano, N., Ogawa, S., Tanaka, T., Mano, H., Yazaki, Y., & Hirai, H. (1994). A novel signaling molecule, p130, forms stable complexes in vivo with v-Crk and v-Src in a tyrosine phosphorylation-dependent manner. *The EMBO Journal*, *13*(16), 3748–3756.

Sakakibara, A., Ohba, Y., Kurokawa, K., Matsuda, M., & Hattori, S. (2002). Novel function of Chat in controlling cell adhesion via Cas-Crk-C3G-pathway-mediated Rap1 activation. *Journal of Cell Science*, *115*(24), 4915–4924.

Sanz-Moreno, V., Gadea, G., Ahn, J., Paterson, H., Marra, P., Pinner, S., Sahai, E., & Marshall, C. J. (2008). Rac Activation and Inactivation Control Plasticity of Tumor Cell Movement. *Cell*, *135*(3), 510–523.

Sauka-Spengler, T., & Bronner-Fraser, M. (2008). A gene regulatory network orchestrates neural crest formation. *Nature Reviews Molecular Cell Biology* (Vol. 9, Issue 7). 557-568

Saw, T. B., Jain, S., Ladoux, B., & Lim, C. T. (2015). Mechanobiology of Collective Cell Migration. *Cellular and Molecular Bioengineering*, *8*(1), 3–13.

Sawada, Y., & Sheetz, M. P. (2002). Force transduction by Triton cytoskeletons. *Journal of Cell Biology*, *156*(4). 609-615

Sawada, Y., Tamada, M., Dubin-Thaler, B. J., Cherniavskaya, O., Sakai, R., Tanaka, S., & Sheetz, M. P. (2006). Force Sensing by Mechanical Extension of the Src Family Kinase Substrate p130Cas. *Cell*, *127*(5). 1015–26,

Scarpa, E., Szabó, A., Bibonne, A., Theveneau, E., Parsons, M., & Mayor, R. (2015). Cadherin Switch during EMT in Neural Crest Cells Leads to Contact Inhibition of Locomotion via Repolarization of Forces. *Developmental Cell*, *34*(4) 421-434

Schlaepfer, D. D., Broome, M. A., & Hunter, T. (1997). Fibronectin-stimulated signaling from a focal adhesion kinase-c-Src complex: involvement of the Grb2, p130cas, and Nck adaptor proteins. *Molecular and Cellular Biology*, *17*(3), 1702–1713.

Selleck, M. A. J., & Bronner-Fraser, M. (1995). Origins of the avian neural crest: The role of neural plate-epidermal interactions. *Development*, *121*(2). 525-538

Sharma, A., & Mayer, B. J. (2008). Phosphorylation of p130Cas initiates Rac activation and membrane ruffling. *BMC Cell Biology*, *9*.

Shellard, A., Szabó, A., Trepat, X. and Mayor, R., 2018. Supracellular contraction at the rear of neural crest cell groups drives collective chemotaxis. *Science*, 362(6412), pp.339-343.

Shi, J., Severson, C., Yang, J., Wedlich, D., & Klymkowsky, M. W. (2011). Snail2 controls mesodermal bmp/wnt induction of neural crest. *Development*, *138*(15). 3135-3145

Shin, N., Dise, R., Schneider-Mergener, J., Ritchie, M., Kilkenny, D. and Hanks, S., 2004. Subsets of the Major Tyrosine Phosphorylation Sites in Crk-associated Substrate (CAS) Are Sufficient to Promote Cell Migration. *Journal of Biological Chemistry*, 279(37), pp.38331-38337.

Simpson, K. J., Selfors, L. M., Bui, J., Reynolds, A., Leake, D., Khvorova, A., & Brugge, J. S. (2008). Identification of genes that regulate epithelial cell migration using an siRNA screening approach. *Nature Cell Biology*, *10*(9).

Singh, M. K., Dadke, D., Nicolas, E., Serebriiskii, I. G., Apostolou, S., Canutescu, A., Egleston, B. L., & Golemis, E. A. (2008). A novel Cas family member, HEPL, regulates FAK and cell spreading. *Molecular Biology of the Cell*, *19*(4), 1627–1636.

Small, J. V., Rottner, K., Kaverina, I., & Anderson, K. I. (1998). Assembling an actin cytoskeleton for cell attachment and movement. *Biochimica et Biophysica Acta - Molecular Cell Research* (Vol. 1404, Issue 3). 271-281

Smith, A., Robinson, V., Patel, K., & Wilkinson, D. G. (1997). The EphA4 and EphB1 receptor tyrosine kinases and ephrin-B2 ligand regulate targeted of branchial neural crest cells. *Current Biology*, *7*(8), 561–570.

Soofi, S., Last, J., Liliensiek, S., Nealey, P. and Murphy, C., 2009. The elastic modulus of Matrigel™ as determined by atomic force microscopy. Journal of Structural Biology, 167(3), pp.216-219.

Stephenson, R. E., & Miller, A. L. (2017). Tools for live imaging of active Rho GTPases in Xenopus. *Genesis* (Vol. 55, Issues 1–2).

Svitkina, T. M., Bulanova, E. A., Chaga, O. Y., Vignjevic, D. M., Kojima, S. ichiro, Vasiliev, J. M., & Borisy, G. G. (2003). Mechanism of filopodia initiation by reorganization of a dendritic network. *Journal of Cell Biology*, *160*(3). 409-421

Szabó, A., Theveneau, E., Turan, M., & Mayor, R. (2019). Neural crest streaming as an emergent property of tissue interactions during morphogenesis. *PLoS Computational Biology*, *15*(4).

Tachibana, K., Urano, T., Fujitat, H., Ohashi, Y., Kamiguchi, K., Iwata, S., Hirai, H., & Morimoto, C. (1997). Tyrosine phosphorylation of Crk-associated substrates by focal adhesion kinase. A putative mechanism for the integrin-mediated tyrosine phosphorylation of Crk-associated substrates. *Journal of Biological Chemistry*, *272*(46), 29083–29090.

Theveneau, E. and Mayor, R., 2012. Neural crest delamination and migration: From epithelium-to-mesenchyme transition to collective cell migration. *Developmental Biology*, 366(1), pp.34-54.

Theveneau, E., & Mayor, R. (2013). Collective cell migration of epithelial and mesenchymal cells. *Cellular and Molecular Life Sciences* (Vol. 70, Issue 19). 3481-3492

Theveneau, E., Marchant, L., Kuriyama, S., Gull, M., Moepps, B., Parsons, M., & Mayor, R. (2010). Collective Chemotaxis Requires Contact-Dependent Cell Polarity. *Developmental Cell*, *19*(1), 39–53.

Theveneau, E., Steventon, B., Scarpa, E., Garcia, S., Trepat, X., Streit, A., & Mayor, R. (2013). Chase-and-run between adjacent cell populations promotes directional collective migration. *Nature Cell Biology*, *15*(7), 763–772.

Thiery, J. P., & Morgan, M. (2004). Breast cancer progression with a Twist. *Nature Medicine*, *10*(8), 777–778.

Thiery, J. P., Acloque, H., Huang, R. Y. J., & Nieto, M. A. (2009). Epithelial-Mesenchymal Transitions in Development and Disease. *Cell* (Vol. 139, Issue 5) , 871-890.

Tikhmyanova, N., & Golemis, E. A. (2011). NEDD9 and BCAR1 negatively regulate E-cadherin membrane localization, and promote E-cadherin degradation. *PLoS ONE*, *6*(7). 25-35

Tikhmyanova, N., Little, J. L., & Golemis, E. A. (2010). CAS proteins in normal and pathological cell growth control. *Cellular and Molecular Life Sciences* (Vol. 67, Issue 7, pp. 1025–1048).

Tríbulo, C., Aybar, M. J., Nguyen, V. H., Mullins, M. C., & Mayor, R. (2003). Regulation of Msx genes by a Bmp gradient is essential for neural crest specification. *Development*, *130*(26), 6441-6452

Trichet, L., Le Digabel, J., Hawkins, R. J., Vedula, S. R. K., Gupta, M., Ribrault, C., Hersen, P., Voituriez, R., & Ladoux, B. (2012). Evidence of a large-scale mechanosensing mechanism for cellular adaptation to substrate stiffness. *Proceedings of the National Academy of Sciences of the United States of America*, *109*(18), 6933–6938.

Trujillo, S. et al. (2020) 'Engineered 3D hydrogels with full-length fibronectin that sequester and present growth factors', Biomaterials. Elsevier Ltd, 252, p. 120104. doi: 10.1016/j.biomaterials.2020.120104.

Tsuji, T., Ishizaki, T., Okamoto, M., Higashida, C., Kimura, K., Furuyashiki, T., Arakawa, Y., Birge, R. B., Nakamoto, T., Hirai, H., & Narumiya, S. (2002). ROCK and mDia1 antagonize in Rho-dependent Rac activation in Swiss 3T3 fibroblasts. *Journal of Cell Biology*, *157*(5). 819-830

Vandewalle, C., Comijn, J., De Craene, B., Vermassen, P., Bruyneel, E., Andersen, H., Tulchinsky, E., Van Roy, F., & Berx, G. (2005). SIP1/ZEB2 induces EMT by repressing genes of different epithelial cell-cell junctions. *Nucleic Acids Research*, *33*(20). 6566-6578.

Wang, H. U., & Anderson, D. J. (1997). Eph family transmembrane ligands can mediate repulsive guidance of trunk neural crest migration and motor axon outgrowth. *Neuron*, *18*(3), 383–396.

Wang, N., Butler, J. P., & Ingber, D. E. (1993). Mechanotransduction across the cell surface and through the cytoskeleton. *Science*, *260*(5111). 1124-1127

Wang, X., Weng, L. P., & Yu, Q. (2000). Specific inhibition of FGF-induced MAPK activation by the receptor-like protein tyrosine phosphatase LAR. *Oncogene*, *19*(19), 2346–2353.

Wang, Y. L. (1985). Exchange of actin subunits at the leading edge of living fibroblasts: Possible role of treadmilling. *Journal of Cell Biology*, *101*(2). 597-602

Watanabe, N., Bodin, L., Pandey, M., Krause, M., Coughlin, S., Boussiotis, V. A., Ginsberg, M. H., & Shattil, S. J. (2008). Mechanisms and consequences of agonist-induced talin recruitment to platelet integrin αIIbβ3. *Journal of Cell Biology*, *181*(7). 1211-1222

Webb, D. J., Donais, K., Whitmore, L. A., Thomas, S. M., Turner, C. E., Parsons, J. T., & Horwitz, A. F. (2004). FAK-Src signalling through paxillin, ERK and MLCK regulates adhesion disassembly. *Nature Cell Biology*, *6*(2), 154–161.

Wehrle-Haller, B., 2012. Assembly and disassembly of cell matrix adhesions. Current Opinion in Cell Biology, 24(5), pp.569-581.

Wehrle-Haller, B., & Imhof, B. A. (2003). Actin, microtubules and focal adhesion dynamics during cell migration. *International Journal of Biochemistry and Cell Biology* (Vol. 35, Issue 1, pp. 39–50).

Welch, M. D., & Mullins, R. D. (2002). Cellular Control of Actin Nucleation. *Annual Review of Cell and Developmental Biology*, *18*(1). 247-288

Wheeler, A. P., & Ridley, A. J. (2004). Why three Rho proteins? RhoA, RhoB, RhoC, and cell motility. In *Experimental Cell Research* (Vol. 301, Issue 1). 43-49

Winklbauer, R., Selchow, A., Nagel, M. and Angres, B., 1992. Cell interaction and its role in mesoderm cell migration during Xenopus gastrulation. *Developmental Dynamics*, 195(4), pp.290-302.

Woda, J. M., Pastagia, J., Mercola, M., & Artinger, K. B. (2003). Dlx proteins position the neural plate border and determine adjacent cell fates. *Development* (Vol. 130, Issue 2). 331-342

Wolfenson, H., Lavelin, I., & Geiger, B. (2013). Dynamic Regulation of the Structure and Functions of Integrin Adhesions. In *Developmental Cell* (Vol. 24, Issue 5, pp. 447–458).

Woods, M. L., Carmona-Fontaine, C., Barnes, C. P., Couzin, I. D., Mayor, R., & Page, K. M. (2014). Directional collective cell migration emerges as a property of cell interactions. *PLoS ONE, 9*.

Wu, Y. I., Frey, D., Lungu, O. I., Jaehrig, A., Schlichting, I., Kuhlman, B., & Hahn, K. M. (2009). A genetically encoded photoactivatable Rac controls the motility of Tikving cells. *Nature*, *461*(7260), 104–108.

Yang, J. *et al.* (2020) 'Guidelines and definitions for research on epithelial–mesenchymal transition', *Nature Reviews Molecular Cell Biology*. Nature Research, pp. 341–352.

Yang, W.-H. (2012). RAC1 activation mediates Twist1-induced cancer cell migration Immunotherapy for Inflammatory diseases View project Membrane receptors in nuclear View project. *Article in Nature Cell Biology*. 366–374

Yi, J., Kloeker, S., Jensen, C. C., Bockholt, S., Honda, H., Hirai, H., & Beckerle, M. C. (2002). Members of the zyxin family of LIM proteins interact with members of the p130Cas family of signal transducers. *Journal of Biological Chemistry*, *277*(11). 9580-9589

Yu, C. H., Law, J. B. K., Suryana, M., Low, H. Y., & Sheetz, M. P. (2011). Early integrin binding to Arg-Gly-Asp peptide activates actin polymerization and contractile movement that stimulates outward translocation. *Proceedings of the National Academy of Sciences of the United States of America*, *108*(51), 20585–20590.

Zaidel-Bar, R., Ballestrem, C., Kam, Z., & Geiger, B. (2003). Early molecular events in the assembly of matrix adhesions at the leading edge of migrating cells. *Journal of Cell Science*, *116*(22), 4605–4613.

Zaidel-Bar, R., Itzkovitz, S., Ma'ayan, A., Iyengar, R., & Geiger, B. (2007a). Functional atlas of the integrin adhesome. *Nature Cell Biology*, *9*(8). 858-867

Zaidel-Bar, R., Kam, Z., & Geiger, B. (2005). Polarized downregulation of the paxillin-p130CAS-Rac1 pathway induced by shear flow. *Journal of Cell Science*, *118*(17), 3997– 4007

Zaidel-Bar, R., Milo, R., Kam, Z., & Geiger, B. (2007b). A paxillin tyrosine phosphorylation switch regulates the assembly and form of cell-matrix adhesions. *Journal of Cell Science*, *120*(1). 137-148

Zamir, E., Katz, M., Posen, Y., Erez, N., Yamada, K. M., Katz, B. Z., Lin, S., Lin, D. C., Bershadsky, A., Kam, Z., & Geiger, B. (2000). Dynamics and segregation of cell-matrix adhesions in cultured fibroblasts. *Nature Cell Biology*, *2*(4), 191–196.

Zhang, Z., Lei, A., Xu, L., Chen, L., Chen, Y., Zhang, X., Gao, Y., Yang, X., Zhang, M., & Cao, Y. (2017). Similarity in gene-regulatory networks suggests that cancer cells share characteristics of embryonic neural cells. *Journal of Biological Chemistry*, *292*(31), 12842–12859.

Zhong, J., Baquiran, J., Bonakdar, N., Lees, J., Ching, Y., Pugacheva, E., Fabry, B. and O'Neill, G., 2012. NEDD9 Stabilizes Focal Adhesions, Increases Binding to the Extra-Cellular Matrix and Differentially Effects 2D versus 3D Cell Migration. *PLoS ONE*, 7(4), p.e35058.